

TECHNICAL UNIVERSITY OF CRETE



School of Electrical & Computer Engineering  
Digital Image & Signal Processing Laboratory  
(DISPLAY)

---

**Delineating the Epileptogenic Zone by Accurately  
Determining the High Frequency Oscillation  
(HFO) Area using Classification of the Extracted  
Features**

---

DIPLOMA THESIS

Olympia K. Gallou

Thesis Committee:  
Professor Zervakis Michalis (Thesis Supervisor)  
Associate Professor Michail G. Lagoudakis  
Dr. Vassilios Diakouloukas

Chania, October 2021





Σχολή Ηλεκτρολόγων Μηχανικών και Μηχανικών Υπολογιστών  
Εργαστήριο Ψηφιακής Επεξεργασίας Σήματος και Εικόνας  
(DISPLAY)

---

**Οριοθέτηση της Επιληπτογόνου Ζώνης με  
Ακριβή Προσδιορισμό της Περιοχής Υψηλής  
Συχνότητας Ταλάντωσης (HFO)  
χρησιμοποιώντας την Ταξινόμηση των  
Εξαγόμενων Χαρακτηριστικών**

---

ΔΙΠΛΩΜΑΤΙΚΗ ΕΡΓΑΣΙΑ

Ολυμπία Κ. Γάλλου

Επιτροπή Διπλωματικής:  
Καθηγητής Ζερβάκης Μιχάλης (Επιβλέπων)  
Αναπληρωτής Καθηγητής Μιχαήλ Γ. Λαγουδάκης  
Δρ. Βασίλειος Διακολουκάς

Chania, October 2021





## Abstract

Epilepsy is a common complex neurological disorder characterized by unprovoked seizures. A significant percentage of epileptic patients worldwide do not respond to anti-epileptic drugs (AED) and as a result experience recurrent unpredictable seizures with increased risks. Epilepsy surgery is proved to be the most effective treatment to achieve seizure freedom in that percentage of drug-resistant patients with focal epilepsy. The main principle of epilepsy surgery is the accurate localization and resection or disconnection of the Epileptogenic Zone (EZ). Invasive techniques such as electrocorticography (ECoG) with high spatiotemporal precision, are crucial in the presurgical evaluation, in order to resect accurately the cortical tissues related to epileptogenesis. Interictal High Frequency Oscillations (HFO) are promising biomarkers in intracranial electroencephalography (iEEG). Recent studies have shown that the resection of the tissue generating HFOs may improve presurgical diagnosis and surgical outcomes of drug-resistant patients. High-frequency oscillations were defined in the Ripple (80–250 Hz) and the Fast Ripple (250–500 Hz) frequency bands. The electrode contacts with the highest rate of Ripples co-occurring with Fast Ripples designated the HFO area. In the current study, the goal was to investigate the association of the different types of interictal HFOs with the seizure onset zone (SOZ), resected area, and the surgical seizure outcome (ILAE) in 20 consecutive patients, who underwent resective surgery in University Hospital Zurich. We analyzed samples of long-term invasive recordings segmented in 5-minute intervals of interictal slow-wave sleep. We have developed an event-based machine learning method for automated prospective identification of the pathological HFO and the non-pathological HFO area using features extracted from interictal iEEG data in clinical settings. Thus, we provide a prospective definition of pathological HFOs that are clinically relevant. The proposed approach is based on supervised learning algorithms, including SVM and Random Forests cross-validated with ten-fold cross-validation and Leave One Patient Out, to sort epileptic and non-epileptic events using distinctive features of HFOs. From the results, we achieve high performance in detecting the epileptic foci and predicting the seizure outcome at the intra-, as well as inter-subject level. These results corroborate findings from previous studies and thus they might enable future prospective multicenter studies testing the clinical application of the HFO.





## Περίληψη

Η επιληψία είναι μια συχνή περίπλοκη νευρολογική διαταραχή που χαρακτηρίζεται από απρόκλητες κρίσεις. Ένα σημαντικό ποσοστό ασθενών παγκοσμίως πάσχει από φαρμακοανθεκτική επιληψία και ως αποτέλεσμα βιώνει επαναλαμβανόμενες απρόβλεπτες κρίσεις με αυξημένους κινδύνους. Η χειρουργική επέμβαση επιληψίας έχει αποδειχθεί ότι είναι η πιο αποτελεσματική θεραπεία για την επίτευξη παρατεταμένης ελευθερίας κρίσεων σε αυτό το ποσοστό φαρμακοανθεκτικών ασθενών με εστιακή επιληψία. Η κύρια αρχή της χειρουργικής επιληψίας είναι ο ακριβής εντοπισμός και η εκτομή ή αποσύνδεση της Επιληπτογενούς Ζώνης (EZ). Επεμβατικές τεχνικές, όπως η ηλεκτροκορτικογραφία (ECoG) με υψηλή χωροχρονική ακρίβεια, κρίνονται απαραίτητες στην προεγχειρητική αξιολόγηση, προκειμένου να εκτομηθεί με ακρίβεια ο ιστός του φλοιού που σχετίζεται με την επιληπτογένεση. Οι μεταξύ επιληπτικών κρίσεων Υψίσυχνες Ταλαντώσεις (HFO) αποτελούν έναν πολλά υποσχόμενο βιοδείκτη στο ενδοκρανιακό ηλεκτροεγκεφαλογράφημα (iEEG). Πρόσφατες μελέτες έχουν δείξει ότι η εκτομή των ιστών που παράγουν HFO μπορεί να βελτιώσει την προεγχειρητική διάγνωση και τα χειρουργικά αποτελέσματα ασθενών ανθεκτικών σε φαρμακευτική αγωγή. Οι ταλαντώσεις υψηλής συχνότητας ορίστηκαν στις ζώνες συχνότητων Ripples (80–250 Hz) και Fast Ripples (250–500 Hz). Οι επαφές των ηλεκτροδίων με τον υψηλότερο ρυθμό Ripples που συμβαίνουν ταυτόχρονα με Fast Ripples, ορίζουν την περιοχή HFO. Στην τρέχουσα μελέτη, ο στόχος ήταν να διερευνηθεί η συσχέτιση των διαφόρων τύπων μεταξύ επιληπτικών κρίσεων HFO με τη ζώνη έναρξης επιληπτικών κρίσεων (SOZ), την περιοχή που αφαιρέθηκε και το αποτέλεσμα της χειρουργικής κρίσης (σύμφωνα με την ILAE). Το σύνολο δεδομένων αποτελείται από 20 διαδοχικούς ασθενείς που υποβλήθηκαν σε χειρουργική επέμβαση επιληψίας στο Πανεπιστημιακό Νοσοκομείο της Ζυρίχης. Αναλύσαμε δείγματα μακροχρόνιων επεμβατικών ηχογραφήσεων τμηματοποιημένα σε πεντάλεπτα διαστήματα ύπνου αργού κύματος (SWS). Έχουμε αναπτύξει μια μέθοδο μηχανικής μάθησης που βασίζεται σε γεγονότα για αυτοματοποιημένη ταυτοποίηση της παθολογικής HFO περιοχής και της μη παθολογικής, χρησιμοποιώντας χαρακτηριστικά που εξάγονται από interictal δεδομένα iEEG σε κλινικά περιβάλλοντα. Έτσι, παρέχουμε έναν ενδεχόμενο ορισμό μιας παθολογικής περιοχής κλινικά σημαντικών HFO. Η προτεινόμενη προσέγγιση βασίζεται σε εποπτευόμενους αλγόριθμους μάθησης, συμπεριλαμβανομένων των Μηχανών Διανυσμάτων Υποστήριξης (SVM) και των Τυχαίων Δασών (Random Forests) που διασταυρώνονται με μεθόδους διασταυρούμενης επικύρωσης 10-fold Cross Validation

και Leave-One-Out, για την ταξινόμηση των επιληπτικών και μη επιληπτικών συμβάντων χρησιμοποιώντας χαρακτηριστικά των HFO. Από τα αποτελέσματα, επιτυγχάνουμε υψηλές επιδόσεις στην ταξινόμηση των παθολογικών HFO εστιών και στην πρόβλεψη του αποτελέσματος ελέγχου κρίσεων στον μεμονωμένο ασθενή, καθώς και μεταξύ διαφορετικών ασθενών. Αυτά τα αποτελέσματα ενισχύουν ευρήματα από προηγούμενες μελέτες και επομένως θα μπορούσαν να οδηγήσουν σε μελλοντικές πολυκεντρικές μελέτες που θα δοκιμάζουν την κλινική εφαρμογή των HFO.

## Acknowledgements

*First, I would like to thank my supervisor Professor Michalis Zervakis for giving me the opportunity to elaborate this thesis work, for all his kind support, patient guidance and overall feedback, despite the difficult times of the covid-19 pandemic. Furthermore, I would like to express my deep gratitude to Vasileios Dimakopoulos, PhD candidate at University of Zürich and ETH, for his constant presence and advice when in need despite the distance, and for all his support and contribution both in theoretical and technical parts of this project. I would like to cordially thank my professor and team leader of Kouretes Michalis Lagoudakis for his mentoring and for being the first to instill my love in artificial intelligence. Also, I would like to thank Marios Antonakakis, PhD Student at University of Münster for his valuable feedback.*

*Last, but not least, I would like to express my deepest gratitude to my parents, for their remarkable patience and resilience, as well as for their overall support at any level throughout my education. Additionally, I would like specially to thank my brother Yiannis, for sharing his academic influence and stimuli, as well as for his priceless advice and mental empowerment throughout the difficult phases of my studies. Finally, I thank my dear friends for believing in me and standing beside me.*

*Chania, 2021*

*Olympia Gallou*



# Table of Contents

Table of Contents .....	11
List of Figures.....	12
Chapter 1 Introduction.....	15
Motivation.....	16
Related Work .....	17
Contribution and Innovation.....	17
Thesis Outline.....	18
Chapter 2 Brain Physiology .....	21
Overview of the Nervous System.....	21
Brain Structure and Brain Compartments.....	26
Chapter 3 Epilepsy & Epilepsy Surgery .....	37
Introduction to Epilepsy.....	37
Overview of Epilepsies & Seizures .....	37
Epilepsy Diagnosis and Imaging Techniques .....	42
Epileptic Activity and Abnormal Waveforms .....	50
Epilepsy Treatment .....	53
Intracranial Data.....	58
Chapter 4 Classification of Epileptic Events .....	67
Feature Extraction and Feature Selection.....	67
Machine Learning Classification Approach .....	84
Experimental Scenarios, Results and Evaluation .....	96
Chapter 5 Conclusions & Future Work.....	108
References.....	110

# List of Figures

Figure 1 Neuron Structure (Source: SEER.Cancer[34]) .....	22
Figure 2 Cerebral Cortex with Gyri, Sulci, White and Grey Matter .....	23
Figure 3 Electrical signal in the postsynaptic neuron, caused by the release of neurotransmitters and generated by an action potential or spike (source by Thomas Splettstoesser/CC BY-SA 4.0) .....	24
Figure 4 Types of glia cells in the nervous system, Blausen.com staff (2014) .....	26
Figure 5 General Regions of the Brain [41].....	27
Figure 6 Nerves and functional parts.....	30
Figure 7 Representative scheme of Meninges .....	31
Figure 8 Functional Areas of the Brain (Adapted from Kayt Sukel Dana Foundation).....	32
Figure 9 Brain Lobes .....	33
Figure 10 Framework for classification of the epilepsies. *Denotes onset of seizure (by Epilepsia ILAE).....	38
Figure 11 A combination of the PET and CT imaging systems for anatomic imaging [66].....	45
Figure 12 The 10-20 system in EEG (Source: Wikipedia).....	46
Figure 13 Comparison of Invasive and Non-Invasive Techniques .....	48
Figure 14 Example of ECoG, electrode placement on patient 14 in our dataset. One can see that on the cortical surface are placed after craniotomy a combination of subdural strips, grids and one depth electrode. The electrode placement is according to the findings of the non-invasive presurgical evaluation. ....	48
Figure 15 Invasive ECoG records electrical activity from the cerebral cortex, Source: Wikipedia .....	49
Figure 16 Abnormal Electrical Activity (Source: Johns Hopkins Medicine) .....	50
Figure 17 Epilepsy outcome classification according to ILAE classification with respect to epileptic seizures following epilepsy surgery .....	55
Figure 18 Schematic representation of the overlapping cortical zones in epilepsy [13].....	58
Figure 19 Sleep Stage Sequence in EEG recordings, from Sinauer Associates Neuroscience 2 <sup>nd</sup> edition .....	61
Figure 20 Table of Patients, adapted from [15].....	64
Figure 21 Patient - Electrode placement, strips, grids, depth .....	65
Figure 22 Patient - Electrode placement, only depth electrodes .....	65
Figure 23 Values and Locations of Peaks in HFO, .....	73
Figure 24 Values and Locations of Restricted Peaks in HFO, .....	73
Figure 25 Statistical Analysis Tree, for the investigation of statistical significance of features .....	79
Figure 26 The core idea of SVM classifier (Source: Wikipedia) .....	86
Figure 27 non-linearly separable data on the left, and after the kernel trick on the right the data is linearly separable in the feature space obtained by the kernel (source Wikipedia).....	88
Figure 28 Hard Margin Vs Soft Margin source by Donthi Suraj.....	89
Figure 29 Combining classifiers with different decision boundaries reduce error (Source Scholarpedia). ....	92
Figure 30 Simplified RF Classification (Source: Medium). A RF Classifier consists of numerous decision trees. Every decision tree has a root node, decision nodes and leaves. The leaf node is the final output-product of each tree. The final prediction of Random Forests follows a majority voting system.).....	94
Figure 31 Framework for Ensemble Learning by MathWorks [113] .....	95
Figure 32 Example of A Weak Learner: Stump (Source: Wikipedia) .....	95
Figure 33 AdaBoost algorithmic steps .....	96
Figure 34 Nested (Double) Cross Validation .....	99
Figure 35 ROC Curves in intra-subject prediction .....	101
Figure 36 Leave One Patient Out (LOPO CV).....	102
Figure 37 Out Of Bag Error in Bagging RF, expresses the misclassification probability during training .....	106
Figure 38 COMPARISON TABLE OF ALGORITHMS.....	107

*To My Parents*



# Chapter 1 Introduction

Neuroscience is an interdisciplinary massively growing domain with biology science at its core, that combines other disciplines such as chemistry, computer science, mathematics, medicine, engineering, psychology, and philosophy. Because of its wide range in scientific areas studying about the nervous system and the brain, neuroscience is often referred to in the plural, as Neurosciences. In the past two decades, cutting-edge technologies have been advanced and neuroscientists achieved many research breakthroughs with the help of computational power and computer intelligence. Undoubtedly, because of the complexity of the neurobiological systems, there are many gates still to be open and questions to be answered about modeling the brain, its interpretation and behavior. Some of the major branches of modern neuroscience include behavioral, affective, cellular, clinical, cognitive, molecular and computational neuroscience [1]. Mathematics, computer science and engineering bring innovations in neuroscience research by combining techniques and mechanisms to better understand, model, examine, repair or improve neural systems. Also, through mathematical modeling can be examined the links between the various brain networks, the neural connections and patterns, the processing and transfer of information [2], [3]. Relevant emerging fields that often overlap are neuroimaging, neuroinformatics and neurolinguistics. Neuroimaging methods allow us to visualize the brain, its functions and its abnormalities and thus identify epileptogenic regions in case of epilepsy [4], [5], [6].

In order to diagnose neurological pathologies like epilepsy or investigate potential neurological abnormalities is important to examine brain physiology through mathematical modeling [7]–[9]. The abnormal brain signals that can lead to excessive or synchronous electrical activity in epilepsy have a neurophysiological basis and is essential to study them at a cellular level. The complexity of human brain is mirrored in the different kinds of epilepsies and epileptic seizures. Through computational models and experimentation, we can study, simulate and interpret this complexity, non-linearity and variability of the nervous system and its pathophysiology [9], [10]. As a result, through multidisciplinary laboratory and clinical approaches, scientists move each time one step closer to more accurate predictions, better diagnosis and treatments. In the case of epilepsy, collaborative neuroscience research is constantly developing, by advancing both invasive and non-invasive neuroimaging techniques and introducing new potential biomarkers of epileptogenicity.

## Motivation

As performed in most epilepsy centers, in the pyramid of the presurgical diagnosis of epilepsy, there is a significant percentage of patients that do not respond to anti-seizure medication [10]. Approximately 20-30% of epileptic patients is diagnosed with drug-resistant epilepsy and experiences recurrent seizures with increased risks [10]. As a result, this target epileptic group has no way of knowing if a seizure will occur in daily activities such as driving. For that reason, in the complex case of patients with drug-resistant focal epilepsy, surgery is suggested and proved to be the most effective treatment. The main principle of epilepsy surgery is the accurate localization and resection of the Epileptogenic Zone [11]–[13]. A complete resection of the Epileptogenic Zone can lead to a seizure-free outcome. In this diploma thesis, we aim to investigate the association of the different types of interictal HFOs with the Seizure Onset Zone, the Resected Area by the surgeons and the post-surgical seizure outcome according to the International League Against Epilepsy (ILAE).

However, epilepsy includes complex brain dynamic phenomena, and the actual Epileptogenic Zone can only be estimated through other cortical zones that are considered to be indicators. Some of these indicators are the High Frequency Oscillation Zone, which is our zone of interest in this present thesis, and the Seizure Onset Zone, which is considered to be the gold standard of the presurgical evaluation. The importance of Seizure Onset Zone in the presurgical evaluation leads to the search of new, better and more reliable biomarkers. A biomarker is defined as an objectively measured characteristic of a normal or abnormal biologic process [14]. Recent studies have shown that the resection of the tissue generating HFOs may improve presurgical diagnosis and surgical outcomes of drug-resistant patients [15]. Although High Frequency Oscillations are indicators of epileptic activity, they can also be generated across different areas of the brain and be physiological oscillations. In order to discriminate the SOZ, we need to differentiate the pathological from non-pathological HFO, but here are the challenges. There is yet to be found a method to distinguish HFOs generated from the epileptogenic Zone and HFOs from other brain areas. Epileptologists combine non-invasive and invasive techniques, place implanted electrodes and experts rely on long-term intracranial recordings. This is a time-consuming procedure with inter-rater reliability that needs manual visual inspection (manual annotation of the onset times) and sometimes can lead to failed surgical outcomes [16].

Over the last few years, there is an intense research interest in finding a combination of significant relevant HFO features that can be used in all patients, in order

to identify automatically more accurately the interictal Seizure Onset Zone[17]. By analyzing HFO characteristics in intracranial EEG (iEEG) that constitute electrophysiological information, and with respect to the post-surgical outcome, we could gain insights into the underlying epileptogenesis in the individual patient, as well as between different patients. One of our first goal is to examine if there are statistically significant features from our dataset at different domains in order to discriminate pathological HFO area and with respect to the seizure outcome. Finally, by proving the novelty of the HFO as a biomarker in intracranial EEG with the help of machine learning approaches, we could delineate the patient's Epileptogenic Zone more accurately.

## **Related Work**

Over the last decade, epilepsy studies proliferate and some of them have led to significant breakthroughs in epilepsy treatment. In our work, the target group is patients with drug-resistant epilepsy (DRE), also referred as refractory or intractable, in which Anti-Epileptic Drugs (ADE) cannot control seizures. Lately, an increasing percentage of the research has transferred its focus from Spikes on to the pathological High Frequency Oscillations and their close relation to the Epileptogenic Zone, setting the establishment of HFO in the clinical routine as a long-term purpose[18]. Up to now, there is still no consensus among researchers on how the HFO area should be defined and identified in clinical settings. In more detail, there are different approaches based on the identification of the clinical Seizure Onset Zone[15], [19], [20]. Some of the most interesting machine learning approaches applied with the goal to detect and differentiate normal from epileptic brain patterns, demonstrate classifiers with algorithms such as SVM, k-NN, Discriminant Analysis, k-Means Clustering, Decision Trees, Random Forests, Gaussian Mixture Models, Logistic Regression and Neural Networks[16], [21]–[24] [25]. However, the conditions of each study vary (dataset, HFO criteria and definition, clinical relevance, validation strategies) and as a result, there is no way of knowing which algorithm is preferred based on its performance alone. Also, there are different views on determining valuable attributes for HFO Zone, in order to be a reliable estimator of the EZ.

## **Contribution and Innovation**

In the current thesis, our aim was to explore clinically relevant epileptic and non-

epileptic HFO events, based on their electrophysiology. Ideally, resective surgery should remove the entire epileptogenic zone sparing any adjacent cortexes that are not part of it [26]. Our feature extraction methods based on the temporal and spatial distribution of HFOs and the further prospective classification, provides a distinct separation of pathological and non-pathological HFO area. Thus, we determine a clinically relevant HFO area with respect to the seizure outcome according to the International League Against Epilepsy (ILAE) [27]. We predicted the seizure outcome across different types of patients, by evaluating our classifiers with different validation strategies. The most important validation strategies were the leave one patient out cross validation, where we trained our classification models with the events of all patients and the double cross validation in the individual patient. We confirmed that the surgery outcome could have been improved with HFO guidance and that the delineation of Epileptogenic Zone could have been more accurate by resecting the highest-rated HFO channels. In current research techniques, HFO area is determined by its persistence in time and by testing against random effects. With this proposed event-based approach we might be able to avoid this by checking spectral and morphological features of the HFOs on different domains and categories such as frequency, time, time-frequency, power, entropy and complexity. The results of our classification models suggest that the prospective HFO definition could possibly long-term contribute in surgical planning. To our best knowledge, in this current thesis, we present the first attempt of a methodic structural event-wise classification of pathological HFO with respect to the surgical seizure outcome, by extracting statistically significant discriminative HFO features. In our dataset, Fast Ripples and Ripples (FRandR), which is the simultaneous occurrence of Ripples and Fast Ripples appears to be the best indicator of epileptogenesis compared to the other two separately. In addition, we observed that in all the patients with Temporal Lobe Epilepsy (TLE), the Seizure Onset Zone (SOZ) and HFO area overlap. The patients with failed surgical outcomes, where there was a slight overlap or no overlapping between Seizure Onset Zone and HFO area, had Extratemporal Lobe Epilepsy (ETE). In research, stays obscure in case HFOs are primarily delivered by obsessively changed tissue with harmed neuronal networks, or they happen autonomously of pathology as an epileptiform sign in SOZ [28].

## Thesis Outline

In **Chapter 2 – Brain Physiology**, a review of the theoretical background of the

brain anatomy and physiology is presented. It is divided in two main sections about the overview of the nervous system and the brain structure and its compartments. Brain physiology is an important prerequisite to understand the human behavior and brain functionality, all the building blocks and how they interact, how neurons transmit electrochemical signals and how the brain interprets information and embodies it to essence. This is translated into brain regions, compartments, lobes, and frequency bands (brain waves). In order to study and analyze epilepsy as a neurological disease, let alone epilepsy surgery and its practices, it is critical to understand the underlying human brain physiology. At the end of this chapter, we present the brain waves at the different frequency bands and briefly introduce for the first time to the reader the High Frequency Oscillations, that are often called high gamma.

In **Chapter 3 – Epilepsy & Epilepsy Surgery**, we present in detail an overview of the different epilepsies and seizures according to the framework of International League Against Epilepsy (2017). Secondly, we describe the phases of a seizure, as well as the tools and principles used in epilepsy diagnosis. Different imaging techniques and their principles are mentioned and differentiated in invasive and non-invasive, including fMRI , PET, CT, EEG, MEG , ECoG. A different subsection about the main attributes of epileptic activity and abnormal waveforms in EEG, is presented and includes a detailed description of interictal spikes, the event-related potentials and fields and the high frequency oscillations. A comparison of invasive and non-invasive techniques, its limitations, and advantages, leads to the conclusion that epilepsy surgery is the best treatment choice for the significant drug-resistant percentage of patients. In epilepsy surgery, we cannot know We move on to a definition of important cortical zones and a thorough understanding of their association with the Epileptogenic Zone (EZ) in presurgical evaluation. The Seizure Onset Zone is up to now the gold standard and in most studies is being investigated with different approaches. High Frequency Oscillation (HFO) Zone, which is our target Zone of interest and often overlaps with other estimators of EZ, appears to improve presurgical diagnosis and surgical outcomes of drug-resistant patients in recent studies. The only way to evaluate the success of the epilepsy surgery is by looking at the postsurgical outcome. For that reason, we explain the classification of postsurgical outcome according to ILAE. Finally we move on to the subsection of intracranial EEG data, where there are also the data reading and processing steps on our dataset used in this thesis. There, we present the slow wave sleep characteristics in EEG recordings, describe the data acquisition and equipment, the participants and electrode placement and there is also a literature comparison between the contribution of scalp-HFO and interictal intracranial HFO for epileptogenicity.

In **Chapter 4 – Classification of Epileptic Events**, all the necessary steps for the final separation of the pathological and non-pathological HFO area are covered. More specifically, the first part includes a description of HFO types and rates in different frequency bands in our dataset. Also, a formulation of the problem hypothesis is displayed with our prospective definition of the HFO area. An HFO exploratory analysis and an extensive investigation of the most likely discriminative features are performed, with the goal to end up with the optimal subset of features. The feature extraction techniques include time domain, frequency domain and time-frequency domain features. We present all the extracted features tested, based on exploratory analysis and a combination of previous research.

From the total amount of extracted features, we had to test which of them are actually statistically important for all patients. Univariate and multivariate filter-based techniques were applied in order to conclude with our final feature vector before the classification of the events, including statistical analysis and pearson's rank correlation coefficients. The channel selection is based on our hypothesis and problem statement. Inside cross-validation, embedded methods to measure the feature importance, as part of the learning process during training were applied. Before applying the classification algorithms, data preparation is important to avoid bias.

After feature selection, our machine learning classification approach based on the HFO events is depicted. After, we move on to a brief explanation of the main supervised algorithms and the main idea of ensemble learning that were used in this thesis, including Support Vector Machines (SVM), k-Nearest Neighbors (kNN), Decision Trees and tree-based ensembles such as Random Forest, Bagging and Adaptive Boosting (AdaBoost). Finally, we present the results of our binary classification problem along with the best-performed validation strategies in the individual patient and inter-patient, which were our two experimental scenarios. The validation strategies include double nested cross validation with inner 10-fold cross validation in the individual patient and leave-one-out cross validation in all the patients together. In order to ensure that our model can be generalized, we evaluated our results with a classification report and confusion matrices that provide us the most important metrics related to our problem. A comparison of the classification algorithms is depicted based on their performance in intra-subject and inter-subject level.

In **Chapter 5 – Conclusions & Future Work**, we conclude with a summary of the overall work, discuss about future steps and how we can advance further our research. The results of this proposed approach and its limitations are also discussed.

# Chapter 2 Brain Physiology

## Overview of the Nervous System

### Nervous System: CNS and PNS

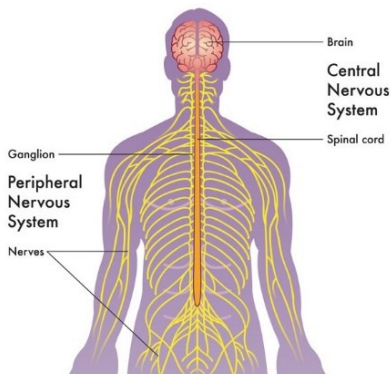


*Figure 1 – Central and Peripheral Nervous System: The CNS includes the brain and spinal cord, the PNS includes nerves (nerve and glia cells)*

Starting from the basics of neuroanatomy, the nervous system is based on the interaction of the two distinct anatomical regions that together form it as a whole, the Central Nervous System (CNS) and the Peripheral Nervous System (PNS) [29] [30]. The CNS is composed of the brain and the spinal cord, which are located in the dorsal body cavity and CNS is also surrounded by connective membranes, called meninges, and by cerebrospinal fluid. Subsequently, the brain is surrounded by the cranium, and the spinal cord is protected by the vertebrae. The human brain is continuous with the spinal cord at the foramen magnum, on average weighs about 1.4 kg (approximately 2% of total body weight) and offers numerous properties with other vertebrate brains, including: the cerebrum, the cerebellum, the brainstem and the limbic system[31]. The spinal cord is a long bundle of nerve tissue that runs from the base of the skull down to the center of the back, carrying messages between the brain and the rest of the body, and having as a result the control of vital functions and human senses [32].

The PNS is composed of pairs of nerves that branch from the spinal cord and the cranial nerves that arise from the brainstem and neuromuscular junctions. In addition, the PNS can be divided into different nervous systems, determined by the functional areas. Generally, by analyzing the building blocks of the brain, one can understand the brain complexity, both in structure and in function.

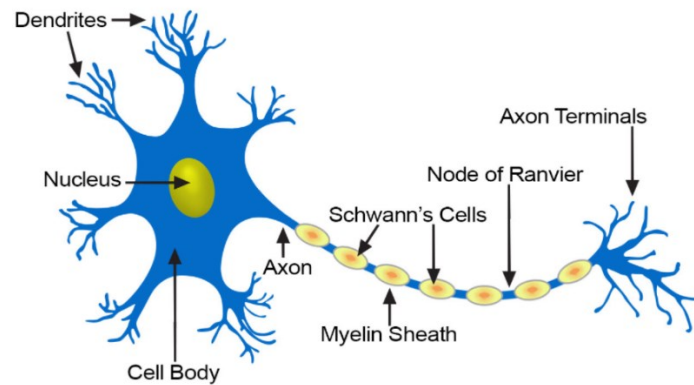


Figure 1 Neuron Structure (Source: SEER.Cancer[34])

## Types of Neurons

Although the nervous system is very complex, there are only two main classes of cells in the nerve tissue. The actual nerve cell is the neuron, that's why most of the times nerve cells are referred as neurons. A typical neuron is the “conducting” cell that transmits impulses and the structural processing unit of the nervous system. The second type of cells is neuroglia (sometimes called glial cells). The etymology of this word “neuroglia” has a Greek origin and can be translated as “nerve glue”. This special type of cells is nonconductive and provide a great support and nourishing system for the neurons. In addition, neuroglia are far more numerous than neurons and, unlike neurons, are capable of mitosis, the fundamental process of cell division. Summarizing these two, neurons play the main information processing role, while the glial cells play the supporting and feeding role of the nerve cells.

In more detail, neurons are comprised of three main regions: the cell body (soma), the dendrites and the axons. They are often called information messengers, as they use electrical impulses and chemical signals in the nervous system to transmit information between different areas of the brain and between the rest of the nervous system, as well. In addition, neurons are highly specialized and amiotic, namely they do not go through mitosis and cannot be replaced if damaged. First, their cell body has a nucleus with at least one nucleolus, contains all the genetic information and synthesizes the cells' proteins. Dendrites and axons are cytoplasmic extensions, or processes, that project from the cell body. More specifically, dendrites, often referred as fibers, are usually short and branching like trees, which increases their surface to receive signals from other neurons, and thus improves the incoming signal capacity. Dendrites are called afferent processes, because they transmit impulses to the neuron's cell body. From each cell body, there is only one axon that projects.

Axons that can convey electrical signals with high speeds, may have infrequent branches called axon collaterals. Axons and axon collaterals terminate in many short

branches or telodendria and the distal ends of the telodendria are slightly enlarged to form synaptic bulbs. It is also substantive to highlight the action potentials, which are the signals that are transferred to the axons from the cell bodies and they are initiated from the initial segment, a trigger region close to the axon hillock. Many axons have also in their surrounded area, a segmented, fatty, white substance called myelin or else the myelin sheath. Myelin's role is to protect and electrically insulate fibers, prevent depolarisation, as well as to increase the transmission speed of nerve impulses. The fibers that are myelinated designate the known "white matter" of the CNS, while cell bodies and unmyelinated fibers designate the "gray matter".

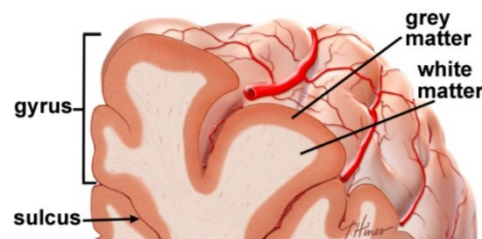


Figure 2 Cerebral Cortex with Gyri, Sulci, White and Grey Matter

In the PNS, Schwann cells produce myelin. A Schwann cell consists of the cytoplasm, a nucleus, and the outer cell membrane that forms a tight covering around the myelin and around the axon of the nodes of Ranvier[35]. This specific covering is the neurilemma, which plays an important role in the regeneration of the nerve fibers. In the CNS, oligodendrocytes produce the myelin, but there is no neurilemma there and that explains why fibers within the central nervous system do not regenerate [36]. Lastly, at the end point of an axon, we have a division into zones which shape branches for the communication of the neighboring nerve cells, called synapses.

A synapse is basically a junction that mediates information transfer from one neuron to the next to an effector cell [27]. At this point of communication, the firing of an action potential in one sending neuron causes the transmission of a signal (presynaptic) to another receiving neuron (postsynaptic) making the postsynaptic neuron more or less likely to fire its own action potential.

## Brain Circuits and Electricity

While reading a paragraph -like this one right now- the brain is sending off electrochemical signals to interpret and understand the meaning of it. CNS' main organ is made of around 86 billion neurons, connecting and creating networks that communicate electrochemically with each other, more specifically by using electrical charges and chemicals called ions. As a result, neurons carry an electrochemical

charge, and this charge changes, depending on whether the neuron is sending a signal or is at rest. In simple words, a brain circuit is basically the path that the electrical activity moves and follows from one nerve cell to the other, and eventually can reach to an effector organ such as a muscle or a gland, causing ultimately a coordinated behavior. A fluid exists inside and between neurons, that contains particles, which are atoms or molecules that have a negative or positive charge. At the point when a neuron is very still, there are more negative ions inside and more certain particles outside of it, giving the neuronal film a negative charge. At the point when cerebrum movement happens, positive particles surge in through diverts in the neuronal layer and, when the charge gets sufficiently high, the neuron conveys a message to speak with adjacent neurons. Because brain activity is caused by electrical charges, that means the brain functioning can change in case of electrical stimulations. At the end of a neuron, is a very important part called synapses [37].

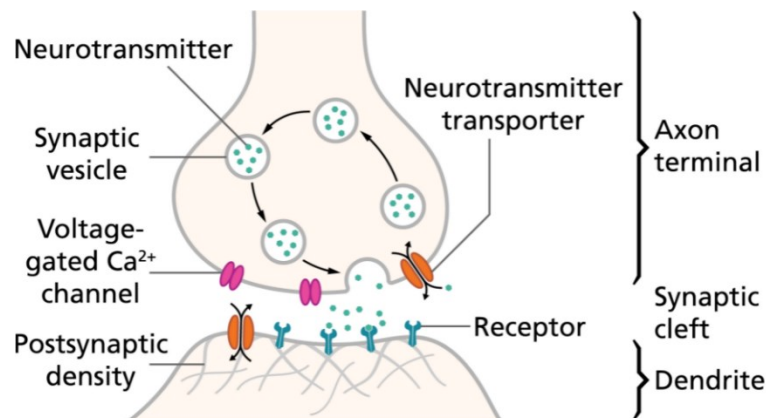


Figure 3– Electrical signal in the postsynaptic neuron, caused by the release of neurotransmitters and generated by an action potential or spike (source by Thomas Spletstoesser/CC BY-SA 4.0)

Synaptic transmission triggers the release of several neurotransmitters (such as epinephrine, dopamine, acetylcholine), which can in turn cause to the cell membrane voltage change. Inhibitory or excitatory activity between the neurons, have synapses as entryways. In more detail, synapses pass information through impulses across neurons in two ways, inhibitory and excitatory. Inhibitory decreases the chance of the subsequent neuron signaling and excitatory increases the chance of the subsequent neuron signaling. Synapses can be thought of as converting an electrical signal (the action potential) into a chemical signal in the form of neurotransmitter release, and then, upon binding of the transmitter to the postsynaptic receptor, switching the signal back again into an electrical form, as charged ions flow into or out of the postsynaptic neuron. Action potentials are the most important units, that neurons use to communicate with each other and occur when the sum total of all of the excitatory and

inhibitory inputs makes the neuron's membrane potential reach around  $-50$  mV, this value is called the **action potential threshold**. These action potentials are often referred as 'spikes', because it is like a spike had fired or 'spiked'. When an action potential reaches the presynaptic terminal, it causes neurotransmitter to be released from the neuron into the **synaptic cleft**, a 20–40nm gap between the presynaptic axon terminal and the postsynaptic dendrite (often a spine). The transmitter, travels across the synaptic cleft and after is being attached to neurotransmitter receptors on the postsynaptic side, and depending on the neurotransmitter that was released (based on the type of neuron), negative ions ( $\text{Cl}^-$ ) or particular positive (such as  $\text{Na}^+$ ,  $\text{K}^+$ ,  $\text{Ca}^+$ ) will travel through channels, that span the membrane.

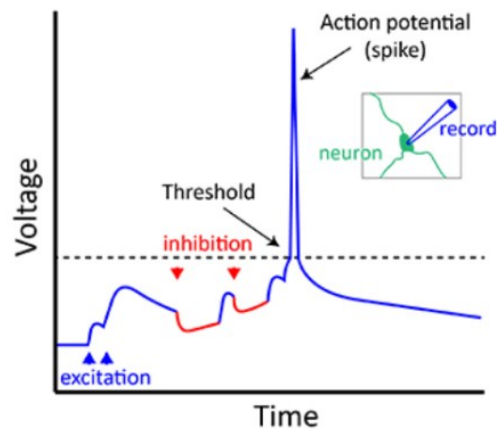


Figure 12.1.1 – Here we can see a neuron that 'spiked' (action potential) when a combination of all the inhibition and excitation makes it reach threshold (source by Alan Woodruff/QBI)

Neurons are classified based on their functionality, as efferent, afferent, or interneurons according to the direction in which they transmit to the CNS impulses. Afferent or else sensory neurons carry impulses from peripheral sense receptors to the CNS. Afferent often have long dendrites and relatively short axons. On the other hand, efferent or else motor neurons usually have long axons, short dendrites and transmit impulses from the CNS to effector organs, such as glands and muscles. Last but not least, interneurons or else association neurons, are located within the CNS entirely and link the afferent and efferent neurons. Interneurons have short dendrites, with either a short or long axon.

Among the other nerve units, glia cells, there are two main types, namely microglia and macroglia [38], [39]. First, **microglia** are the brain's immune cells, spiderlike phagocytes that dispose of debris, including bacteria and dead brain cells.

They also prune synapses. In some cases, such as Alzheimer's disease, they may become hyper-activated and cause too much inflammation. Microglia, play an important role in the control of homeostasis, neuronal defense and repair, scar formation, and also affect electrical impulses. When respond to an injury, microglia cause inflammation as part of the healing process. That is believed to lead to the amyloid plaques and other problems associated with the disease. Second, macroglia could be divided into three basic categories: oligodendrocytes, Schwann cells, and astrocytes. The oligodendrocytes are glia, their flat extensions are wrapped tightly around the nerve fibers and by this way, they produce myelin sheaths, which are fatty insulating coverings [38]. In turn, in the PNS we have Schwann cells that form the myelin sheaths around nerve fibers. Next, the astrocytes are characterized as abundant, star-shaped cells. These cells are responsible for nearly half of the neural tissue. Ependymal cells are also glial cells that line the central brain cavities, as well as the spinal's cord. The beating of their cilia assists the circulation of the cerebrospinal fluid and forms a protective cushion around the CNS. Last but not least, satellite cells are cushioning cells, offering various protective mechanisms.

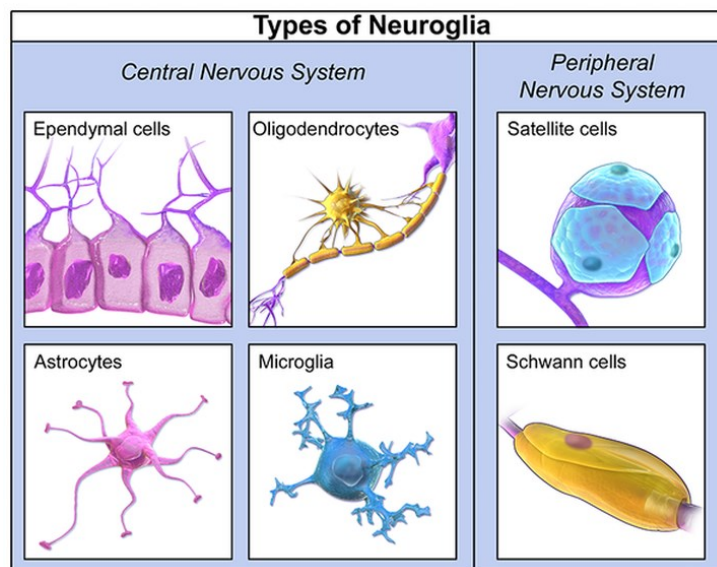


Figure 4 Types of glia cells in the nervous system, Blausen.com staff (2014)

## Brain Structure and Brain Compartments

### Brain Regions

Moving on to the brain structure itself, this intricate organ is separated into several anatomical and functional regions. First of all, the brain lies within the skull and the cranial cavity of the skull and can be divided anatomically into these 3 regions, the *forebrain*, the *midbrain* (or mesencephalon) and the *hindbrain*.

The **forebrain** consists of the cerebrum and the diencephalon (basal ganglia, thalamus, hypothalamus). The **cerebrum** or cortex is the largest part of the human brain and divided into two lateral regions, the left and right hemisphere, which are connected through a bundle of nerve fibers, called corpus callosum. Each hemisphere controls the opposite side of the body, so if a stroke occurs on the left side of the brain, then the right arm or leg may be weak or paralyzed. The two hemispheres consist of the cerebral cortex, which is an outer shell made up of cell bodies with a gray appearance, that's why it's called gray matter. The cerebral cortex has a highly convoluted topography of sulci/sulcus (grooves or furrows) and gyri/gyrus (bumps or ridges). The folding of the brain, and the functionality of gyri and sulci, increases its surface area and as a result enables efficiently more cerebral cortex matter to fit inside the skull. If it was possible to spread out all of these furrows and ridges, the result would be a total cerebral brain surface area of about 2500 cm<sup>2</sup>, which is almost the size of a pillow case 50x50 cm [40].

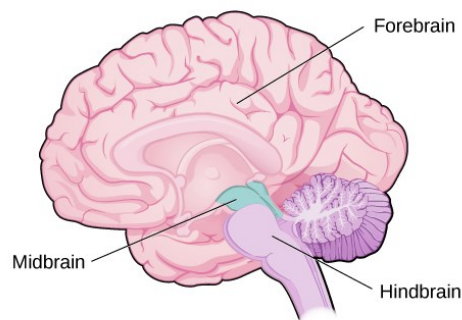
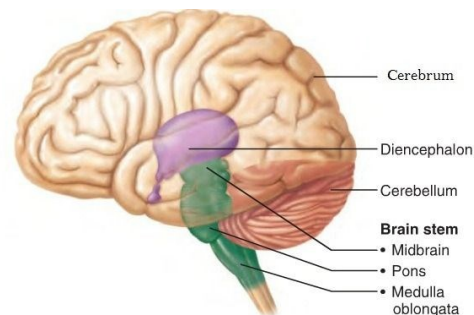


Figure 5 General Regions of the Brain [41]

The part of the brain called **cerebrum**, includes the most significant and vital brain functions such as thinking and reasoning, planning and processing, interpreting and processing inputs from our senses, such as vision, hearing, taste, touch, and smell. Cerebral cortex is the outer layer of cerebrum, is called the cerebral cortex, and in each hemisphere, it is traditionally divided into four main lobes - frontal, parietal, occipital and temporal. A fifth lobe, the insula or Island of Reil, lies deep within the lateral sulcus. Lateral sulcus separates the temporal lobe with the parietal and frontal lobes and the central sulcus separates the parietal from the frontal. Corpus callosum maintains the communication between the two hemispheres. Beneath the surface, there are large knots of neurons called basal ganglia, which specialize in programming and executing motor functions. A characteristic disease example, where ganglia are affected is Parkinson, and there patients suffer from uncontrolled movements and tremors. In correspondence to the gray matter, the white matter is the inner area where there are myelinated fibers that give into this layer the white tint, because of the myelin.

After the forebrain, the **midbrain** consists of various cranial nerve nuclei, tectum, colliculi, tegmentum, and crura cerebri. The **hindbrain**, sometimes also called **brainstem**, consists of the medulla, pons, cranial nerves, and cerebellum. The **cerebellum** has two hemispheres which have widely folded surfaces and looks like a layered, wrinkly coral. Also, Cerebellum, which means 'little brain', helps to control and regulate fine movements, balance, and posture. If damaged, the cerebellum could lead in muscle contractions and loss of equilibrium. Moreover, cerebellum receives input from the sensory systems of the spinal cord and other brain areas and finally integrates these inputs to fine-tune motor activity.

Just underneath the midbrain and bulbous in shape, the **pons** (in Latin means 'bridge'), connects the rest of the cerebral cortex to the brainstem, and constitutes a coordination center for signals and communications that flow between the spinal cord and the two brain hemispheres. The



crania] nerves of Pons are four and more specifically, the abducens nerve that helps coordinate eye movement, the facial nerve for the coordination of movement and sensation in the face. Also, the vestibulocochlear nerve, which has the goals of processing different sounds and balance maintenance, and then we have the trigeminal nerve which is responsible for the coordination of chewing and for carrying carries sensory information.

The lower part of both the brainstem and hindbrain is the **medulla oblongata**, where the brain transitions to the spinal cord. Medulla is only about 3 cm long, and controls autonomic vital functions such as breathing, heart rate, blood pressure, and many in voluntary reflexes such as swallowing and sneezing. In addition, the medulla oblongata contains both white and grey matter. Some important cranial nerves stem from medulla, these are called vagus, glossopharyngeal, accessory nerve hypoglossal nerve. All the ascending and descending nerve fibers, pass through the medulla.

One of the most efficacious CNS components that goes along with the brain, is the **brainstem**. This component is at the low part of the brain and is also the oldest. Brainstem is often called the reptilian brain and controls vital autonomic body processes, such as breathing, heartbeat, bladder function and sense of equilibrium.

**Diencephalon's components** are also important to be inspected and evaluated. First, **thalamus** is located in the central of the brain, between brainstem

and cerebrum. This component is made up of a series of nuclei which are responsible for the relay of the different sensory signals and since there is a connection between the limbic system structures to the anterior nuclei of the thalamus, this part is also involved in the regulation of sleep and wakefulness, in learning and memory. Secondly, hypothalamus is a small area about the size of an almond, in the center of the brain between the pituitary gland and thalamus, that plays an important role in hormone production and the maintenance of homeostasis. The pituitary gland is a small gland, that is located behind the nose at the base of the brain, in an area called the pituitary fossa or Sella turcica, but pituitary is often called the "master gland" as it is responsible for the secretion of hormones (growth and development, function of various body organs such as kidneys, uterus and other glands such as thyroid).

Back to **hypothalamus**, when it receives a signal from the nervous system, then it secretes substances known as neurohormones, that control the secretion of pituitary hormones. Moreover, hypothalamus helps to stimulate many important processes in the body, such as temperature, thirst, sleep cycles, appetite and weight control, sex drive, balancing body fluids, childbirth and others, as it is considered to be the link between the nervous system and the endocrine system. For example, if the hypothalamus receives a signal related to body temperature, that for example is too high, then the body will get a sign to start sweating. If the body temperature is too low, then the body will produce heat on its own by shivering. Even smaller than the hypothalamus, about the length of a grain of rice, is the **pineal gland**, tucked between the two lobes of the thalamus and involved in regulating functions related to hormones. This little area has a shape of a very small pinecone and its objective is to produce the important hormone melatonin, that regulates sleep-wake cycles.

The **hippocampus** comes in structure as a pair, one in each hemisphere of the brain, just like other structures inside brain. Hippocampus resembles the shape of a curvy seahorse and is essentially the memory center of our brains. The connections inside hippocampus, lead us to associate memories with various senses. The hippocampus plays also a significant role in spatial orientation, navigation memory formation, and also is a part of the brain, where new nerve cells are made from adult stem cells. This is known as neurogenesis and is a key brain structure for learning new things.

Next to the hippocampus, is located another important region called **amygdalae**. The name amygdala refers to its shape that looks like an almond. The left and right amygdalae have a central role in human emotional responses. More specifically, attaches emotional content to the human memories, such as fear and anxiety or pleasure and determines how robustly those memories can be stored. The

amygdala has a key role in forming new memories specifically related to fear. Fearful memories are able to be formed after only a few repetitions and that is why 'fear learning' constitutes a popular way to investigate the mechanisms of memory formation, consolidation and recall. Memories with strong emotional charge, have a greater emotional weight and thus tend to stick.

Another important aspect of the brain is the **limbic system**, which is often referred as the brain of emotions. This part is located deep within the brain, underneath the cerebral cortex and above the brainstem, constitutes an evolutionarily old structure and is involved in our behavioral and emotional responses, especially when it comes to survival modes/situations: thirst, feeding, reproduction, caring for the young, and arousing fight-or-flight responses. The limbic system's actions include the components of diencephalon (thalamus, hypothalamus), along with the corpus callosum, basal ganglia and amygdala. The interconnected group of all the previous components is associated with emotional experience, learning and a set of different endocrine functions.

The brain communicates with the entire body through the spinal cord and twelve pairs of cranial nerves. Posterior fossa, is the name of a cavity in the back part of the skull which contains the cerebellum, brainstem and the cranial nerves numbered from five to twelve. In addition, ten of the twelve pairs of these cranial nerves, originate in the brainstem and they are responsible for controlling the eyes, hearing and facial sensations, how we move different kind of muscles such as the tongue muscles or those responsible for moving the neck (swallowing) or face. In the cerebrum one can find the cranial nerves that control vision and smell. These nerves are named and numbered with their specific functions, as shown in the figure:

No.	Name	Function
I	olfactory	smell
II	optic	sight
III	oculomotor	moves eye, pupil
IV	trochlear	moves eye
V	trigeminal	face sensation
VI	abducens	moves eye
VII	facial	moves face, salivate
VIII	vestibulocochlear	hearing & balance
IX	glossopharyngeal	taste, swallow
X	vagus	heart rate, digestion
XI	accessory	moves head
XII	hypoglossal	moves tongue

*Figure 6 Nerves and functional parts*

**Meninges** consists of three protective tissue layers that cover all the CNS, brain and spinal cord. As the brain is housed inside the bony covering called the cranium for injury protection, between the brain and the skull exists the meninges, which in turn is divided in the dura mater, the arachnoid and the pia mater. Dura mater consists of two layers of a nonelastic film or whitish membrane and the second outer

layer is called the periosteum. The inner layer, called dura, lines the inside of the entire skull and creates little folds or compartments for the protection of the brain parts inside. The names of the two special folds of the dura, are falx and tentorium. The falx separates the right and left half of the brain and the tentorium separates the upper and lower parts of the brain. Then, follows the second layer of the meninges, the arachnoid. Arachnoid membrane is thin and delicate, while consists of an elastic tissue and blood vessels of varying sizes, that cover the entire brain. Also, there is a space between the two previously mentioned membranes, arachnoid and dura, with the name subdural space. After that, the layer of meninges closest to the surface of the brain is called the pia mater. This layer is full of blood vessels that can reach so deep into the surface. The space that separates the arachnoid and the pia is called the subarachnoid space, where the cerebrospinal fluid flows. The pia covers the entire surface of the brain and follows the folds of the brain. The major arteries supply the human brain, by providing the pia with its blood vessels.

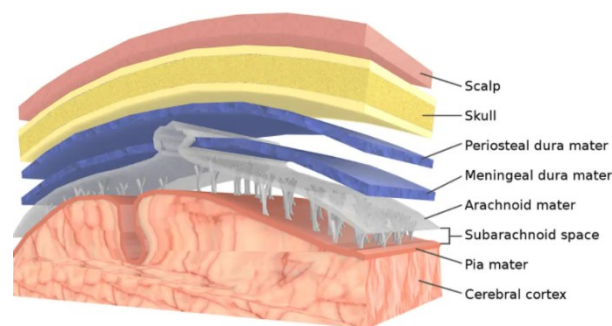


*Figure 7 Representative scheme of Meninges*

Another essential part within the brain and around the brain and spinal cord, is the **CerebroSpinal Fluid (CSF)**. CSF is a clear, watery fluid-substance that helps to cushion the brain and spinal cord from injury and potential damages, it circulates through channels around the CNS, constantly being absorbed and replenished. This particular fluid is part of the ventricular system, is produced and secreted in the brain within hollow channels, called ventricles. A specialized structure within each ventricle, called the choroid plexus, controls the majority of CSF production. Also, the arachnoid space is filled with this fluid, while at the same time helps the blood vessels to reach the brain.

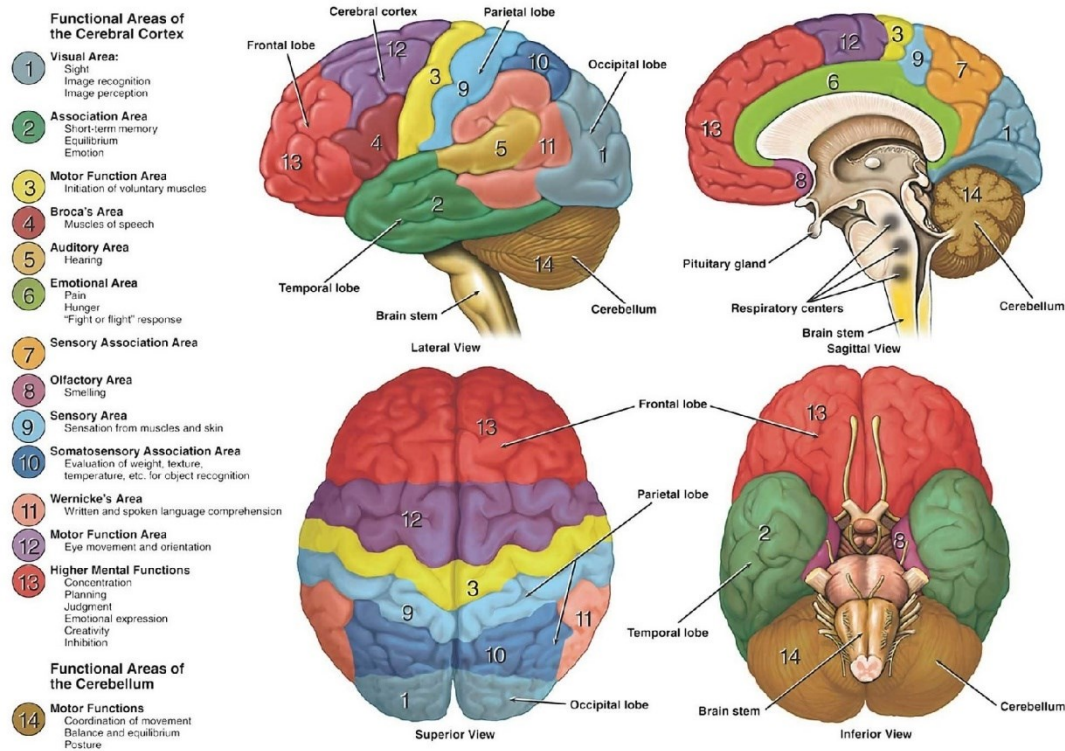


Figure 8 Functional Areas of the Brain (Adapted from Kayt Sukel Dana Foundation)

## Brain Lobes

A fundamental separation is still made between four lobes: Occipital, Temporal, Parietal, and Frontal. The **occipital lobe** is located in the rearmost portion of the skull. Furthermore, it is the major visual processing center, including important functional processes such as orientation or spatial frequency, how we differentiate colors and patterns, and perceive motions. The **primary visual cortex (V1)**, receives visual information directly from our eyes. This information is relayed to several secondary visual processing areas, which interpret distance, location, depth, and others. Lastly, because of all these mentioned, occipital lesions are connected with agnosia (in colors or movements), hallucinations, as well as blindness.

Separated from the frontal lobe by the lateral fissure, the **temporal lobe** is responsible for long-term memory and contains also regions dedicated to processing sensory information, extremely important for hearing, recognizing language, emotional association and forming visual memories. Likewise, temporal lobe contains the primary auditory cortex. The auditory cortex is responsible for receiving and processing information directly from the ears and secondary areas, too. The left temporal cortex helps in the comprehension of languages (reading or hearing), this is often called Wernicke's area, and Wernicke's aphasia is a language disorder associated with damages to these regions that control language. Moreover, the medial temporal lobe (closer to the middle) contains the **hippocampus**, an important brain region

strongly related to learning, memory, and emotions. In some certain areas of the temporal lobe, the process of complex visual information such as faces or scenes is possible.

The **parietal lobe** is behind the frontal lobe, separated by the sulcus and is all about integrating information stemming from external sources, as well as internal sensory feedback (including touch, temperature, pressure and pain) from skeletal muscles, limbs, eyes, otoliths and others. More specifically, because of the processing that occurs in the parietal lobe, a human can discern nearby points that are distinct, rather than one object (two-point discrimination). Depending on the brain area, there is a different amount of sensory receptors and as a result a different sensitivity. The parietal cortex gives us a coherent representation of our surroundings and spatial associations (people, objects, distances, environment), by merging all the information sources. All the tasks that require the participation or the cooperation of different sensors, such as our eyes or hands, are controlled by parietal cortex. Different processes (storing information) that parietal cortex coordinates are related to the morphology of the surroundings, such as size and shape, or their spatial orientation. Parietal cortex if damaged, then a human experiences severe disruptions, especially disruptions that have to do with motor behavior.

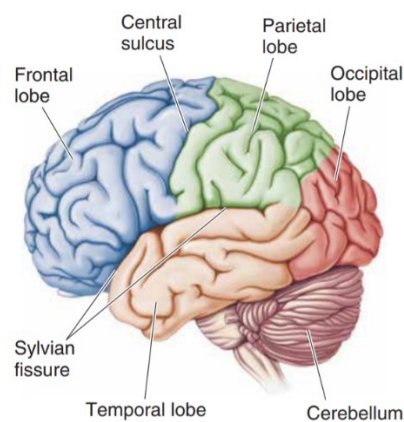


Figure 9 Brain Lobes

The region of the **frontal lobe**, where most of the conscious thoughts and decisions are made, is separated from the parietal lobe by a space area called the **central sulcus**, and from the temporal lobe by the **lateral sulcus**. The activity of frontal lobe is very important, as it allows to connect current actions, project future consequences from them and make appropriate decisions. Frontal lobe is related to the personality and learning history of a subject, and as a result frontal lesions have been shown to cause severe changes in categories such as personality with social behavior and action control or taste preferences. Generally, the frontal lobe exists where higher executive functions occur, including emotional regulation, reasoning, planning and

problem solving. Also, the frontal cortex, contains most of the neurons that are related to dopamine system. More specifically, frontal lobe contains motor areas where voluntary movements are controlled (such as walking upstairs or picking up a cup of coffee), as well as conscious thought (for example thinking about what to have for dinner). The dopamine system controls cognitive processing associated with reward, attention, emotional expression, planning, short-term memory and motivation[42].

<b>Brain Parts</b>	<b>Functions</b>
Frontal Lobe	Problem solving, concentration, judgement, inhibition of behavior, attention, anticipation, organization, speaking (expressive language), emotional expression, mental flexibility, self-monitoring, motor planning, behavioral control, initiation, sexual behavior, personality, social skills
Temporal Lobe	Understanding language, information retrieval, memory, hearing, learning and awareness, organizing and sequencing
Parietal Lobe	Sense of touch and pain, smell and taste, spatial perception, reading and writing, math calculations, differentiation of size, shape and color
Occipital Lobe	Processing visual information (color, light), reading (perception, recognition)
Cerebellum	Coordination of voluntary movement, balance and equilibrium, attention, emotion regulation
Brain Stem	Vestibular function, breathing, heart control and heart rate, digestion, blood pressure and blood vessel control, consciousness, temperature, alertness, sweating, reflexes to seeing and hearing, ability to sleep
Thalamus	Spatial attention, depth perception, consciousness, alertness, sleep
Basal Ganglia	Memory, emotion, coordination of muscle movement
Spinal Cord	Breathing, body temperature, swallowing, digestion, sleep

Encephalography is one of the oldest and most important tests that can facilitate in epilepsy diagnosis and treatment, as well as in other neurological disorders. More specifically, EEG can localize where the seizure is originated and aid in this way as a workup for possible epilepsy surgery, characterize seizures and determine next treatment choices. Some of the key components of studying neural oscillations measured with EEG, are frequency, which is the number of oscillations per second, power, which is the amount of energy in a frequency band, and phase, which is the stage of alignment and synchronization of sources. In reality, the signal (brain

signal activity) consists of underlying base frequencies in different bands, which are considered to mirror certain affective, cognitive and attentional states of a human. Researchers classify the brain waves into the following distinguished bands [49]: Delta frequency band – delta waves [1 – 4 Hz], theta frequency band – theta waves [4 – 8 Hz], alpha frequency band – alpha waves [8 – 12 Hz], beta band – beta waves [13 – 25 Hz] and gamma frequency band – gamma waves [ $> 25$  Hz].

## **Brain Frequency Bands**

### **Delta band [1 - 4 Hz, <4]**

Starting with the Delta band, the delta waves are the slowest brainwaves with the highest amplitude in the range [1 – 4 Hz]. Delta oscillations are found most often during the stage 3 of slow wave sleep (SWS), sometimes also called non-REM. The stronger the delta rhythm, the deeper the sleep. Memory consolidation is very important and is related to cycles of sleep. With the help of EEG monitoring, and with recordings from deep sleep, we can get insights and analyze the depth of sleep or its quality, including sleep disorders, alcoholism and side effects (decrease SWS) and last but not least temporal lobe epilepsy. Sleep disorders and many disruptions are often connected to certain neurological diseases, in patients with Schizophrenia, Parkinson, dementia or epilepsy. In addition, delta waves present more often in the right hemisphere with higher frequencies, and more specifically they come from the thalamus, but they can also present in the cortex.

### **Theta band [4 - 8 Hz, 4-7]**

Brain oscillations within the frequency range 4 – 8 Hz are known as theta waves and belong to the theta band. Theta waves can be detected from all over cortex, including involving frontal, central, parietal areas and medial temporal cortices. Also, in general theta is associated with brain processes underlying mental workload or memory [44]. This is due to the fact that theta frequencies are strongly related with mental operations, such as attention, focus and information processing, learning and recall. Many studies have shown that frontal theta activity is more prominent with increasing level difficulty and challenges. For example, in spatial navigation, in real environments or in virtual reality, theta frequencies and workload have been proved to get stronger in complex levels and mazes or at key landmarks along routes, where the brain needs to be focused the most [45].

### **Alpha band [8 - 12 Hz, 7-12]**

Alpha band, first discovered in 1929 by Burger, is defined within the frequency range

of 8 – 12 Hz, where the oscillations are called alpha waves. Alpha waves correlate to various functions, such as motor and memory. These oscillations are reported to get increased during relaxation and rest states, where eyes are closed. In opposite, when eyes are open, alpha power is reduced, or suppressed, during mental or physical activity. During focused attention and coordination of any stimulus, alpha waves start to decrease and this implies probably intellectual activities or engagement in problem [44], [46]. Social, spatial and semantic attention are related to alpha power and in research for example, there are many experiments showing that with poor performance and distraction, generally alpha power gets higher [47]. Next, in meditation studies, alpha band typically reflects relaxation and sensory inhibition and there are comparisons in states of experienced and inexperienced meditators, that can be differentiated by the alpha [48].

### **Beta band [12- 25 Hz, 12-30]**

Frequency oscillations within the 12 – 25 Hz range are commonly referred to as beta waves. Beta activity is generated in posterior and also in frontal region. Higher beta power is generally known to be correlated with busy, anxious or active thinking, alertness and concentration. Beta power over central cortex (along the motor strip), becomes higher when movements are planned or executed, and particularly when reaching or grasping requires attention and fine finger movements. Moreover, beta frequencies are often monitored during stimulation with extreme stimuli in light or sound, psychostimulants modifying levels of alertness and attentional processing. Also, in studies, clinical populations such as patients suffering from Parkinson's, Multiple Sclerosis (MS) or other neurodegenerative disorders are compared to age-matched healthy controls [49].

### **Gamma band [above 25 Hz, 30-50]**

Gamma frequencies are still considered to be a part of intense research, as the studies have not yet exactly figured out where gamma waves are generated in the brain and what exactly their presence reflects in different cases. Future research has to shed light and address how gamma frequencies affect the brain procedures better in the following years. High frequency oscillations are often called high gamma. Some researchers support that gamma serves as a carrier frequency that connects and binds different sensory impressions and mirrors theta waves (at the engagement and attention phases). Other scientists, argue that gamma is a by-product of other neural processes such as movement of the eye, and because of that they are not related to cognitive procedures.

# Chapter 3 Epilepsy & Epilepsy Surgery

## Introduction to Epilepsy

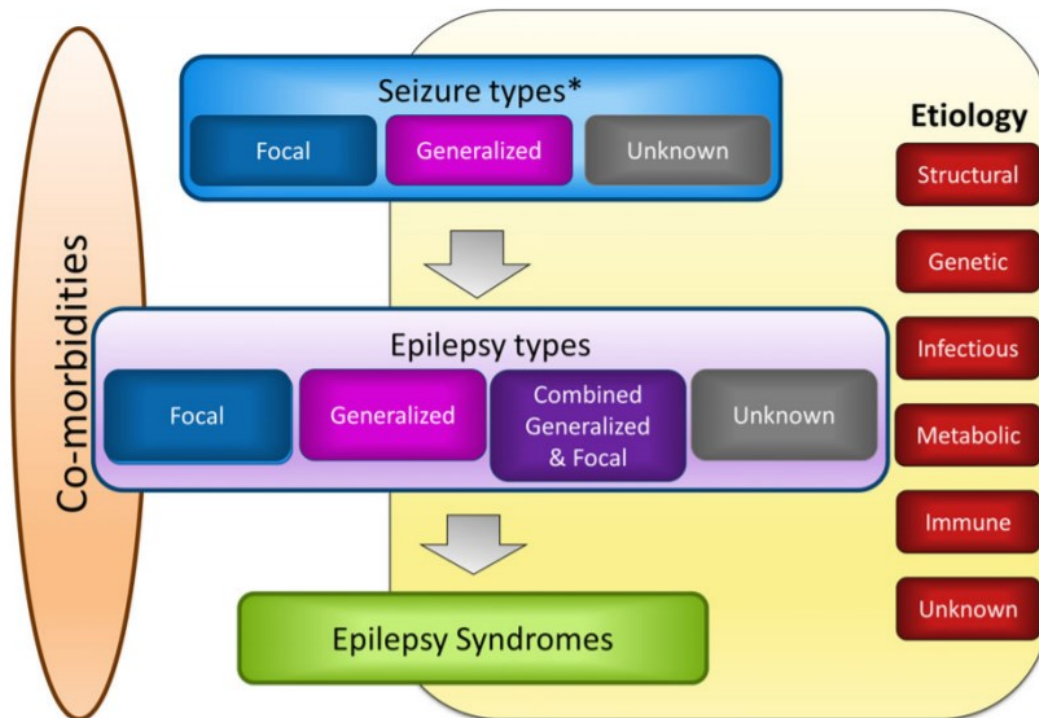
Epilepsy is a diverse brain condition described as a tendency to manifest unprovoked recurrent seizures in cerebral cortical neurons, by systemic or neurologic insults. Epilepsy can start at any age and affect any gender or race, is divided in many different types, and is only diagnosed if clinically there is a high chance that the person could have more than one seizure episode. Epileptic activity is characterized by bursts of uncontrolled electrical activity between nerve cells, sort of like an electrical storm, that can cause temporary abnormalities in behaviors, mental functions, muscle tones or movements, sensations or states of awareness. Anyone can have a one-off seizure and some types of epilepsy last for a limited time before they eventually stop. Nonetheless, for many people on a world-wide scale, with incidence approximately 48/100,000 per year, epilepsy is a serious life-long condition [51]. A seizure could be highly connected with impairment of mental function, disruption of consciousness and disturbance in sensation and movement. Uncontrollable jerking, confusion, losing awareness, sense of fear, collapsing and strange sensations (i.e. *deja-vu*) are some of the most common epilepsy symptoms [52]. In Drug Resistance Epilepsy (DRE), the treatment choices aim to maximize the quality of patients' life, optimize the long-term seizure control, minimize side-effects, maximize adherence and manage co-morbidities. Living with severe symptoms of epilepsy means consequences. These consequences can affect the every day life of a patient including psychological dysfunction, social stigmatization, inability to drive, increased mortality rate. The question that rises here is if the risk of uncontrolled epilepsy outweighs the risk of treatment. It is shown through studies that after ensuring drug-resistant epilepsy, resective surgery is suggested as the best treatment choice. Many different research approaches are ongoing, as with the years they dive more into the causes, treatment, and possible therapies for epilepsy.

## Overview of Epilepsies & Seizures

What makes epilepsy even more complex, is the fact that comes in different syndromes with a broad prism of symptoms which arise from different brain areas [7], [53], [54]. As a result, this disorder can affect people in different ways, but is characterized by the uncontrolled excessive activity of either part or all of the Central Neural System. Formerly, used to be classified into 3 main categories as grand mal epilepsy (generalized tonic-clonic), petit mal epilepsy (absence epilepsy) and focal epilepsy,

based on how the abnormal brain activity is generated. However, the most recent classification of seizures and epilepsies was the International League Against Epilepsy (ILAE), 2017, which was published in March 2017. This new classification lists some new seizure types and is better organized with a clear elucidation of new terminologies.

Figure 10 Framework for classification of the epilepsies. \*Denotes onset of seizure (by Epilepsia ILAE)



In this current classification by ILAE, the clinical features of epilepsy are categorized into these 3 levels: the seizures, the epilepsies, and the epilepsy syndromes. Also, epilepsy is declared now as a disease and a curable one, rather than a neurological disorder. Sometimes it can be resolved after 10 years of being seizure-free with the last 5 years without medications, or the patient for epilepsy syndromes that have to do with age, is not in danger anymore [55]. At the start, the clinician needs to classify according to the type of seizure and then the classification of patient's epilepsy type follows. When epilepsy seizure and epilepsy type is in the same entity, then diagnosis and epilepsy management can be easier, because in epilepsy drugs are used according to the classifications of the seizure types and sometimes they can be more effective.

Seizures based on the onset Zone are classified into **focal onset, generalized onset, and unknown onset**. Sometimes and mostly at the first epileptic seizures, classification according to the seizure type is the first diagnosis, if there are no available imaging diagnostic tools or access. In other cases, there may simply be too little available information for a higher-level diagnosis, such as when a patient has reported

only a single seizure. When a seizure appears to result from abnormal activity in just one area of the brain and affects only a part of the brain, it is called focal (partial) seizure. However, a focal seizure can turn often into a generalized seizure. **Focal seizures** are divided into seizures without loss of consciousness and into seizures with impaired awareness. Simple partial seizures can alter sometimes emotions or change the way a patient looks, feels, tastes or hears (without to lose their consciousness). Other possible symptoms may be involuntary jerking in body parts, such in an arm or leg, spontaneous sensory symptoms such as tingling, dizziness and flashing lights. On the other side, complex partial seizures, involve most of the times loss or at least a change of consciousness or awareness. During such a seizure, the patient may stare into space with no response to the environment or perform abnormal activities and repetitive movements (i.e. chewing, rubbing, swallowing). Status epilepticus consists of a dangerous seizure that lasts at least five minutes or by more seizures that occur without a complete recovery of interictal consciousness between the seizures. This specific kind of seizure is a life-threatening medical emergency that requires immediate medical attention. Not infrequently, the symptoms of a focal seizure may be confused with other brain disorders (migraines and mental illness), that is why testing and thorough examination are considered necessary for a clear diagnosis.

**Generalized seizures** appear to involve all areas of the brain and are further separated into motor (tonic-clonic, clonic, tonic, myoclonic, myoclonic-tonic-clonic, atonic, epileptic spasm) and non-motor (myoclonic, typical, atypical, eyelid myoclonia). Absence seizures, previously known as petit mal seizures, often occur in children and are characterized by staring into space or subtle body movements, such as eye blinking, lip smacking or rhythmic limb movement. These seizures may occur in clusters and cause a brief loss of awareness. Next, clonic seizures are associated with repeated or rhythmic, jerking muscle movements and usually affect the neck, face and arms. Moving on to tonic-clonic seizures, previously known as grand mal seizures, these are the most dramatic type of epileptic seizure and can cause an abrupt loss of consciousness, body stiffening and shaking, and sometimes loss of bladder control or tongue biting. Tonic seizures cause stiffening of your muscles, usually affect muscles in back, arms and legs and may cause a fall. Atonic seizures, also known as drop seizures, cause a loss of muscle control, which may cause a sudden collapse or fall down. Last but not least, myoclonic seizures usually appear as sudden brief jerks or twitches of arms and legs.

As shown in the diagram 10, the epilepsy syndromes are defined by the **epilepsy types**, which in turn are defined by the previously analysed seizure types. Until now, there are no approved ILAE epilepsy syndromes. But normally, syndromes

are defined again by focal and generalized seizures, by etiology, and by whether it is idiopathic or symptomatic. Focal epilepsy is characterized by focal seizures, that could start from any local brain part or deeper structures of brainstem. Most often focal epilepsy has to do with organic lesions from brain injuries, functional abnormalities (for example tumors) or infections. The abnormal electrical activity can spread to adjacent brain areas a few millimetres or centimetres away and then maybe it could become generalized. Generalized epilepsy consists of abnormal discharges throughout all the areas of the cerebral cortex or deep parts of cerebrum and brainstem. General seizures could affect the spinal cord, causing tonic seizures with either sudden or rhythmic muscle contractions. In addition, there is the combined epilepsy type that includes both generalized and focal seizures. Last but not least the unknown type (not yet known) exists and this term declares the patient's epilepsy, but it is not possible to denote (insufficient clinical information or normal EEG) whether it is focal, generalized, or combined focal and generalized.

In the ILAE classification figure 10, one can also notice the entity of comorbidities. Comorbidities range in type and severity (for example learning disabilities, intellectual disabilities, behavioral problems, psychiatric spectrum disorders, cerebral palsy) and are often associated with epilepsies. Just like etiology, it is necessary for every patient, that the presence of comorbidities be considered at each stage of epilepsy classification. These two sections, co-morbidities and etiology, have an important role to raise and increase awareness and to enable early identification, diagnosis, and better management.

### **The Stages of a Seizure**

To every epileptic seizure episode, there are some phases that need to be cleared out and shortly according to Epilepsy Foundation are referred to as **preictal, ictal, interictal and postictal**. Firstly, **preictal** or else prodrome stage, is referred to the time before the actual seizure. Preictal can last from minutes to days and the feeling of this can vary from patient to patient. Not every patient experience something at this stage of a seizure and for those who experience it is considered to be subjective. Approximately 20% of individuals with epilepsy experience this stage [56]. Often, people that experience this stage, describe it as a warning or a strange state. Many people have an aura before a seizure and this realistically may cause nausea, tremor, headache, weird feelings such as confusion, irritability, anger or mood disturbances, a sense of déjà vu or others [57]. Technically, an aura was used to be described as a simple partial seizure and is the earliest epileptiform sign. An aura can remain localized or progress to other brain areas with the person's awareness becoming

impaired to varying degrees. Sometimes, an aura can also spread to both brain hemispheres and then it can become a secondarily generalized seizure within seconds to minutes [58]. That is why sometimes the aura is characterized as an early ictal, for those people with epilepsy that experience it.

Then sometimes follows the middle **ictal** phase, which is basically the actual seizure. During ictal, there will be actual physical changes in the patient's body that again vary from patient to patient, as this is the time that abnormal electrical discharges happen. If the person having the epileptic seizure, happened to be monitored by an EEG system during this phase, a neurologist could see all the cardiovascular and metabolic changes, and determine the point of seizure's origin and as result the type of seizure. This stage is different for every person living with epilepsy and causes a variety of symptoms. Some of these symptoms include memory lapses, drooling, twitching, eye or head movement in one direction, inability to respond and to control the bladder or the bowel, pupil dilation, tremors, vision loss or blurring, hearing loss, difficulty breathing, chewing or lip-smacking, arm or leg stiffening.

Moving on to the next stage, **interictal** is the time between seizures. A lot of people, including more than half of all people with Temporal Lobe Epilepsy, have recurrent seizures and suffer from emotional disturbances between them. The effects of interictal stage range from mild fear to pathological levels of anxiety and depression. Sadly, anxiety disorders, interictal panic attacks and depression that are by far the most common in relevant epilepsy types, are in cases difficult to be controlled.

At last, the **postictal** or co-interictal, is the final phase and is described as the recovery period after an epileptic episode. In most cases can last from 5 to 30 minutes, but it can also last hours (or days) and vary quite a bit, partly depending on the intensity, duration and severity of the seizure, as well as the specific seizure type itself (brain region affected). Quite often, many people cannot remember anything that happened during the seizure. Among other things, postictal might leave the person feeling tired and/or bewildered, confused, with hypertension, nausea, drowsiness, headache or migraine, body soreness, an agitated behavior or altered consciousness and other disorienting symptoms. Sometimes symptoms from this phase can help doctors diagnose the starting origin of the seizure, too.

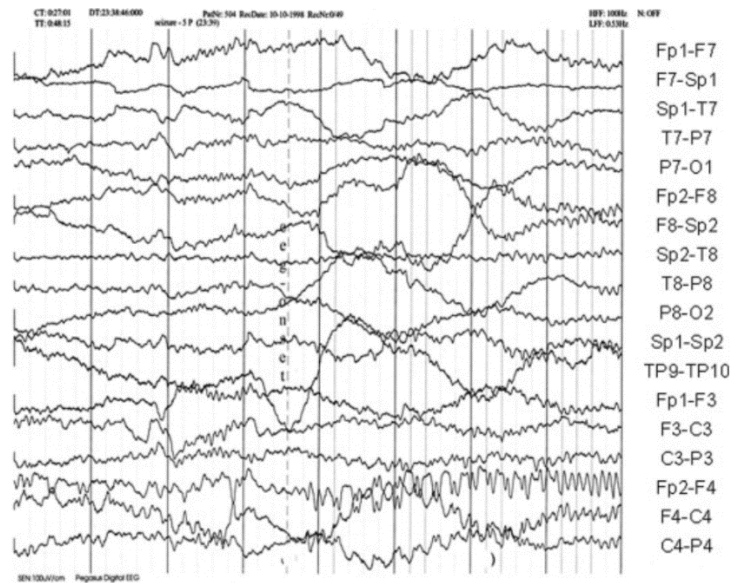


*Figure 12.1.1 – Ictal electroencephalogram showing a regional right frontal seizure discharge (maximum at electrode F4) in a patient with right-sided lateral frontal lobe epilepsy. Source by Handbook of Clinical Neurology, 2012 Christoph Baumgartner, Susanne Pirker*

## Epilepsy Diagnosis and Imaging Techniques

May epilepsy be one of the most common brain conditions and highly correlated with unpredicted seizures, but there are also other disorders that can be confused with epilepsy. For that reason, accurate epilepsy diagnosis is critical and requires many thorough steps of testing and examination. The evaluation includes a neurological exam, blood tests and tests to monitor and detect possible brain abnormalities. A neurological exam by a neurologist, includes questions about medical history (e.g. indication of hereditary predisposition or triggers by psychological problems) and neurological tests for behavior, senses (sensory testing), cranial nerves, motor abilities (muscle function), mental status and functions (memory tests, simple math calculations), coordination (walking in a straight line), reflexes (knee jerk, plantar reflex to test abnormalities in the voluntary control of muscles), gait and station. After that, the neurologist often gathers and suggests additional information such as blood tests (for example shortly after an epileptic seizure, increased levels of prolactin can be detected in blood or low glucose levels) and imaging tests.

The main goal of these brain imaging tests, are to monitor and detect brain abnormalities and to determine problematic areas. One can record brain abnormalities, with electrodes attached on the scalp that are able to capture electric activity from deep structures of the brain with high temporal resolution. So as to increase the levels of certainty and accuracy of the medical report, doctors often combine EEG/MEG with MRI scans, called Magnetic Resonance Imaging (MRI) and functional MRI that have high spatial resolution. These brain scans can further

facilitate, since they could find brain regions with lesions or injuries that could possibly trigger brain abnormalities or seizures. In many cases, the doctor could also order a computed tomography (CT) scan of the brain or a Positron Emission Tomography (PET) to identify areas that maybe are indicative epileptic postictal markers. The PET scan is more supplementary to the scan results of Single Photon Emission Computed Tomography (SPECT).

## FMRI

Functional magnetic resonance imaging, or f-MRI, is one of the most widely known technology for recording neural activity, by detecting changes on brain regions associated with blood flow and not by recording the neurons' activity. More precisely, the active regions require more oxygenated blood, and so despite being indirect, fMRI allows scientists to infer activity patterns of neurons. When a brain area is more active, then it consumes more oxygen and to meet this increased demand, blood flow increases to the active area. FMRI can produce activation maps showing which parts of the brain are involved in a particular mental process, it is non-invasive, doesn't involve radiation, it has high spatial resolution, but not the high temporal resolution of an EEG [59]. Therefore, this neuroimaging technique has become a stable of neuroscience research the last decades, even though it does have some significant limitations, that scientists continue to research ways to surpass and improve for example the spatial and temporal resolution. Connecting f-MRI to epilepsy, some major applications include the localization of task-correlated language and memory function, the localization of ictal and paroxysmal phenomena and presurgical planning for the localization of epileptic brain functions [60]. FMRI provides comparable results to intracarotid amobarbital testing, in language lateralization and promising memory lateralization[6], [61].

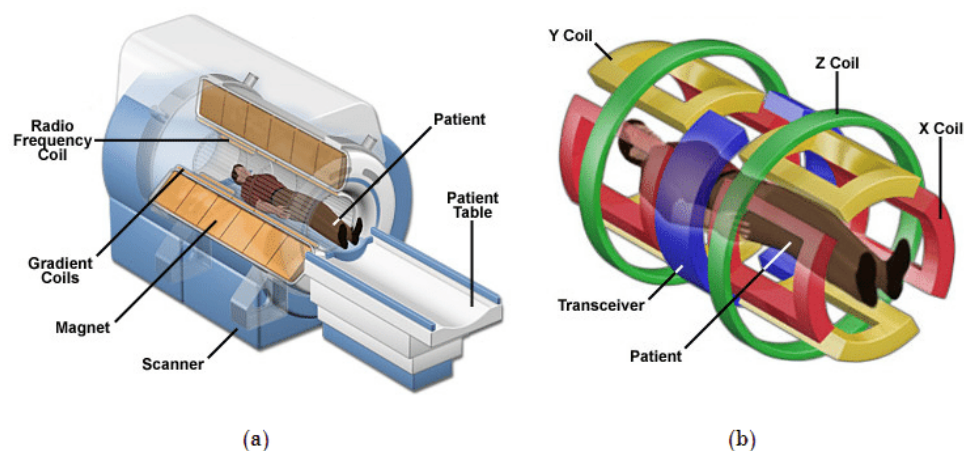


Figure 12.1.1 – (a) MRI Scanner Cutaway (b) MRI Scanner Gradient Magnets (MRI: A Guided Tour, 2015)

### **Computed Tomography (CT)**

Computed Tomography or else CT is a technique based on the measured attenuation of X-rays with uniform and specific energies, that are emitted by an external source beam [62]. The emitter and the detector both placed on the opposite site, rotate around the patient during scanning. Given the known attenuation coefficient of tissues in the body, 3-dimensional anatomical images can be constructed [63]. Each time the X-ray source completes one full rotation, the CT computer constructs a 2D image slice of the patient. The thickness of the tissue that is presented in each image slice can vary depending on the CT scanner with an average range of 1-10 millimeters. After a full slice is shaped, then the motorized bed is moved forward incrementally into the gantry for the process to continue for another slice, until we reach to the desired slices.

### **Positron emission tomography (PET)**

Position Emission Tomography or else PET is a nuclear imaging technique based on gamma rays caused by decaying radionuclides that are inside the body. With this brain imaging technique, one can monitor metabolic activity like glucose levels of neurons during cognitive activity. In a PET scan, the patient lies on a table that slides into the middle of the scanner and receives a short half-lived radiopharmaceutical (produced by a cyclotron) and the most widely used radiopharmaceutical is called FDG [5], [64]. In addition, because FDG is a positron-emitting compound and does not stay 'alive' for a long time, radiation exposure is from several chest rays. As the positrons encounter electrons within the body, gamma rays are produced. FDG-PET is most commonly used in oncology, cardiology or in neurology to diagnose various neurological conditions and disorders. Within the PET scanner, rings of detectors containing special crystals produce light when they are struck by a gamma ray [64]. The electronics of the scanner record detected gamma rays and map an image of the area, where the radiopharmaceutical has stayed. The radiopharmaceutical contains a chemical commonly used by the body as glucose and PET enables to see the location of these metabolic processes. For example, we can see if we combine a radioisotope with glucose, where glucose is used in the brain the most, the heart muscle or in a tumor.

It is also important to be noted, that while PET scans are more robust towards artifacts, they do not have the high time resolution of EEG. In contrast with CT and MRI, PET shows metabolic activity or function and physiology [5]. In hybrid PET/CT scanners, the density map based on the CT allows to result in increased image quality [65]. Finally, SPECT scanner integrates CT and a radioactive tracer, has a similar use to PET and offers accurate localization in 3D space.

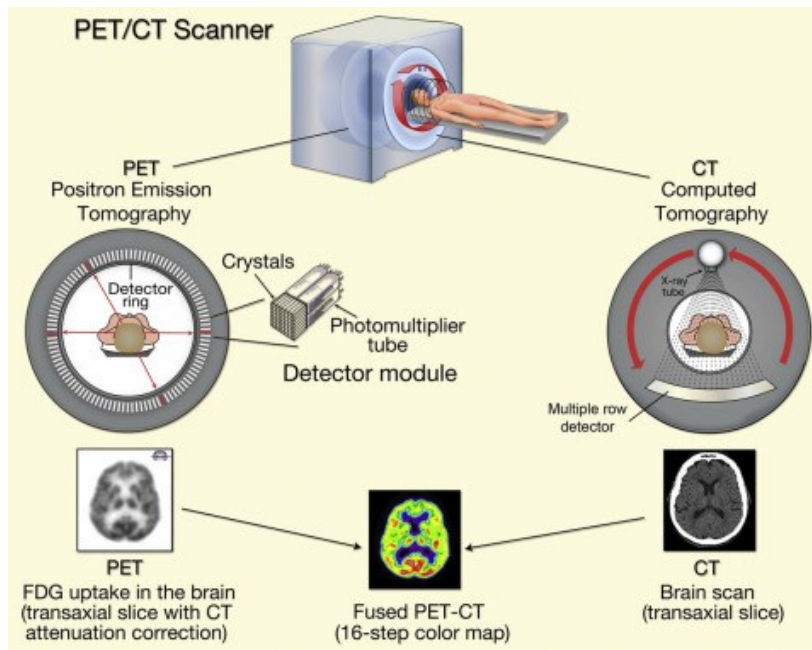


Figure 11 A combination of the PET and CT imaging systems for anatomic imaging [66]

### Electroencephalography (EEG)

One of the most important brain imaging technology until today, that first applied to humans by neurologist Hans Burger (Jung & Berger,1979), is called EEG or else electroencephalography. Electrical brain activity was at first attempted to be recorded by using galvanometers. This technology consists the ancestor of modern EEG, since the galvanometers led to the invention of electrometers and consequently of the electrodes. Proceeding to the digital era and moving from paper to digital data, scientists decided to transform EEG signals in digital form and analyze, interpret and process it with higher computing power. The digitization procedure for the EEG, requires sampling, quantization, encoding devices and signal processing tools embedded in the computer systems. The bandwidth of EEG is limited to 100 Hz thus 200 samples per second (according to Nyquist criterion) but in some applications it is feasible to record even at 2000 samples per second. In modern EEG setups the representation of each sample is performed with 16 bits maintaining thus the diagnostic information in an accurate and high level.

Nowadays, the most common systems for EEG placement have been provided by the American Encephalographic Society (10-20 system) and Oostenveld & Praamstra (10-5 system). In the **10-20 system**, electrodes are placed according to the name at 10% and 20% along the longitude and latitude lines[67]. Nasion referred as Nz is marked between the eyes at the top of the nose and Inion referred as Iz is marked at the back of the head. Often the measurement is taken across the top of the head,

from Nz to Iz. Also other important parts are the left and right pre-auricular points that can be felt by the fingers as depressions just anterior to the ears when the mouth is open and closed. The vertical line that connects Nz and Iz, as well as the horizontal line connecting left and right pre-auricular points, is divided into ten equal sections. Moreover, in the 10-20 system, electrode names derive from their location and begin with one or two letters, due to their placement in the brain regions (Fp = pre-frontal, F = frontal, P = parietal, O = occipital, T = temporal, C = central). Each electrode name has a number or letter at the end of the word, indicating the distance to the midline. Also, odd numbers are for the left hemisphere and even for the right. The electrode placement at the midline is labeled with the letter Z from zero. The larger are the numbers, the greater distances they indicate from the midline. For example in the following representation of the system, the electrode labeled as Fz is placed in the Frontal lobe over the midline and the electrode labeled as T6 is placed in the Temporal lobe over the right hemisphere and farther from the midline.

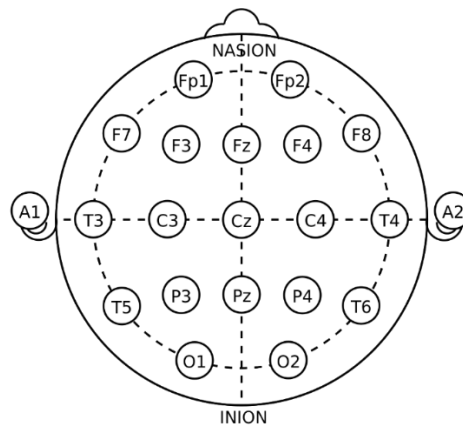


Figure 12 The 10-20 system in EEG (Source: Wikipedia)

EEG recordings are particularly well-suited to studies that examine functional or effective connectivity and research, where high temporal resolution is essential [68]. EEG is used to record electrical brain activity in a non-invasive way and is also a painless recording technique. EEG practitioners, simply place carefully at the scalp surface the EEG electrodes and record. Although, there are cases, where invasive electroencephalography, that requires craniotomy for the placing of sensors, cannot be avoided (intracranial EEG). One of the most significant benefits of EEG technique, is its high time resolution that can take hundreds to thousands of snapshots from multiple electrodes (ranging from 10 to 500+ electrodes depending on the experiment), within a single second. Since the electrical brain signals are small, the recorded data is digitized and sent to an amplifier. Once the data amplification is finished, EEG record can be displayed as a time series of voltage values. EEG Channels are the digital signals recorded by the amplifiers and is important to distinguish them

from the sensors (electrodes). Channels consist of two electrodes whose activity is referenced to another more distant electrode to form the signal (referential montages). Some things that are important for an EEG system are the number and quality of the electrodes, the digitization and sampling rate of the amplifier and as a consequence, the quality of the final recording.

Regardless of whether it's neural activity, the applauding of a group or an earthquake, these phenomena happen due to synchronization of wave patterns. If postsynaptic potentials happen simultaneously, rhythmically and in synchrony for countless neurons, then, at some point, they summarize, tune and produce an electric field, which is quickly continued through cerebrum tissue and the skull. In the end, one can measure it from the scalp. This is very similar to an audience that starts to applaud. At first every individual in the crowd applauds in their own way, making white noise. After a brief time, the crowd gets synchronized by applauding with the same rhythm. This synchronized applauding is a lot stronger than the repetitive sound

This is very similar to an audience that starts to applaud. At first every person in the audience claps with their own rhythm, causing white noise, without any observable rhythmic pattern. After a short while, however, the audience gets in sync (clapping in the same rhythm). This synchronized clapping is much louder than the white noise [67], [69], [70].

### **Magnetoencephalography (MEG)**

In 1972 David Cohen developed a new modality for measuring the brain activity, by means of detecting magnetic fields generated by neural currents, that is known as Magnetoencephalography (MEG). MEG has some advantages over both EEG and fMRI. More specifically, MEG has a very high temporal resolution, a good spatial resolution and often captures much better than EEG (deeper). Furthermore, MEG is housed inside a magnetically room, to attenuate the external magnetic noise and MEG fields pass through the head without any distortion. This is a significant advantage of MEG over electroencephalography. fMRI signals compared to MEG, reflect indirectly the brain activity by measuring the oxygenation of blood flow near the active neurons. Magnetoencephalography is most sensitive to activity originating in sulci, provides temporal brain characteristics much more precisely (in the range of sub milliseconds), whereas fMRI performs poorly in temporal information. Lastly, MEG scanners (require superconducting quantum interference sensors – SQUID) are large, stationary and very expensive, as their range is of femto-tesla to pico-tesla. They also require heavy technical maintenance and training resources. Connecting MEG with epilepsy condition and epilepsy surgery, this technique could be useful in detecting

where the seizures were generated and showing the exact location or in mapping of the functioning areas near lesions, such as tumors and as a result help in resective surgery. For patients who had undergone surgery, MEG could show if a further surgery is required, providing the required information easily and non-invasively. Summing up, EEG has a spatial resolution of centimeters and limited below cortical surface, fMRI has a spatial resolution of millimeters and is not limited to cortical areas, whereas MEG has a spatial resolution of millimeters at cortex, but is less precise for deep sources.

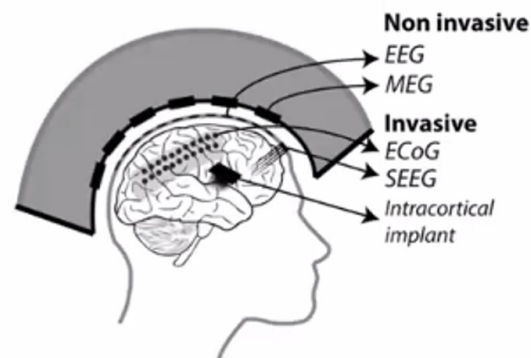


Figure 13 Comparison of Invasive and Non-Invasive Techniques

## Patient 14

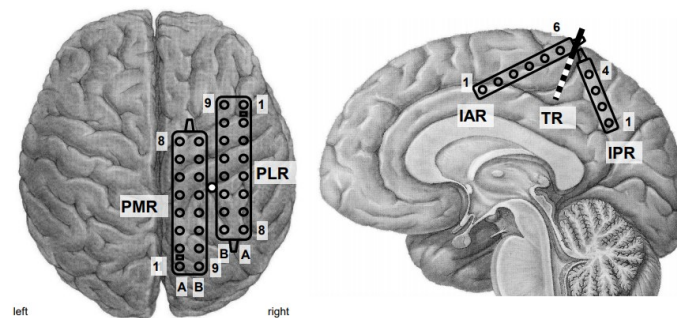


Figure 14 Example of ECoG, electrode placement on patient 14 in our dataset. One can see that on the cortical surface are placed after craniotomy a combination of subdural strips, grids and one depth electrode. The electrode placement is according to the findings of the non-invasive presurgical evaluation.

### Electrocorticography (ECoG)

Almost similar to EEG's way of working, Electrocorticography (ECoG) measures the combined oscillatory activity of millions of neurons, but with a significant difference. In contrast with EEG, ECoG is invasive, requires insertion of the electrode array under the scalp, and therefore requires craniotomy. For this reason, ECoG is only

suitable for patients already scheduled to undergo surgery that involves craniotomy. In addition, ECoG gives significantly improved localization of the activity source, as well as the recording of higher frequency electrical activity. Both of these advantages of ECoG are key factors to presurgical epilepsy evaluation. ECoG is considered to be the best way of assessing the abnormalities in refractory epilepsy, is established in presurgical planning, and plays an important part in surgical guidance.

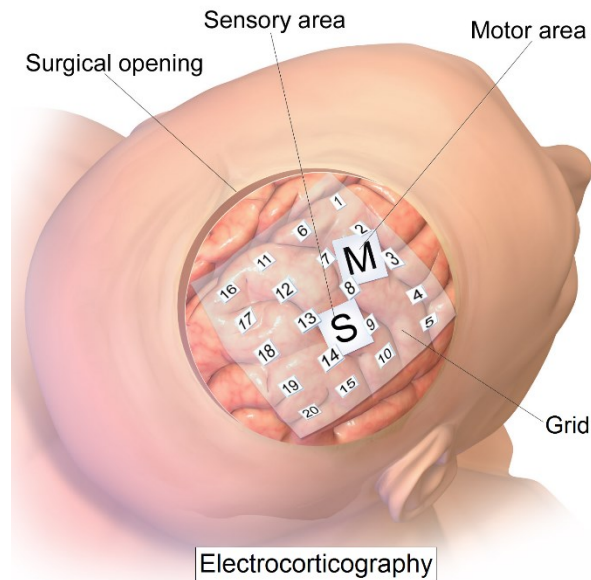


Figure 15 Invasive ECoG records electrical activity from the cerebral cortex, Source: Wikipedia

The invasive method mentioned above can be performed either *during surgery*, called **intraoperative ECoG**, or *outside of surgery*, called **extraoperative ECoG**. In epilepsy surgery, the goal is to remove the epileptogenic tissue without causing neurological damage to other brain structures. For that reason, the precise identification and localization of the Epileptogenic Zone plays a critical role in the surgical outcome. ECoG is often combined with a functional cortical simulation mapping tool, also known as Direct Cortical Electrical Simulation (DCES), in order to preserve the functional areas of the patient safe. Functional mapping allows the patient to interact with the surgeons, therefore he is under local anesthesia rather than general. Important functional areas (eloquent cortex) include sensory processing, speech, motor coordination and somatosensory integration. During surgery, the implanted electrodes can monitor the epileptic activity of the tissue and aid the surgeons to ensure that the pathological region is resected. Sometimes though, additional surgeries may be necessary to completely eradicate epileptic activity and eliminate seizures. As for the extraoperative ECoG, it is considered again after ensuring that the patient needs to undergo epilepsy surgery (and as a result skull opening). First, an MRI is performed to demonstrate where is the abnormal epileptogenic lesion, in combination and support by EEG recordings and pathological evidence. Once the epileptogenic

lesion has been identified, then extraoperative ECoG may be applied to determine more precisely the location and extent of the lesion in relation with the other indicators of the EZ. The traditional scalp-EEG in this case is not precise enough to provide sufficient data for the localization of the epileptogenic tissue. Additionally, extraoperative ECoG is used to localize important functional areas, vital to be preserved during epilepsy surgery[71].

In the last decades, combined with neuroimaging and computational tools, human electrocorticography has become increasingly more amenable for research studies and its popularity trend among neuroscientists is on a steady rise[72]. ECoG data can provide guidance and insights that no other non-invasive technique can offer in intractable epilepsy.

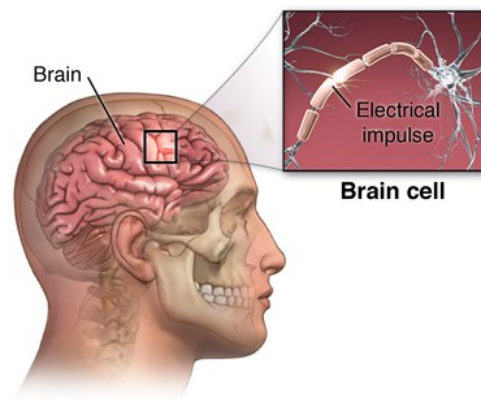


Figure 16 Abnormal Electrical Activity (Source: Johns Hopkins Medicine)

## Epileptic Activity and Abnormal Waveforms

Epileptic seizures are often unpredictable and appear frequently or at specific patterns, that are still being investigated. In any EEG recording is highly important to be able to detect the abnormal waveforms, which include epileptiform and non-epileptiform abnormalities. If we want to identify abnormal waveforms in EEG and recognize artifacts, a basic understanding of the normal EEG patterns and benign variants in various physiological states and in a variety of adults and children, is needed.

### Interictal Spikes

Clinical epileptic seizures contain often only a small proportion of all the brain abnormalities, which includes subclinical seizures, interictal spikes, bursts and high-frequency oscillations. **Interictal spikes** are actually the bursts from a group of neurons that had synchronized and results in an electrical paroxysmal discharge. The

spikes are very brief and fast waves, and are generated by the synchronous discharges of a group of neurons in a region called **epileptic focus**. Their name comes from their shape on the encephalography, where they really stand out comparing to other marks and shapes. Each spike normally lasts less than 80ms and are often followed by slow delta waves. Sometimes, sharp waves can also be seen in recordings and these happen over 80-200 milliseconds. Not all interictal spikes or sharp waves are associated with seizures. These spikes associated with epilepsy, known also as Interictal Epileptiform Discharges (IED) are used to diagnose epilepsy, localize the EZ and provide a further insight on the epileptic pathological areas.

### **Evoked/Event -Related Potentials and Fields**

ERPs or Event related potentials measured by means of electroencephalography (EEG), are actually small fluctuations as direct response to a stimulus (of a specific sensory, cognitive or motor event). The magnetoencephalography's equivalent of ERP is called event-related field or else ERF. The evoked potentials and induced potentials are subtypes of ERP's. In more detail, evoked potentials (EP) are an electrical triggered potential in following a stimulus recorded/seen in spontaneous EEG and is not time-locked to the event. So, the primary derivatives of the traditional, non-invasive scalp EEG are evoked potentials and event-related potentials. Time-locked/event-related potentials (ERP) are measured by brain responses that are a direct result of stimulus presentation and are time-locked to the event. In general, ERPs provide a noninvasive way to evaluate brain functionality and are useful for checking the sensory pathways and for detecting brain dysfunctions or abnormalities. Regarding the Event Related Fields (ERFs) they share the same principles with the ERPs, but the difference is on the record of summed postsynaptic magnetic fields, which serve complementary to the ERPs for the diagnostic tests.

### **High Frequency Oscillations (HFO)**

In recent years, with the high manufacturing electrophysiological systems and setups, the recording of electrical potentials with high spatiotemporal resolution is possible. After the gamma band, there are even higher in frequency brain waves, faster than ~80 Hz, and they are generated by neuronal cells. In older studies, researchers used to refer to these oscillations as high gamma or just high frequency oscillations. Nowadays, high frequency oscillations or else HFO have become a new promising biomarker of epileptogenic zone and are also associated in many studies with pathophysiology of the brain, psychiatric disorders and psychotic episodes, such as in schizophrenia.

High Frequency Oscillations are actually brain signals with sinusoidal-like

morphology of high frequency (>80 Hz), recorded by EEG or ECOG due to the transient local field potential -LFP. HFO studies and definitions vary, but shortly in most cases HFOs have a frequency range of 80-500 Hz and are classified into two subtypes, Ripples (80-250 Hz) and Fast Ripples (250-500 Hz). There are also some sub-bands that are often called low gamma band (30-80 Hz), high gamma band (80-150 Hz) that overlaps with the Ripple band and some recent epilepsy studies have also named oscillations >600 Hz as very high frequency oscillations (VHFO). VHFOs are further classified into very-fast ripples (500-1000 Hz) and ultra-fast Ripples (1000-2000 Hz)[73].

Pathological High Frequency Oscillations are arguably one of the strongest candidates that marks neuronal hyperexcitability [28], [74], [75]. They are considered to be generated in the seizure onset zone (SOZ), or in the first-propagation zone. Analysis of HFOs may accelerate the identification and narrow down the location of the seizure-onset area compared to the routine EEG analysis of interictal and ictal epileptic activities. While physiological HFOs maybe express the summated synchronous inhibitory postsynaptic potentials (IPSP) generated by interneuronal cell subpopulations and their discharges, epileptic pathological HFOs might reflect the field potentials which are formed by the activity from clusters with bursting pyramidal cells, generating population spikes, and decreased inhibitory interneuron firing. For this reason, pathological HFOs may be a new biomarker of SOZ [76].

However, there is up to no “uniform definition” of pathological HFOs. Even though HFOs have been discovered more than two decades ago, there are still many questions about their biomarker-utility in clinical practice and about their relationship with the epileptogenic zone. Until now, multiple studies and approaches have been sought to distinguish non-pathological and pathological HFOs. The nature of the problem lies in the overlapping frequency range that these two types of HFOs can occur. In terms of duration, amplitude, and frequency, there exists a large overlap between physiological and pathological ripples found in normal and in epileptic conditions. In severe cases of epilepsy, HFOs is considered to be an important interictal indicator of focal epileptogenic zones and have been also used to localize such areas clinically [59], [60]. It is worth highlighting, that the removal of HFO-generating areas led to improved surgical outcomes [77]–[79] [80] [81]. Thus, HFOs seem to be reasonably suitable markers of the epileptogenic zone. Potentially HFOs can be investigated as biomarkers to mark and predict the epileptogenesis, to link the severity of epilepsy, to predict the occurrence of seizures, and to evaluate the outcome of a medical or surgical treatment.

Many studies have analyzed the relationship between the SOZ and HFO

occurrence and the correlation between removal of HFO generating tissue and postsurgical seizure freedom. Without doubt, HFOs have been proved useful to delineate the SOZ -seizure onset zone and to validate the application of excitability. However, some studies cast also some doubt on the precision with which HFO can delineate the epileptic tissue [82]. In order to provide broadly applicable, clinically useful predictors, non-invasive recording techniques would have to be established. For example, the use of HFO biomarkers in conjunction with behavioral state, and/or other EEG biomarkers such as interictal spikes, may combined together prove to be useful to optimize the predictive efficacy of HFOs [14]. In addition, high-sampling rate MEG systems might constitute a promising candidate method to test the validity of HFOs as biomarkers in human epilepsy [83], [84]. Up to now, HFO analysis is not included in the clinical practice as a part of presurgical evaluation.

## Epilepsy Treatment

After a concrete epilepsy diagnosis, epilepsy treatment follows and addresses different ways of enhancing the patient's quality of life, by eliminating seizures and abnormalities. The key choices of treating epilepsy can be listed as follows: Anti-Epileptic Drugs (AED), Vagus Nerve Stimulation, Ketogenic Diet, Epilepsy Surgery and Deep Brain Stimulation (DBS) [54], [12], [37]. The anti-epileptic drugs are modifying chemicals for the brain excessive electrical activity, that can reduce the number of seizures and in many cases even eliminate them (according to studies, AEDs control seizures in about 70% of the cases when taken strictly as prescribed). It is worth-noting that drugs do not cure epilepsy, but they can often control seizures efficiently. Vagus Nerve Stimulation is a procedure that includes a device implantation, that stimulates vagus nerves with electrical impulses and helps to prevent seizures. This specific device is surgically placed under the skin on the chest and electrically stimulates the nerves that run through the neck, preventing irregular electrical activity. Nevertheless, it requires maintenance and is also an expensive invasive method, which renders it as a second choice. Ketogenic Diet is a high fat, low carbohydrate protein diet, suitable mostly for limited seizure types (mostly myoclonic seizures) and more than half of patients that fail to be treated by medication benefit from it. During this diet, the body is forced to use fat for energy instead of glucose, a process called ketosis. Last but not least, deep brain stimulation (DBS) may be used as a surgical treatment (electrode implantation), for drug-resistant patients that cannot have resective epilepsy surgery. Now if medication can't decrease the number of seizures, surgery is the next option, especially in severe cases with brain-tumors or injuries. Resective epilepsy surgery

involves removing the part of the brain where seizures originate. One surgical plan for example is the resection of the temporal lobe, in a procedure known as temporal lobectomy, and often can be very effective leading to seizure freedom. After surgery, some people are able to cut down on AEDs and increase a lot their life quality. Although, there are risks to any surgery, including a bad reaction to anesthesia, bleeding, infection or cognitive changes.

### **Epilepsy Surgery**

According to Epilepsy Foundation, at least 30-40% of people with epilepsy continue to have seizures despite optimal treatment with AED. Only 44% of people taking seizure medications reported being seizure-free, so that leads to the option of surgery as a way of controlling the seizures. Epilepsy Surgery is applied to eliminate the seizures to drug-resistant patients and there is a good medical evidence of its effectiveness and safety. By taking out the seizure foci in the brain, epilepsy surgery can, in most cases, successfully and safely reduce or stop seizures. Around 70% of people, who have temporal lobe surgery become seizure-free, and for a further 20% their seizures are reduced. Around 50% of people, who have temporal lobe surgery are still seizure-free 10 years after their surgery, but most of these people will still take their Anti-Seizure Medication (ASM) for some time. If the seizures cannot be controlled and after adequate trials of different medication (two or three), then surgery evaluation should be brought early to the table [81].

There are many different types of epilepsy surgery, which involve either the resection of tissues associated with epileptogenesis (resective surgery) or with pathways to treat seizures focal or generalized. Technology has improved tremendously the ability to detect where seizures begin in the brain. The ultimate goal is to split the connection pathway between the hemispheres to cut down the flow of abnormal activity from one part to another. A significant step of the overall evaluation by the neurosurgeons, is the presurgical evaluation, which aims at detecting the actual region of epileptogenesis, using intracranial electrodes with craniotomy, invasive ECoG. Of course, EEG or MEG tests precede, give the first insights and guide the next steps for future operation. Some of the different surgeries for different epilepsies, include Focal Resection that is branched into Temporal Lobe and Extratemporal Resection (frontal, parietal and occipital), Laser Interstitial Thermal Therapy, Multiple Subpial Transections, Lesionectomy, Corpus Callosotomy, Anatomical or Functional Hemispherectomy, Stereotactic Radiosurgery and Neurostimulation Device Implantations (Vagus Nerve Stimulation-VNS, Responsive Neurostimulation-RNS and Deep Brain Stimulation-DBS). The brain surgery for epilepsy, aims at removing the epileptic foci by stopping

the abnormal activity, while preserving at the same time the vital eloquent cortex. Neurologists call eloquent cortex, the brain regions that if resected will cause severe neurological damage, such as paralysis, loss of linguistic ability or loss of somatosensory processing.

One essential part to mention for this research work, is the predefined and modified from the ILAE classification outcome in respect to the epileptic seizures following epilepsy surgery [85]. According to ILAE, there are 6 different postsurgical outcomes, where starting from ILAE 1 is the completely seizure-free outcome with no auras. ILAE 2 includes only auras and no other seizures after surgery. Moving on to worse outcomes, ILAE 3 and further, where there are still seizures after surgery and the patient can have from one to three seizure days per year, including or not auras if is classified with ILAE 3. The worst outcomes after surgery can be ILAE 5 or 6 where the patients can have daily seizures or auras or even worse, more than 100% increase of baseline seizures or auras daily. Surgery outcomes with patients still suffering from recurrent disabling seizures (with no seizure reduction), are typically considered as failures. Consequently, re-evaluation and re-operation may be considered, in a selected group of patients with an unfavorable postsurgical outcome.

OUTCOME CLASS ILAE	CONTROL OF SEIZURES
1	Completely seizure free (no auras)
2	Only auras; no other seizures
3	One to three seizure days per year (+auras)
4	Four to 12 seizure days per year (+auras)
5	Daily seizures (+auras)
6	More than 100% increase of baseline seizure days (+auras)

*Figure 17 Epilepsy outcome classification according to ILAE classification with respect to epileptic seizures following epilepsy surgery*

As the surgical success rate rises, there are two epilepsy types worth mentioning, as they are often associated with surgical treatment, when there is also in the table drug-resistancy. The patients of this thesis iEEG study have also these types of epilepsy, were drug-resistant and all underwent surgery epilepsy. The two types of epilepsy are called Temporal Lobe Epilepsy and Extratemporal Lobe Epilepsy and are presented in more detail below:

### **Temporal Lobe Epilepsy (TLE)**

TLE or else Temporal Lobe Epilepsy is the most common form of focal epilepsy, characterized by recurrent, unprovoked focal seizures that originate in the temporal lobe of the brain, and usually last about one or two minutes[86], [87]. Focal Seizures in TLE start or involve in one or both temporal lobes in the brain. Shortly, there are two types of TLE, the Mesial temporal lobe epilepsy (MTLE), that involves the medial or internal structures of the temporal lobe and the neocortical or lateral temporal lobe epilepsy that involves the outer part of the temporal lobe. In the MTLE epilepsy, that accounts for almost 80% of all the temporal lobe seizures, seizures often begin in the hippocampus or in its surrounding area. Most of the time the cause of TLE is unknown and some possible causes may be previous prolonged febrile seizures brain injuries or head traumas. aware seizures, such as auras and focal impaired awareness seizures. MTLE is often associated with abnormalities on MRI scans. One of the most common MRI findings is scarring in the temporal lobe and is called hippocampal sclerosis. It may look like the hippocampus on one side, or both, has shrunk or is smaller. When the MRI is abnormal, seizures often do not stop with anti-epileptic drugs. In this case, epilepsy surgery is the next best option for many patients.

### **Extratemporal Lobe Epilepsy (ETE or ETLE)**

Another important and more diverse seizure type is called Extratemporal Lobe Epilepsy, characterized by its extratemporal seizures, namely seizures that can happen outside of the temporal lobe, originating in the parietal, frontal or occipital lobes, or even more than one lobe. They have a wide spectrum of semiological presentation depending on the site of origin and they can be further divided and analyzed. Often when extratemporal seizures happen in more than one lobe, then extratemporal cortical resection is a surgery approach to resect, or cut away, brain tissue that contains the seizure focus.

### **Epileptogenic Zone (EZ) in Epilepsy Surgery**

The epileptogenic zone (EZ) is a theoretical construct defined as the minimum amount of cortex to produce seizure freedom and consists of five conceptual cortical abnormal 'zones': symptomatogenic, irritative, seizure-onset, structurally abnormal (epileptogenic lesion) and functional deficit. A successful epilepsy surgery requires a comprehensive preoperative evaluation for the definition of the Epileptogenic Zone. Shortly, EZ is the area of the cortex responsible for the generation of habitual seizures and ideally should be resected in order to achieve seizure freedom. However, there is no diagnostic modality able to unambiguously delineate this zone and the surgery's objective strongly requires a precise and successful identification and delineation of it

[13]. Until now, the only way to evaluate the epilepsy surgery is by examining the postsurgical outcome. If after surgery, the patient is seizure free with minimal or no functional deficits, then that means the EZ has been correctly identified and resected with no damage to the functionally relevant eloquent cortex. Because of its importance, there is still active research for the establishment of EZ markers that can precisely determine it. Some of the indicators of the EZ are the following cortical zones, that can estimate the EZ through diagnostic tests and systemic examination.

Starting with the **Seizure Onset Zone** or else **SOZ**, it is the area of the cortex from which clinical seizures are generated. SOZ is considered to be the best clinical estimate of EZ that doctors can give, and it is removed in the majority of surgeries, as opposed to the actual epileptogenic zone which can be evaluated only post-surgically. Nevertheless, the seizure onset zone is also a zone difficult to identify because of the clinical seizures' nature. Clinical seizures are unpredictable and often difficult to be monitored and captured completely in EEG recordings. Because of all these, the identification of the entire SOZ is not often precise, deviates from EZ and its removal still leads to a significant percentage of unsuccessful surgical outcomes. To sum up, SOZ and EZ are regarded as two different concepts and in some cases the full resection of actual SOZ does not lead to seizure-freedom, in contrast with the EZ where its full resection always leads to seizure-freedom.

Another important zone for the estimation of the EZ is the **Irritative Zone (IZ)**, which is defined by the localization of interictal epileptiform discharges or else IEDs (known as spikes) that occur more frequently than seizures. The manifestation of IEDs can be detrimental to cognitive function in epilepsy syndromes [88], [89]. The big advantage of the IZ is that it can be evaluated during the interictal period independently from the occurrence of seizures. This reduces the recording time, the associated cost and the discomfort of patients. Nevertheless, the irritative zone is often more widespread than the actual EZ, and for that reason is proved to be less specific [90]. Respectively, because in IZ there are IEDs or else spikes, spikes are proved to be less specific than HFOs in HFO Zone. Furthermore, the presence of an epileptogenic lesion close to the irritative zone or the SOZ provides an additional marker. Finally, Functional Deficit Zone (FDZ) is the area of the cortex with a normal functionality between seizures. This zone can be defined by a number of examinations and testings, such as neurological and neuropsychological examination and functional neuroimaging such as SPECT and PET.

Last but not least, **High Frequency Oscillation Zone**, which is our target zone of interest has been recently added in the research scope. From the figure 17 we can observe a clear correlation between the occurrence of HFO zone and the SOZ, as it is

been proved in many cases. In multiple studies it has been proved, that there is a spatial association of HFO with EZ. Some of the studies have also shown that the resection of the tissue generating HFO may help presurgical diagnosis and improve the surgical outcomes of drug-resistant patients. Despite all that, it remains challenging to translate HFOs as epileptogenic biomarkers into the clinical routine. One of the major problems that remains, is to detect and localize HFO with MEG or EEG that are conventional non-invasive methods.

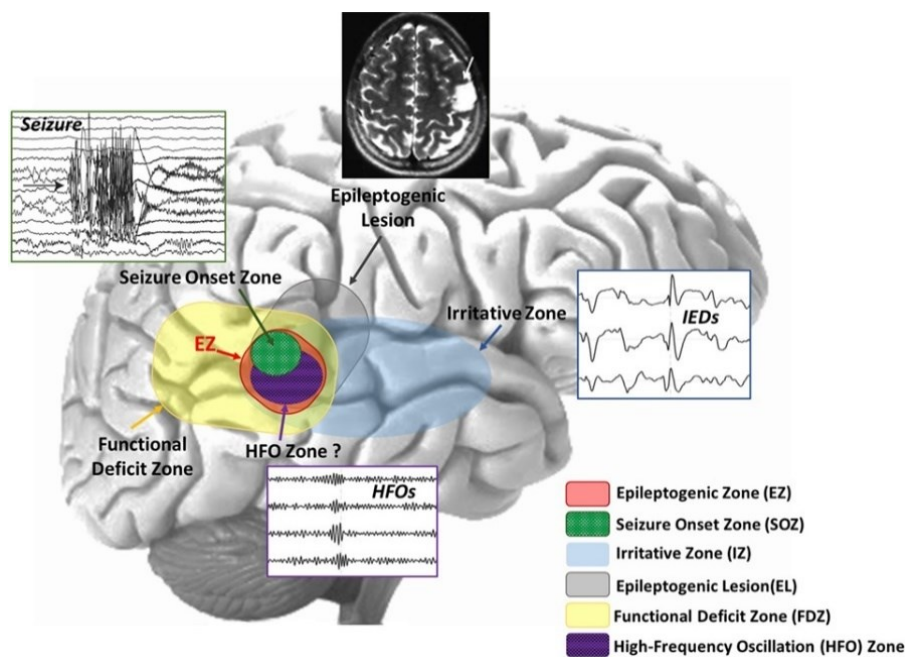


Figure 18 Schematic representation of the overlapping cortical zones in epilepsy [13]

## Intracranial Data

Intracranial EEG (iEEG), also known as electrocorticography (ECoG) using subdural grid electrodes or stereotactic EEG (sEEG) using depth electrodes, is a type of electrophysiological monitoring that is blossoming in various fields of human neurosciences. Pioneered in the early 1950s by Wilder Penfield and Herbert Jasper, this technique uses electrodes placed directly on the exposed surface of the brain in contrast to conventional EEG that monitors the activity from outside the skull. When the EEG recordings are obtained with intracranial electrodes, we refer to it as intracranial EEG (iEEG) either in the form of electrocorticography (ECoG) using strips or grids of electrodes implanted in the subdural space), or stereotactic-EEG (sEEG) using wires of electrodes penetrating the brain and targeting pre-defined deeper sites (e.g., hippocampus) without open craniotomy[64], [46]. Intracranial EEG

involves the surgical implantation of electrodes and is most often used for the mapping of epileptic foci (areas of focused seizure activity) prior to surgical interventions, when AED fail to work. For decades iEEG used to be applied in animal studies, in recent years human iEEG provides new encouraging possibilities for examining human cognition [72].

In intracranial EEG recordings we can observe fluctuations through the implanted electrodes in the voltage of ionic currents produced by neurons. Generally, the sensors of electroencephalography are the electrodes, which form a linking bridge between the brain and the acquisition system. More specifically, in iEEG recordings, electrodes are the physical transducers that perform the analogue recording and are connected to amplifiers, which not only amplify, but also filter the iEEG activity. Intracranial data can be used to study high frequency oscillations and gamma-band responses.

One of the main advantages of iEEG is that it permits direct recording of electrical neurological activity on the exposed cortex, at the individual cell or cellular cluster-level. Other brain imaging techniques, such as fMRI or PET, rely upon signals from the biproducts of neural activity (for example blood oxygen level dependent-BOLD-signal in fMRI). A second advantage of iEEG is the extremely high spatiotemporal resolution that offers, as well as the high signal to noise ratio-SNR. This can be examined in contrast to conventional scalp EEG, which has low spatial accuracy due to physiological barriers outside the skull. According to studies, iEEG can provide neurological data on the millimeter scale in terms of localization and at the millisecond scale can capture temporal-related activity [91].

In contrast to EEG, the iEEG mainly provides recordings that contain local field potentials (LFP). The cortical field potential (CFP), a recording of the activity of a local population of neurons, LFP, which is the direct measurement of a single or much smaller group of neurons and the intracranial event-related potentials (iERP) are the primary derivatives of iEEG[92]. In conclusion, intracranial EEG can provide help to understand the nature of functional activity between different regions of the brain, as well as brain networks, and determine causality through neural electrical stimulation.

### **Intracranial High Frequency Oscillations (HFO)**

In iEEG recording there are two different types of intracranial electrodes that record HFOs, microelectrodes and macroelectrodes (depth or subdural) [93]. High Frequency Oscillations are transient LFP oscillations [94] and they can be similarly detected with microelectrodes, with surface area  $150 \mu\text{m}^2$  [95] and clinical macroelectrodes with surface area: 1-10  $\text{mm}^2$  [96]. Thus, the features of HFOs are

related to the type of recording electrode. The EEG must be sampled above 4 times of the interest upper frequency, in order to form the wave shape [97]. To record HFOs including fast ripples as high as 500 Hz, a sample frequency of 2 000 Hz or above should be attained and an amplifier with wide bandwidth 0.1–500 Hz. A referential montage of epidural reference is used during the recording far from the suspected epileptogenic zone [98]. Recording HFOs with bipolar montages are also recommended as they can neutralize the artifacts carried by two adjacent electrodes [99]. After the EEG signal is filtered at the 80-250Hz Ripple band (Ripple events) and at the 250-500 Hz Fast Ripple band (Fast Ripple events). Mainly, only events including at least 4 continuous oscillations are regarded as HFOs. Events that are separated by at least two non-HFO oscillations, are considered to be two different events [100].

In epilepsy surgery, there are many studies that have proved the spatial association between the HFO and the EZ and report that the removal of HFO Zone can lead to better surgical outcomes for drug-resistant adults and children [101]. Frequency spectrum analysis above 80 Hz is helpful to improve the accuracy of preoperative evaluation. In a study including patients with TLE and ETE epilepsy, it is shown that better surgical outcomes are correlated with the removal of HFO Zone in the whole cohort in the TLE group, but not in the ETE group [100]. Patients with good outcomes (ILAE classes 1–3) had significantly higher Ripple ratio between resected and non-resected contacts than patients with poor outcomes (ILAE classes 4–6).

High Frequency Oscillations are proposed progressively as a new biomarker of epileptogenicity, as their association and efficiency have been proven in both focal epilepsy and symptomatic generalized epilepsy studies. However, there are also still different views and debates. A few studies suggest that physiological and pathological HFOs largely overlap in regions and frequencies [102].

In conclusion, the establishment and application of HFOs as a biomarker is pending, as there are still disagreeing studies. In the future, with the improvement of imaging techniques, the localizing value of pathological HFOs for epileptic foci will be higher and there is hope for advancing the understanding of the pathophysiology of epilepsy better with HFOs. The main problem lies on the inability of current techniques to distinguish epileptic pathological HFOs from physiological HFOs. Thus, even though HFOs are surely a reliable marker of pathological brain activities and networks, their application and adaptation as a biomarker of SOZ in clinical practice is still foggy.

### **Electroencephalographic characteristics of Slow Wave Sleep (SWS)**

By means of electroencephalographic (EEG) recordings, sleep comprises different stages that occur in a characteristic sequence in normal subjects. Deep sleep or else

Slow-Wave Sleep (SWS) follows the stage II sleep, which is the deepest phase of non-rapid eye movement (non-REM) sleep and is characterized by delta waves measured by electroencephalography. During the first hour of sleep, the recordings show the beta activity, which is characterized as the waking state (Awake state) with the eyes open and by high-frequency and low amplitude activity (15–60 Hz,  $\sim 30 \mu\text{V}$ ). When the frequency starts to decrease into 4–8 Hz and the amplitude starts to increase (50–100  $\mu\text{V}$ ), then the stage I of non-REM sleep follows with the theta waves. Descent into stage II non-REM sleep is characterized by 10–15 Hz oscillations (50–150  $\mu\text{V}$ ) called spindles, which occur periodically and last for a few seconds at about 10–12 Hz, generally 1 or 2 seconds and arise because of the interactions between thalamic and cortical neurons. Then, the Stage III non-REM sleep follows and is characterized by slower waves at 2–4 Hz (100–150  $\mu\text{V}$ ). During slow wave sleep dreaming and sleepwalking can occur. Moving on to the Stage IV sleep or deep sleep (1–4 Hz), this phase is defined by the characteristic slow waves with high amplitude at 0.5–2 Hz (100–200  $\mu\text{V}$ ), also known as delta waves. Delta waves are polymorphic, semirhythmic waves accounting for at least 20% of the EEG activity in sleep stages III and IV (slow wave activity or else SWA). Together sleep stage III and IV are known as the slow-wave sleep (SWS), that is characterized by relative body immobility, is maximal in young years and markedly decreases with the age (the elderly may not show SWA at all during many nights of sleep). After reaching this level of deep sleep (last stage of non-REM sleep), the sequence reverses itself and a period of rapid eye movement sleep, or REM sleep, ensues. On average, four additional periods of REM sleep usually occur, each having longer durations. From the first stage of drowsiness (awake state) to the deepest sleep stage IV, all the sleep sequence usually lasts about an hour in a normal subject[103].

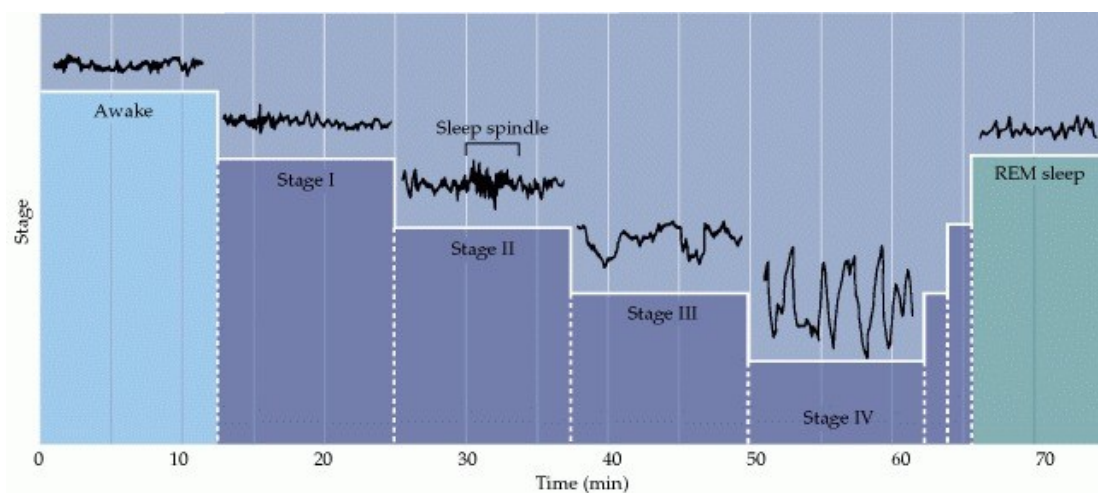


Figure 19 Sleep Stage Sequence in EEG recordings, from Sinauer Associates Neuroscience 2<sup>nd</sup> edition

### **Data Acquisition and equipment in iEEG**

Between EEG and iEEG, the second provides a higher spatial resolution at millimeter scale, a frequency bandwidth of up to 200Hz or higher (which makes ECoG more suitable for dealing with high gamma band than EEG), and higher signal-to-noise ratio. Nevertheless, iEEG has an invasive nature and that means limitation to generalizability of the findings, as most often only patient groups with serious pathology may be sampled, such as in epilepsy. Because iEEG studies are mostly carried out on epileptic patients, the regions studied frequently mirror the focal areas, the temporal and frontal lobes. Because the research takes place in a hospital, the ability to carry out elaborate research paradigms is often more complicated and limited, trials must be timed according to the participant's condition and length of time since the implantation of the electrodes. Consequently, researchers may not be able to meticulously plan for subject participation in the same way that one can with other studies with conventional EEG recordings for example. As a result, obtaining iEEG data is time consuming and relative research includes often fewer participants than studies with traditional EEG. An additional challenge for the quality and the value of the experiments is the clinical environment itself, for example if it is a hospital setting or a university EEG lab. Comparing again iEEG and EEG, iEEG is clearly more rare and requires the involvement of trained clinicians, as well as access to a neurologist to determine where seizure activity has occurred. Moreover, there is a chance that participants may be distracted by sounds and events outside of the researcher's control and that has consequences. Different kinds of iEEG recordings exist based on the type of electrode used and its method of placement. As mentioned before, when the electrical activity in the brain is measured by using subdural grid or strip electrodes, then is called electrocorticography (ECoG) and in case of depth electrodes is called stereotactic EEG (sEEG). Sometimes, there are cases where a combination of different types of electrodes may be used and may be necessary. Two main data acquisition and processing systems for iEEG are the Micromed system, which is an audio-video iEEG monitoring system for sEEG, and the Neurolynx System.

### **Software**

About the analysis software packages, many of the available iEEG systems come with software packages with varying levels of detailed descriptions implemented and with different preprocessing tools. There are several free and commercially available software packages that run on MATLAB, R or Python platforms and offer alternative implementations of data analysis tools. In this thesis project, MATLAB is the dominant software used for the iEEG data preprocessing and processing, analysis, and

visualization. MATLAB is a high-level programming environment, easy to use and access large amounts of data and because the most widely used iEEG analysis packages are MATLAB based (for example most commonly knowns are Fieldtrip or EEGLAB), the iEEG dataset and the largest part of the implementation was completed here. With these packages it is easy to inspect and compare results from different subjects, compute and customize plots of data, that can be exported as pixel-based image files (.jpg, .bmp, .png, .tiff), vector files (.eps), or movies, which can be used to make presentations and publication-quality figures. Because of the high sampling rate of IEEG data, iEEG include generally much larger files than most of the electrophysiological data acquisition systems. As a result, processing iEEG files means that a good amount of RAM is needed. After reading the data in MATLAB memory, a common procedure that was also followed in this thesis, is the downsampling to reduce the sampling rate. Downsampling contributes to subsequent analyses run much faster and facilitates by doing the analysis with less RAM.

### **Data Reading and Processing**

In this thesis, the dataset used was from a paper published in 2017 by Fedele T, Burnos S, Boran E, Krayenbühl N, Hilfiker P, Grunwald T, Sarnthein J . The basic motivation for using and experimenting with this dataset and behind the whole thesis, is that HFO are recognized as a potential biomarker for the SOZ. However, a remaining challenge is the prospective classification of epileptogenic tissue samples by individual electrode contacts. The University Hospital Zurich [18] provided to us the dataset and contains samples of long-term invasive recordings iEEG from 20 consecutive individual patients, who subsequently underwent epilepsy surgery. From each night recording, there are up to six sample intervals and each interval contains five minutes of interictal slow-wave sleep. IEEG recordings were made using subdural strip and grid electrodes, as well as depth electrodes, according to the findings of the non-invasive presurgical evaluation. HFOs were defined prospectively by a previously validated, automated algorithm in the Ripple (R, 80-250 Hz) and the Fast Ripple (FR, 250-500 Hz) frequency band. The HFO detector was generated and validated on datasets from the Montreal Neurological Institute (Burnos et al., 2016). In the sample intervals we detected high frequency oscillations (HFO) and the start and ending times of these events are included in the data set. The contacts with the highest rate of Ripples co-occurring with FR over several five-minute time intervals, finally designated the HFO area.

According to the paper's results of Fedele et al. 2017, the HFO area was **fully** included in the resected area in all 13 patients, who achieved **seizure freedom**

(specificity 100%) and in 3 patients where seizures reoccurred (negative predictive value 81%). On the other side, the HFO area was only **partially** resected in 4 patients suffering from recurrent seizures (positive predictive value 100%, sensitivity 57%). The clinical relevance of the HFO area was validated in the individual patient with an automated procedure. Thus, the resection of the prospectively defined HFO area proved to be highly specific and reproducible in 13/13 patients with seizure freedom, while it may have improved the outcome in 4/7 patients with recurrent seizures. Although, the neurophysiological mechanisms underlying pathological HFO still await clarification and more extensive research.

### Participants and Electrode Placement

The total number of individual patients shaping the dataset is 20 and they all subsequently underwent epilepsy surgery. Subdural strips, grid electrodes, and depth electrodes were placed according to the findings of the non-invasive presurgical evaluation, depending on the individual patient's pathology and type of epilepsy. The age of the patients ranges from 17 to 52 years old. About the epilepsy type, 9/20 patients have TLE and 11/20 have ETE epilepsy. The outcome results for the patients after surgery are as follows: 65% completely seizure free and 35% with seizures. In more detail 13/20 are completely seizure free with ILAE 1, 2/7 still have seizures with ILAE 3, 4/7 with ILAE 5 and 1/7 with ILAE 6.

Patient	Age, Gender	Histology/ Pathology	Epilepsy	Electrode placement	Type of electrodes	Surgery	Nights	Intervals	Test: retest intervals	Test: retest nights	Ripple area resected?	FR area resected?	ERandR area resected?	Outcome (ILAE)	Postoperative follow-up (months)
1	25, M	HS and gliosis	TLE	MTL L R	5 depth, 1 strip 4 × 1, 1 strip 6 × 1	sAHE; Les	4	28	0.99	1.00	N	N	Y	1	12
2	33, M	Glioma	TLE	MTL L R	8 depth	sAHE; Les	2	13	1.00	1.00	Y	Y	Y	1	29
3	20, F	HS	TLE	MTL L R	5 depth	sAHE	5	39	0.78	1.00	N	Y	Y	1	13
4	20, F	HS	TLE	MTL L R	8 depth	sAHE	6	34	1.00	1.00	N	Y	Y	1	41
5	40, M	HS	TLE	MTL L R	8 depth	sAHE	5	35	0.94	1.00	Y	Y	Y	1	14
6	48, M	HS	TLE	MTL L R	8 depth	sAHE	5	35	0.98	1.00	Y	Y	Y	1	11
7	25, M	HS	TLE	MTL L R	8 depth	sAHE	1	1	—	—	Y	Y	Y	3	42
8	21, F	HS	TLE	MTL L R	8 depth	sAHE	2	16	0.67	1.00	Y	Y	Y	3	15
9	52, M	HS	TLE	MTL L R	8 depth	sAHE	2	12	1.00	1.00	Y	Y	Y	5	46
10	37, M	FCD 2b	ELE	Pr R	1 grid 8 × 4; 2 strips 4 × 1	Les	1	6	1.00	—	N	Y	Y	1	36
11	36, M	FCD 2b	ETE	FR	1 grid 8 × 8; 1 depth	Les	3	19	1.00	1.00	Y	Y	Y	1	37
12	49, M	Ganglioglioma	ETE	T-Lat L	1 grid 8 × 4; 1 depth	Les	4	25	0.53	0.67	Y	N	Y	1	25
13	17, M	FCD 1a	ETE	PR	1 grid 8 × 8; 1 depth	Les	2	16	0.75	1.00	N	N	Y	1	25
14	46, F	FCD 1b	ETE	PR	2 grids 8 × 2; 1 strip 6 × 1; 1 strip 4 × 1; 1 depth	Les	2	13	0.97	1.00	Y	Y	Y	1	10
15	31, F	Gliosis	ETE	T-Lat L	1 grid 8 × 4; 2 strips 4 × 1	Les	4	28	0.32	0.33	Y	N	Y	1	25
16	17, F	FCD 2a	ETE	F-Pr-CL	1 grid 8 × 4; 1 depth	Les	2	17	1.00	1.00	N	Y	Y	1	19
17	30, M	FCD 2a	ETE	FR	2 grids 8 × 2; 1 depth	Les	1	1	—	—	Y	Y	N	5	45
18	40, M	FCD 2a	ETE	PR	2 strips 6 × 1; 1 depth	Les	1	5	1.00	—	N	Y	N	5	30
19	38, M	Cavernoma	ETE	TP	1 grids 8 × 4; 1 grids 8 × 2	Les	2	13	0.36	0.00	N	N	N	6	11
20	17, M	FCD 3	ETE	OT	1 grids 8 × 2	Les	4	29	0.23	1.00	N	N	N	5	16

Figure 20 Table of Patients, adapted from [15]

About the placement of electrodes, in TLE patients were implanted bilaterally into the amygdala (labels AL, AR), the entorhinal cortex (ECL, ECR), anterior hippocampus

(AHL, AHR) and the posterior hippocampus (PHL, PHR), depth electrodes (1.3 mm diameter, 8 contacts of 1.6 mm length, spacing between contacts centres 5 mm, ADTech®). On the other hand, in ETE patients, a combination of depth and subdural grid, and strip electrodes (contact diameter 4 mm with a 2.3 mm exposure, spacing between contact centers 10 mm, ADTech®) was placed after craniotomy. Two typical examples of the placement of the electrodes in the epileptic patient are illustrated schematically in the following figures. Post-implantation MR images were used to locate each contact anatomically along the electrode trajectory.

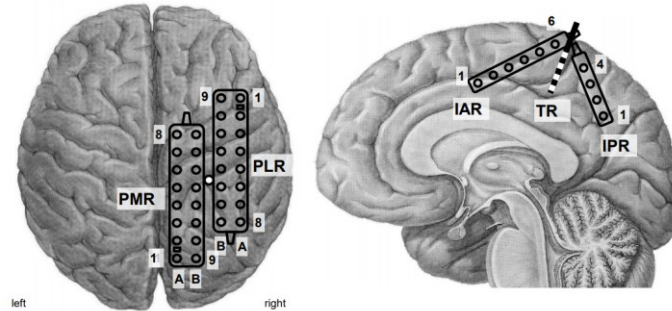


Figure 21 Patient - Electrode placement, strips, grids, depth

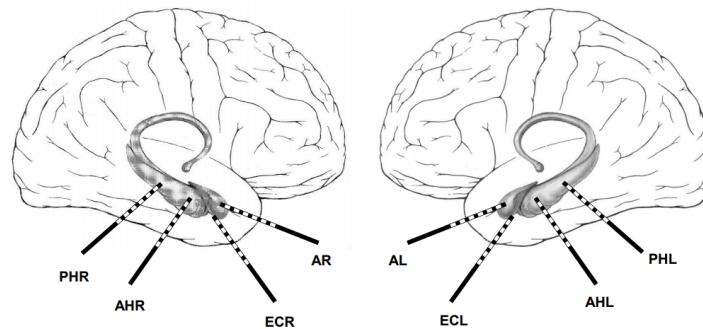


Figure 22 Patient - Electrode placement, only depth electrodes

### Data Acquisition and Selection

The intracranial data was acquired at 4000 Hz sampling frequency with an ATLAS recording Neuralynx system (0.5-1000 Hz pass-band, Neuralynx) and down-sampled to 2000 Hz for HFO analysis. Neuralynx system uses an acquisition software called Cheetah. Also, Neuralynx system outputs its own proprietary file formats and its standard setting is for each individual channel to create a separate file. These channel files are written into a 'dataset directory' and the files therein are able to be read concurrently. The Fieldtrip toolbox contains reading functions that work with these file types. Here [http://www.fieldtriptoolbox.org/getting\\_started/neuralynx/](http://www.fieldtriptoolbox.org/getting_started/neuralynx/) one can find the listing of the exact functions. In addition, scalp EEG were recorded according to the 10-20 system, with minor adaptations in order to avoid the surgical scalp lesions,

and the submental electromyogram (EMG). The iEEG was recorded against a common intracranial reference and then transformed to bipolar channels for further analysis. About the bipolar montage, each channel represents the potential difference between two adjacent active electrodes and the entire montage consists of a series of such channels. Basically, it consists of a display in which each channel connects adjacent electrodes from anterior to posterior in two lines, essentially covering the parasagittal and temporal areas bilaterally. Moreover, for every patient for each night recording were selected up to six intervals of interictal slow-wave sleep and with duration 5 minutes per interval. The number of nights and the number of intervals vary across patients. Sleep scoring was performed based on scalp EEG, electrooculogram, EMG and video recordings. The selection of intervals was carefully done and they were at least three hours apart from epileptic seizures, in order to eliminate the influence of seizure activity on the analysis. Also, all the electrode contacts, where electrical stimulation evoked motor or language responses were excluded from the dataset.

## Chapter 4 Classification of Epileptic Events

### Feature Extraction and Feature Selection

#### A prospective definition of HFO area

In this thesis work and according to [15], so as to facilitate the HFO analysis, a definition of HFOs was proposed, with the purpose of providing a prospective definition of a clinically relevant HFO. In more detail, the focus goes to the electrode contacts with the HFO rate exceeding the 95% percentile of the HFO distribution and on ripples co-occurring with the fast ripples or else FR, thus creating a new entity called Fast Ripples and Ripples or else called FRandR. The designated HFO area consists of FRandR and the resected by the surgeon's channels. The evaluation of the clinical relevance of the final defined HFO, was done by comparing the resected area (RA) with the HFO area and combining the experts markings with the highest-rated HFO channels and then by predicting the seizure outcome in the individual patient. The aim of this HFO definition was not to outperform the visual markings, but to evaluate whether the HFO area was included in the resection area and to quantify the predictive value of the HFO area with respect to the seizure outcome. It is worth noting, that HFO analysis isn't expected or intended to replace surgical planning or the surgeons' decisions, but that it might provide an insightful value in difficult or ambiguous cases.

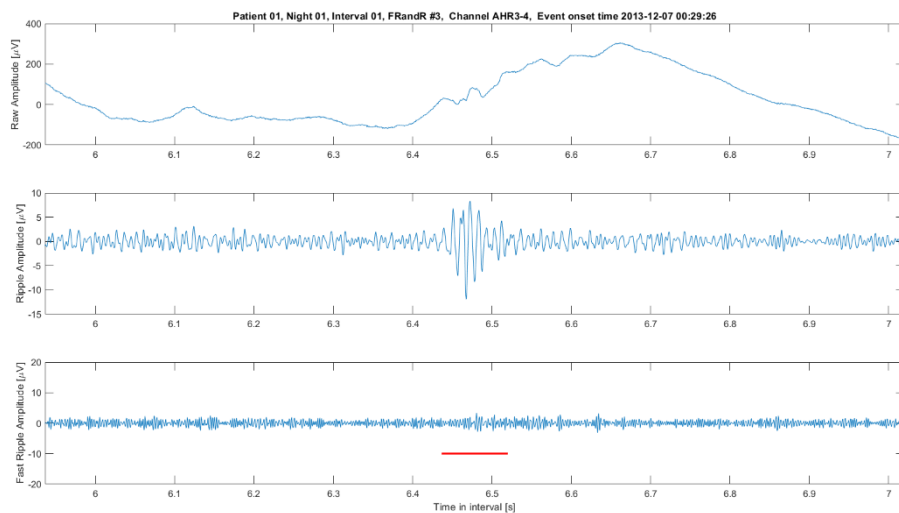


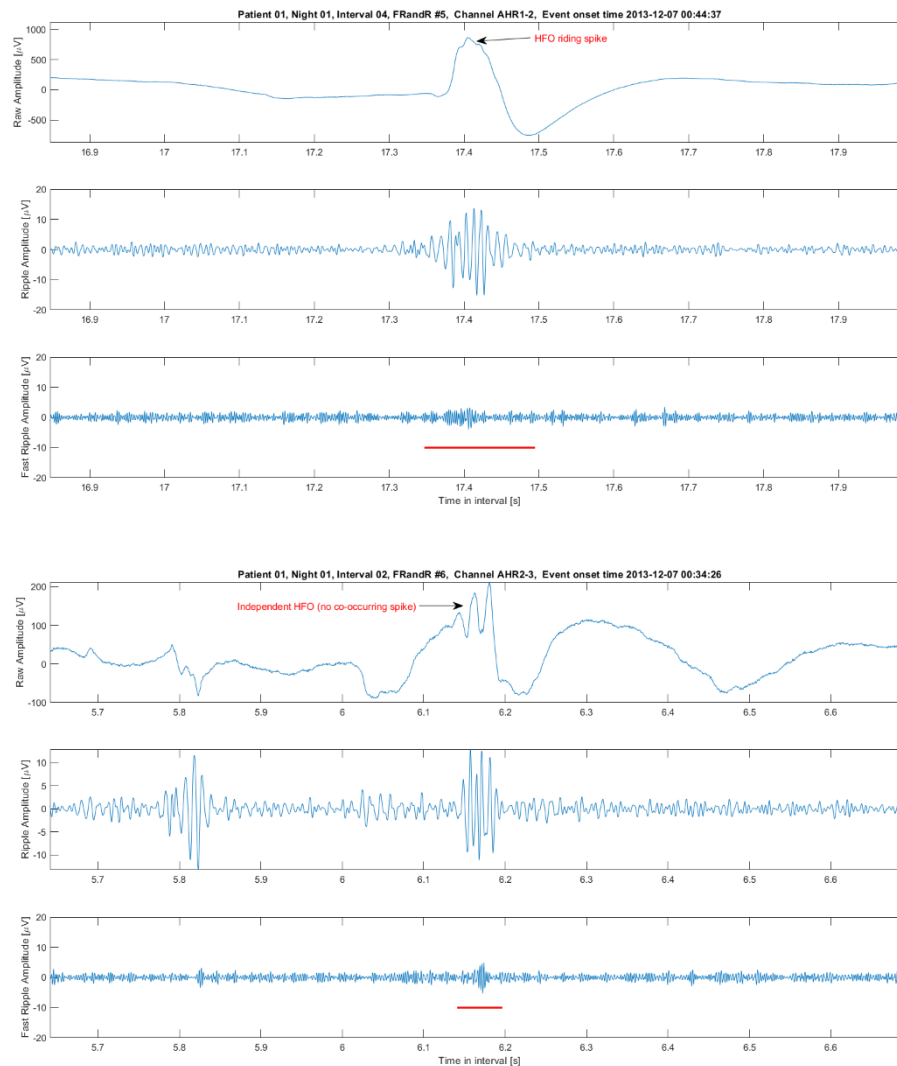
#### Different types of HFO

In the following figures we can see some example events of different HFO bands, where the raw and filtered signal are presented. Specifically, from top to bottom, all the HFO bands are illustrated. On top there is the raw signal, in the middle the filtered R band and on bottom the filtered FR band. The most important part of the data, where the focus goes in this thesis work, is the red line on the FR band, that marks the FRandR area. FRandR band designates the HFO area in this thesis and consists of the contacts with the highest rates of Ripples co-occurring with Fast Ripples over five-minute time intervals of interictal slow wave sleep. Thus, the red line in each event marks the simultaneous occurrence of R and FR, that creates the new band called FRandR. High Frequency Oscillations are short-lasting field potentials, that are both ictal and interictal phenomena and it is confirmed that are connected to normal non-

pathological as well as pathological brain functions. HFOs often have at least 4 peaks, a mean duration of  $\sim 30$  ms, an amplitude of  $\sim 5\mu\text{V}$  in ripple band and  $\sim 1\mu\text{V}$  in fast ripple band.

It is also worth highlighting that there are different types and shapes of HFOs. Spikes are another established interictal marker for epilepsy up to 70 Hz, that is not completely independent of HFOs as they often occur at the same time and at the same brain areas. Quite often, we come across instances, where HFOs are riding spikes, sometimes it is visible in the unfiltered raw signal and sometimes is not. Fast ripples are thought to reflect population spikes from synchronous bursting cells. Sometimes, the HFO amplitude is irregular due to the filter effect of the sharp spike. In recent studies it has been concluded that HFOs can contribute to the understanding of epilepsy beyond the contribution of individual spikes in individual patients. In addition, there are also independent HFOs with no co-occurring spikes. According to some recent studies, all three kinds of HFOs can become in the future valuable biomarkers for identifying the EZ. In the following figures, we can see these basic different cases in our detected HFO events of slow wave sleep:





### HFO Rates in R, FR and FRandR bands

In the following figures are presented the computation of the HFO rates per channel of some characteristic patients/cases. On top of every patient is the postsurgical outcome ILAE, that as previously referred ranges from 1 to 6, starting from the best-case scenario that is seizure-free outcome ILAE 1, continuing to ILAE 3 that is recurrent seizures, and finishing to 5 and 6 that are the worst postsurgical cases. Every rate has been computed in number of events to minutes per channel. Out of all the HFO events detected in different channels, the channels with the HFO rate exceeding the 95% percentile of the HFO distribution, defines eventually the HFO area and these HFO channels are highlighted in green. In red colour are highlighted the channels that were resected by the surgeons in each individual patient. The red channels form the resected area for each patient.

According to these validation tables of channel rates and comparing them to the postoperative results regarding the class of ILAE, green HFO area is a subset of the

red resected area in most of the cases. In all the patients who achieved full seizure freedom, 13 out of 20 patients, the surgeons had removed areas including the HFO areas related to the channels with the highest F<sub>randR</sub> event rates, 13 patients with fully resected HFO area out of the 13 seizure-free patients. In some cases, though with recurrent seizures post-surgically, the detected HFO area that is studied and considered to be epileptogenic, was not removed or was partially removed in 4 out of 7 patients with recurrent seizures. In these 3 cases left, at least the HFO areas and guidance were consistent with the routine surgical planning. Therefore, the role of HFOs proves to be crucial as an indicator in this dataset, and mostly with the focus on F<sub>randR</sub>. Ripples and Fast Ripples separately were also studied, but proved to be less specific than F<sub>randR</sub>.

### **Feature Extraction from HFO events**

The process of feature extraction includes unveiling hidden characteristic information about the input filtered signal events in F<sub>randR</sub> band and its behavior of its sources. HFO events as observations are far too voluminous to be modeled directly by predicting modeling algorithms, such as classification. By reducing the dimensionality of these detected events with millions of attributes at first, the result is a much smaller set of characteristics, that are not redundant or strongly correlated with each other and can be more easily modeled. By identifying relevant features, the insight gets larger into the nature of the corresponding classification problem. At first, it was the HFO detection and second, and most importantly for this work, the classification of the distinctive features that determine the pathological HFO area and the non-pathological.

The first steps before the feature extraction attempts, are related to the construction of the feature vector. The HFO events that were detected in every interval and in every night for each patient, are timeseries that need to be prepared as time segments with their own starting and ending point. At the start, an array based on the number of the detected events and the size of the maximum detected event in duration was constructed and after by cropping, any event was prepared and accessible for the feature computation. The rows of the feature vector are the isolated HFO events, and the columns are the features. At the first attempts, the feature vector contained some basic waveform characteristics, such as the amplitude, the mean, the median, the variance, the standard deviation, and the duration of the detected events. Moreover, some of the most basic features that describe HFOs are the negative or positive peaks and their maximum or minimum values, as well as the peak-to-peak amplitude. Peak-to-peak amplitude expresses the change between the peak, that is the highest

amplitude value, and the trough, that is the lowest amplitude value, which can be negative. However, these basic descriptors are not enough, because we need more information to differentiate among different shapes of HFOs.

HFO shapes and patterns, differ depending on the frequency band, Ripples (80-250Hz) and Fast Ripples (250-500Hz). This variety of HFO shapes, demands an extensive investigation of the most likely discriminative features. It is worth noting, that often there is a co-occurrence between spikes and HFOs, and in the same brain areas. Sometimes HFOs are even visible riding the spikes in the unfiltered raw signal, but not always. There are also completely independent HFOs with no co-occurring spikes. A lot of studies investigating the interaction of both biomarkers, suggest that spikes can be grouped into spikes with and without HFOs co-occurring, and that spikes with HFOs may be more closely related to epileptogenicity than spikes without [104].

Other insightful features of spikes and HFOs, that are used to describe their distributions, are kurtosis, skewness, energy, Renyi entropy, Log-Energy entropy, Wavelet coefficients, median frequency in terms of the sampling rate, mean frequency, interquartile range, in terms of the sampling rate, number of peaks, average prominence of peaks, average width of peaks, and others. Other methods that have been tested in extracting features from intracranial EEG include Fourier Transform (TF) and Wavelet Transform (WT). All these features and methods of extraction were investigated in our case, some of which were rejected at the final feature selection.

**Interquartile range** in descriptive statistics expresses the middle half of the distribution. We can measure it by subtracting the Q1 value, which is the 1<sup>st</sup> quartile or 25<sup>th</sup> percentile, from the Q3 value, which is the 3<sup>rd</sup> quartile or 75<sup>th</sup> percentile of the distribution .

**Kurtosis** measures the tail-heaviness of the distribution and is defined as follows in the following equation. It is used to measure the outliers present in the distribution. The kurtosis of a normal distribution is 3, distributions that are more outlier-prone than the normal distribution have kurtosis greater than 3, and less outlier-prone have kurtosis less than 3.

$$k = \frac{E(x-\mu)^4}{\sigma^4}$$

where  $\mu$  is the mean of  $x$ ,  $\sigma$  is the standard deviation of  $x$ , and  $E(t)$  represents the expected value of the quantity  $t$ .

The kurtosis function computes a sample version of this population value. For that reason, tends to differ from the population kurtosis by a systematic amount based on the sample size and this kurtosis systematic bias needs to be corrected. The bias-corrected kurtosis depends on the sample size  $n$  of every detected event and is

computed as in the following equations:

$$k_1 = \frac{\frac{1}{n} \sum_{i=1}^n (\chi_i - \bar{\chi})^4}{\left(\frac{1}{n} \sum_{i=1}^n (\chi_i - \bar{\chi})^2\right)^2}$$

$$k_0 = \frac{(n-1)((n+1)k_1 - 3(n-1))}{(n-2)(n-3)} + 3, \quad n > 4$$

**Skewness** is a measure of the asymmetry of the data around the sample mean and is defined as follows in the following equation (\*). In a normal distribution or in any perfectly symmetric distribution, the skewness is zero. If skewness is positive, the data spreads out more to the right of the mean than to the left. If skewness is negative, the data spreads out more to the left.

$$s = \frac{E(\chi - \mu)^3}{\sigma^3}$$

where  $\mu$  is the mean of  $x$ ,  $\sigma$  is the standard deviation of  $x$ , and  $E(t)$  represents the expected value of the quantity  $t$ .

The bias-corrected skewness depends on the sample size  $n$  of every detected event and is computed as in the following equations:

$$s_1 = \frac{\frac{1}{n} \sum_{i=1}^n (\chi_i - \bar{\chi})^3}{\left(\sqrt{\frac{1}{n} \sum_{i=1}^n (\chi_i - \bar{\chi})^2}\right)^3}$$

$$s_0 = \frac{\sqrt{n(n-1)}}{(n-2)} s_1, \quad n > 3$$

Another four exploratory features based on the **HFO Peaks** were tested. These features could offer a topological view on different types of HFO and may help explore also new features of complex data through a geometrical perspective. More specifically, we extracted the **number of peaks**, the **average prominence of the peaks**, the **average width of the peaks** and finally the **average value of the peaks**. We approached the number of peaks by identifying local maxima. The prominence of a peak measures how much the peak stands out due to its location relative to other neighboring sample points (surrounding signal baseline). It is defined as the vertical distance between the peak and its lowest contour line. In order to find the number of peaks in the detected events, and knowing that HFO shape has at least 4 peaks in general, we mark as peaks the local maxima of the input signal. In order to make a better estimate of the number of peaks in the cycle of an HFO duration, we restrict in time the peak-to-peak separation based on its standard deviation (threshold).

Figure 23 Values and Locations of Peaks in HFO,  
in this example (Local Maxima), number of Peaks =11

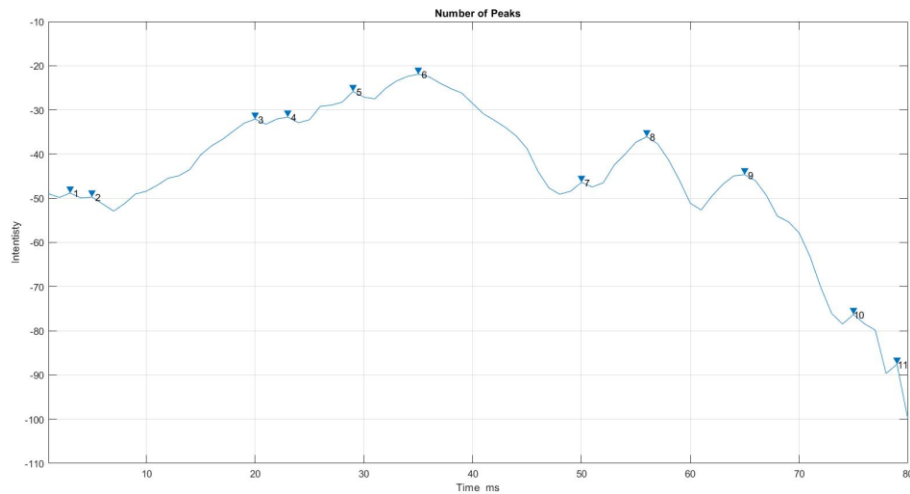
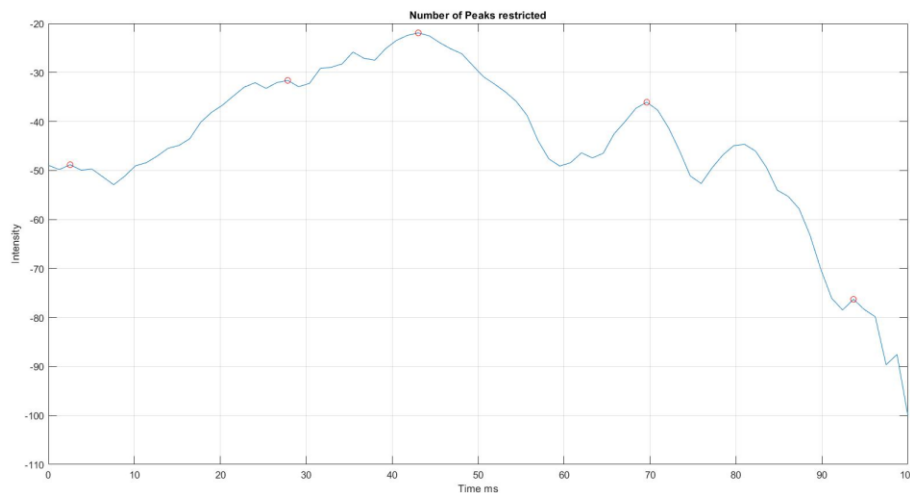


Figure 24 Values and Locations of Restricted Peaks in HFO,  
time restricted the peak-to-peak separation based on its standard deviation, number of peaks = 5



**Entropy** measures for epilepsy are used to quantify in a statistical sense, the diversity, irregularity, or uncertainty in an EEG signal. The lower the approximate entropy, the greater the information obtained by a system, and as a result the greater is the statistical independence, as the signal appears to be more regular or repetitive. Random or irregular signals tend to have higher values for approximate entropy. Renyi entropy, which generalizes Shannon Entropy and min-Entropy, is a measure of randomness. **Renyi Entropy** is generalizing the Kullback–Leibler divergence, that according to it is being quantified how different is a probability

distribution from another. In other words, it is related to the Shannon entropy or else Relative entropy, where the maximum entropy corresponds to distributions that have identical quantities of information. Smaller values of entropy indicate repeatability in a signal and higher values indicate irregularity.

$$H_R(X) = \frac{1}{1-\alpha} \log \sum_{i=1}^n p_i^\alpha,$$

where  $\alpha \geq 0$  and  $\alpha \neq 1$ , alpha is a bias parameter, and the Shannon entropy is recovered in the limit as  $\alpha \rightarrow 1$  (Kullback–Leibler divergence),  $X = \{x_i: i=1, \dots, N\}$  with  $\sum_{i=1}^n p_i = 1$ , is a discrete probability distribution (PDF) with  $N$  the number of possible states of the system under study. In the discrete case, we define a “normalized” Shannon entropy ( $0 \leq H \leq 1$ ) as follows:

$$H_S(X) = \frac{S[P]}{S_{max}} = \frac{\{-\sum_{i=1}^n p_i \log(p_i)\}}{S_{max}},$$

where given a continuous PDF,  $f(x)$  with  $x \in \Delta \subset \mathbb{R}$  and  $\int_{\Delta} f(x) dx = 1$ , associated Shannon Entropy  $S$  is defined as  $S[f] = -\int_{\Delta} f(x) \log(f(x)) dx$ .

As temporal features, **Hjorth parameters** are used often in the analysis of electroencephalography, and they are normalised slope descriptors. These parameters are known as Activity, Mobility and Complexity. Activity is also known as the variance of the signal or else the mean power. In this feature extraction, we computed the mobility and the complexity, as the variance had previously been tested as a basic descriptor. Firstly, Mobility represents the mean frequency or else the proportion of standard deviation of power spectrum.

$$Mobility(x) = \sqrt{\frac{var(\dot{x})}{var(x)}}$$

Secondly, Complexity expresses the change of mobility that is translated as frequency change. The parameter compares the signal's similarity to a pure sin wave, where the value converges to 1 if the signal is more similar.

$$Complexity(x) = \frac{Mobility(\dot{x})}{Mobility(x)}$$

**Fractal dimension (FD)** is a measure of a signal's complexity and self-similarity in the time domain. A **fractal** is a subset of Euclidean space with a fractal dimension, that strictly exceeds its topological dimension (FD is a non-integer dimension of a geometric object). In fractal geometry, the **Higuchi dimension** is an approximate value for the box-counting dimension of the graph of a real-valued timeseries. In biomedical signals, fractal dimension analysis is applied often, when the waveforms are considered geometric figures. The FD number lies in the interval

between 1 and 2. Generally, higher self-similarity and complexity result in higher FD. Higuchi's algorithm (1988) was applied to EEG signal and was demonstrated to be the most appropriate for electrophysiological data. Fractal dimension as mentioned works directly in the time domain. Higuchi's FD works even in the case of short signal segments, like the detected HFO events, and is computationally fast. Important step of the algorithm is the selection of the maximal scale  $K_{max}$ , that in our case was computed based on the maximum duration of all the detected events ( $K_{max} \sim 40$ ).

$$D = \frac{d \log(L(k))}{d \log(k)}$$

**Hurst Exponent** is directly related to fractal dimension and is another measure useful to timeseries, often referred as the "index of independence" of the predictability of the signal. It is a scalar between 0 and 1 which measures long-range correlations of a timeseries. A value of  $H$  between 0.5 and 1 indicates a time series with long-term positive autocorrelation, meaning both that a low value in the series will probably be followed by another low value, and that the values a long time into the future will also tend to be low and vice versa (predictability). On the other side, a value  $H$  between 0 – 0.5 indicates a time series that switches between high and low values in adjacent pairs, meaning that a single high value will probably be followed by a low value, and that the value after that will tend to be high, with this tendency to switch between high and low values, lasting a long time [105].

**Continuous Wavelet Transform** measures the similarity between the signal and a Wavelet Function. One of the key powers of wavelet transform is that given any general function, it can be transformed into an infinite set of wavelets. **Discrete Wavelet Transform** allows the analysis of a signal in a specific segment, in our case isolated detected epileptic events. The procedure consists of expressing a continuous signal to expand coefficients of the internal product between the segment part and a mother wavelet function. As a result, the wavelet transform's discretization changes from a continuous mapping to a finite set of values. This process is done by changing the integral in the definition by an approximation with summations. Hence, the discretization represents the signal in terms of elementary functions accompanied by coefficients. The mother wavelet functions include a set of scale functions. The parent functions represent the fine details of the signal, while the scale functions calculate an approximation. Thus, considering the above, a function or signal can be described as a summation of wavelet functions and scale functions. A signal can be decomposed into various levels from the time domain to the frequency domain in wavelet analysis. The

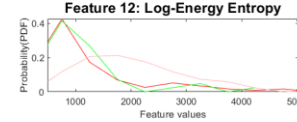
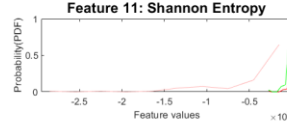
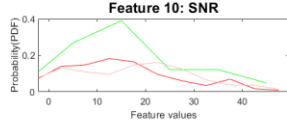
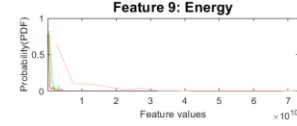
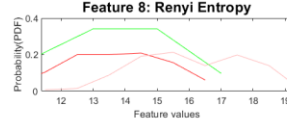
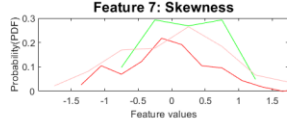
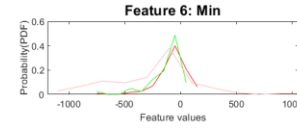
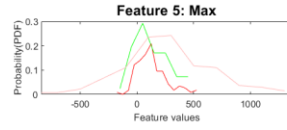
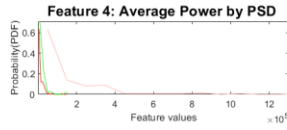
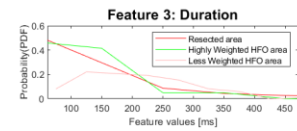
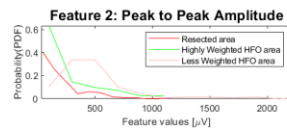
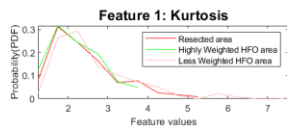
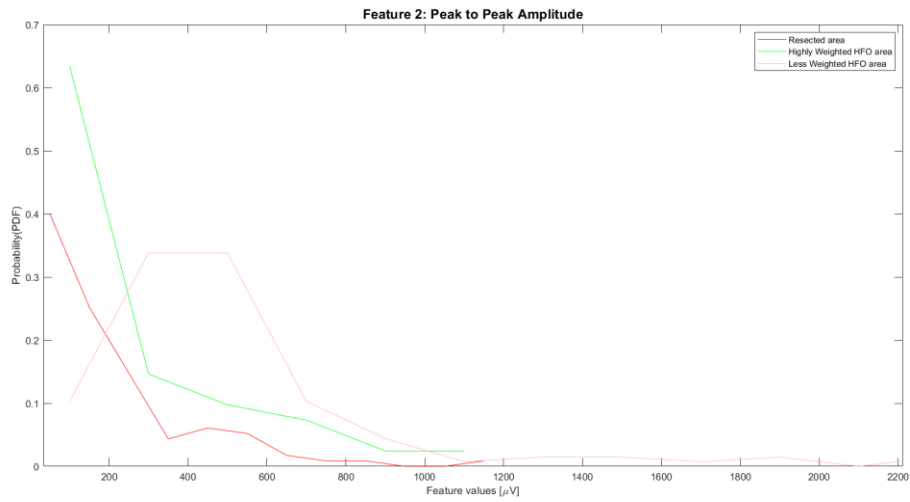
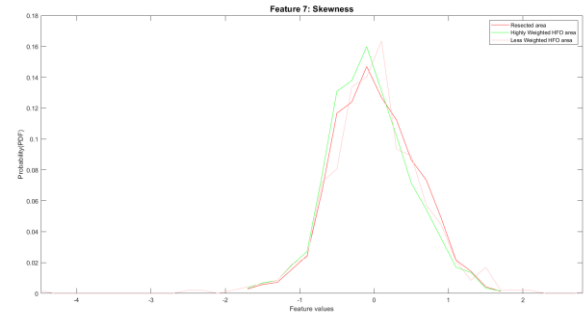
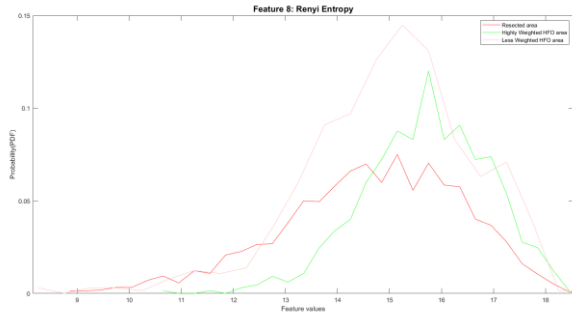
decomposition is done from the detail coefficients as well as the approximation coefficients. The upper level of the tree in wavelet decomposition represents the temporal representation. As the decomposition levels increase, an increase in the compensation in the time–frequency resolution is obtained. In the last level of the tree the representation of the signal frequency is described.

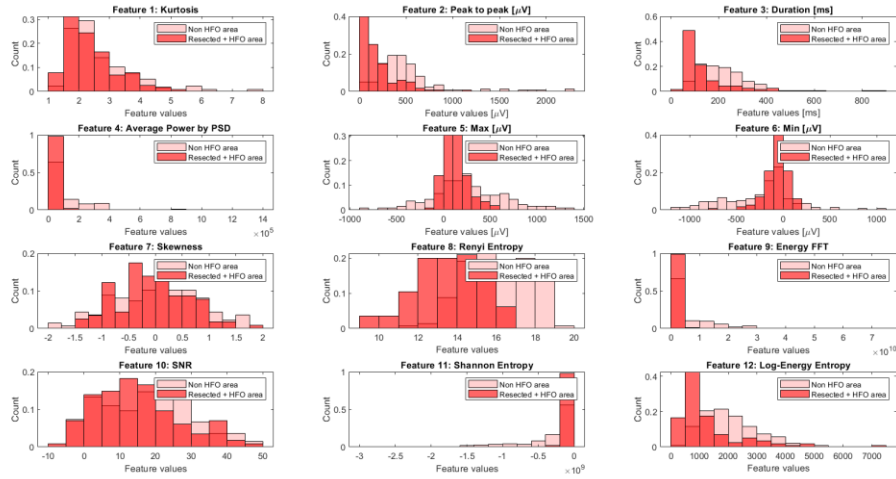
At the end, the Feature Vector was proved to be optimal through is comprised of 12 features for each detected HFO event and thus its dimensionality varies based on the size of the detected events and the recordings of each. After the construction of the feature vector for each individual patient, we can proceed to the HFO classification. In conclusion, the main aim of feature extraction is to end up with fewer features that can summarize and capture the same information, without leading the following classification model to underfitting.

### **Channel Selection**

Before feature selection methods, precedes the important **channel selection** procedure, which is determined by the classification problem statement, and its value is assigned to the key clinical assumption. Our motivation to solve the classification problem was to delineate the epileptogenic zone by classifying the extracted events from the channels. By following a reverse-engineering approach, we started experimenting based on the ground truth that the surgeons resected channels related to epileptogenesis, and these resected channels are colored red and labeled as 1. According to the surgeons, all the other channels that weren't resected should be related to the non-epileptic area. This area was colored salmon and labeled as 0. The question that arises now is how the channels associated with the highest HFO rates should be grouped based on the resective channels. At the start, we grouped them in a separate class with the label 2 and were colored green. Some of the first attempts included investigating the statical significant differences between the distributions of the green channels and the red channels, as well as green channels and salmon channels. It is worth noting, that in the majority of patients the green channels are a small subset of the red resective channels. As a result, we verified that the distributions of the green and red channels are similar, and in consequence, the resected events are related to the highest rated HFO events. Because the red and green events followed the same distribution, they were grouped together in the final analysis and marked as red events, which implies pathology. The aim was to compare their statistical significance to the salmon events, that eventually define the non-epileptogenic area. In conclusion, the events that correspond to the red channels designate the pathological HFO area or else the epileptogenic area (resected + highest HFO rated channels) and the events that

correspond to the salmon channels (remaining channels), designate the non-pathological HFO area or else the non-epileptogenic area.

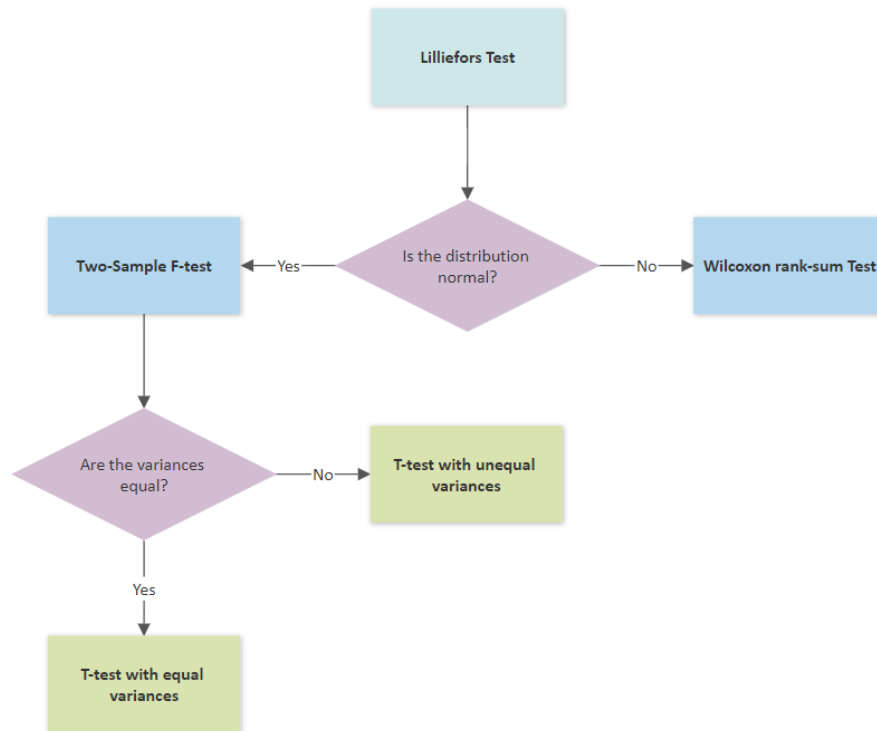




## Feature Selection

After systematic literature search and exploratory analysis for the feature extraction part, the following feature selection methods that have been applied in this work are supervised and more specifically filter-based and intrinsic. The goal of the filter-based approach for adaptive feature selection was to evaluate the relationship between each input variable and the target variable, and then choose the final most suitable input variables that will be used in the predictive classification model. Different combinations of features were tested in individual patients, but in the end 12 features gave the best prediction interpatient in the model. Some of the discriminative features were common in all patients. As the number of features increases, the classifier's performance increases as well until we reach the optimal number of features. Adding more features based on the same size as the training will then degrade the classifier's performance and this is known as the Hughes Phenomenon or else "The Curse of Dimensionality". The first feature vector after feature extraction, included some irrelevant and redundant features, that didn't result in better predictions, needed longer training time and made overall the learning process more difficult. For that reason, we moved on first to a univariate filter feature selection, that evaluates each feature individually such as the following statistical analysis scheme that we built in Figure 22 and selected the 12 highest-ranking features based on their final p-values.

Figure 25 Statistical Analysis Tree, for the investigation of statistical significance of features



At first, we check if the distributions of each individual feature grouped together form a normal distribution or not, by using a **Lilliefors Test**. In more detail, a Lilliefors test, just like the most hypothesis testing approaches, either rejects or accepts the null Hypothesis. We reject the hypothesis if the test is significant at the 5% level and that means the distribution is normal. The Lilliefors test evaluates the hypothesis that a set of data  $X$  has a normal distribution with unspecified mean and variance, against the alternative hypothesis, where there is not a normal distribution. This test compares the empirical distribution of  $X$  with normal distribution and same mean and variance as  $X$ . The idea is similar to the Kolmogorov-Smirnov test, but it adjusts a the point where the parameters of the normal distribution are estimated from  $X$  rather than specified in advance.

$$\hat{D} = \max_x |\hat{F}(x) - G(x)|,$$

where  $\hat{F}$  refers to the empirical cumulative distribution function of the sample data set and  $G$  is the cumulative distribution function of the hypothesized distribution with the estimated parameters equal to the sample parameters (sample mean and standard deviation).

By setting in our statistical analysis tree the threshold parameter alpha as a significance level at  $\alpha=0.05$ , then a p-value  $< 0.05$  is considered significant and a p-value  $\geq 0.05$  is considered not significant. Therefore, our accepted rate of type-I errors in this decision

strategic approach is 0.05. The smaller the p-value, the stronger the evidence to reject the null hypothesis. When the distribution is not normal, we follow a non-parametric approach, the **Wilcoxon rank-sum Test**. The Wilcoxon rank-sum test is a common nonparametric test, sometimes also called Mann Whitney U test, and is used often as an alternative of a t-test for independent populations. More specifically, it is applied to compare the outcomes between two independent sample groups and if they have been derived from the same population, by comparing the medians of the two groups. The procedure for the test involves pooling the observations from the two samples into one combined sample, keeping track of which sample each observation comes from, and then ranking lowest to highest respectively, from 1 to  $(n_1+n_2)$ . The  $R_1$  and  $R_2$  indicate the sums of the ranks in groups 1 and 2. The test statistic for the Wilcoxon rank sum Test is denoted as  $U$  and is the smaller of  $U_1$  and  $U_2$ . The null and two-sided hypotheses, as well as the  $U$  statistics are stated as follows:

### Null hypothesis

$H_0$ : The two populations are equal.

### Alternative hypothesis

$H_a$ : The two populations are not equal.

$$U_1 = n_1 n_2 + \frac{n_1(n_1+1)}{2} - R_1$$

$$U_2 = n_1 n_2 + \frac{n_2(n_2+1)}{2} - R_2 ,$$

where  $U = U_1$  if  $U_1 > U_2$  and  $U = U_2$  if  $U_1 < U_2$

If the distribution is normal, then we check first the variances of the two discrete feature distributions depending on the event label, by using a two-sample F-test. The **two-sample F-test** determines if the variances of the two sets are equal. The test statistic  $F$  is calculated as the ratio of the two sample standard deviations of the groups  $S_1$  and  $S_2$ . The further this ratio deviates from 1, the more likely we are to reject the null hypothesis. Under the null hypothesis, the test statistic  $F$  has a  $F$ -distribution with numerator degrees of freedom equal to  $(N_1 - 1)$  and denominator degrees of freedom equal to  $(N_2 - 1)$ , where  $N_1$  and  $N_2$  are the sample sizes of the two data sets. The Degrees of Freedom in two samples tests, are calculated as  $(N_1 + N_2) - 2$ . By comparing the F-statistic value to the f-table value where  $\alpha=0.05$ , then if the f-table value is smaller than the calculated value, we reject the null hypothesis of this test. The hypotheses and the F test statistic are shown below:

### Null hypothesis

$$H_0: S_1^2 = S_2^2$$

### Alternative hypothesis

$$H_a: S_1^2 > S_2^2 \text{ (one-tailed), reject } H_0 \text{ if the observed } F > F_\alpha$$

$$H_a: S_1^2 \neq S_2^2 \text{ (two-tailed), reject } H_0 \text{ if the observed } F > F_{\alpha/2}.$$

$$F = \frac{S_1^2}{S_2^2}, \text{ assuming } S_1^2 > S_2^2$$

At the final step, we proceed to a parametric test, a **two-sample T-test** based on the equality of the variances. When the variances are unequal, we test if the null hypothesis, that the two data groups are from populations with equal means, is rejected or not, without assuming the populations also have equal variances. In the case where it is assumed that the two data samples are from populations with equal variances, the test statistic under the null hypothesis has Student's *t* distribution with  $n + m - 2$  degrees of freedom, and the sample standard deviations are replaced by the pooled standard deviation  $S_{eq}$ . In the case where it is not assumed that the two data samples are from populations with equal variances, the test statistic under the null hypothesis has an approximate Student's *t* distribution with a number of degrees of freedom given by Satterthwaite's approximation. This subtype test which is an adaptation of Student's *T*-test, with the unequal variances, is sometimes called Welch's *T*-test. The *T*-test statistic is stated in general as follows:

$$t = \frac{\bar{x} - \bar{y}}{\sqrt{\frac{S_x^2}{n} + \frac{S_y^2}{m}}},$$

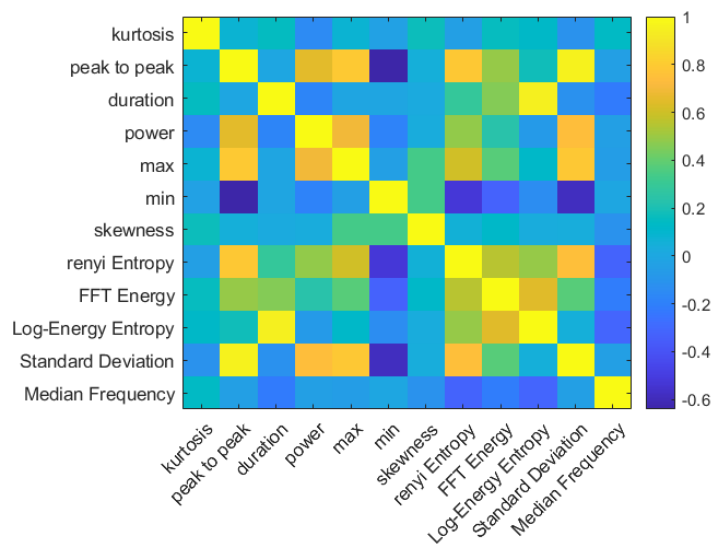
$$S_{eq} = \sqrt{\frac{(n-1)S_x^2 + (m-1)S_y^2}{n+m-2}},$$

where the means are  $\bar{x}$  and  $\bar{y}$ , the sample standard deviations are  $S_x^2$  and  $S_y^2$ , the pooled standard deviation when the variances are equal  $S_{eq}$ , and the sample sizes of the groups are  $n$  and  $m$ . For the final p-values, the Bonferroni correction was applied. This correction adjusts probability (p) values because of the increased risk of a type I error when making multiple statistical tests. In our case, the statistical tree includes 3 tests. The Bonferroni correction simply takes the standard cut-off points for a significant p-value and divides them by the number of tests that were performed. After that a "new" cut-off point p-value is created. In the following table is presented a ranking summary of the HFO feature values based on the final p-values of the previously explained statistical analysis tree:

<b>No.</b>	<b>Category</b>	<b>Feature</b>	<b>Ranking p-value</b>
<b>1</b>	Time Domain	Duration	<b>4</b> (2.69e-106)
<b>2</b>	Time Domain- Amplitude	Peak-to-peak	<b>7</b> (1.07e-39)
<b>3</b>	Time Domain- Amplitude	Max	<b>5</b> (1.43e-68)
<b>4</b>	Time Domain- Amplitude	Min	<b>11</b> (3.40e-18)
<b>5</b>	Frequency Domain	Mean Frequency	<b>16</b> (4.74e-09)
<b>6</b>	Frequency Domain	Median Frequency	<b>13</b> (5.46e-14)
<b>7</b>	Time Domain- Statistics	Standard Deviation	<b>10</b> (3.31e-18)
<b>8</b>	Frequency	SNR	<b>18</b> (1.8527e-2)
<b>9</b>	Frequency Domain - Energy	Energy FFT	<b>3</b> (3.24e-140)
<b>10</b>	Time-Frequency Domain	Power Estimate (PSD)	<b>12</b> (3.31e-15)
<b>11</b>	Frequency Domain - Entropy	Renyi Entropy	<b>1</b> (7.59e-151)
<b>12</b>	Frequency Domain - Entropy	Log-Energy Entropy	<b>2</b> (5.35e-145)
<b>13</b>	Frequency Domain - Entropy	Shannon Entropy	<b>6</b> (4.20e-57)
<b>14</b>	Time Domain- Statistics	Kurtosis	<b>9</b> (1.3321e-25)
<b>15</b>	Time Domain- Statistics	Skewness	<b>8</b> (8.89e-34)
<b>16</b>	Time Domain- Complexity	Hjorth Mobility	<b>17</b> (7.137e-06)
<b>17</b>	Time Domain- Complexity	Hjorth Complexity	<b>14</b> (3.182e-11)
<b>18</b>	Time Domain- Complexity	Higuchi Fractal Dimension	<b>20</b> (3.674e-1)
<b>19</b>	Time Domain- Complexity	Hurst Exponent	<b>19</b> (1.071e-1)
<b>20</b>	Time Domain-	Interquartile range	<b>15</b> (6.68e-25)

	Statistics		
--	------------	--	--

The existence of correlated features in isolation makes it possible to select important, but redundant features too. The obvious consequences of this issue are that too many features are chosen and, as a result, collinearity problems arise. To avoid collinearity, we moved on to a multivariate feature selection approach, such as the following correlation filter method that is shown below by using Pearson's correlation coefficients. Multivariate filter methods evaluate the entire feature space, test the relation amongst all features in the vector and identify the most correlated. In this figure, we can see depicted the most correlated features of two optimal subsets of features for all patients. We can see the positive correlation between max and peak-to-peak features or between entropies. Also, some interesting correlations are the negative correlation of min and peak-to-peak value, as well as the positive correlation between power and max values.



The Pearson correlation coefficients is a popular statistical measure, used to summarize the strength of the linear relationship between two data variables, which can vary between 1 and -1. The coefficient returns a value between -1 and 1 range, representing the limits of correlation from full negative to a full positive correlation. When the values of one variable increase as the values of another increase, then there is a positive correlation or else values between 0 and 1. On the other side, when the values of one variable decrease as the values of another increase, that means negative correlation or values between 0 and -1. The value must be interpreted, where often a value above 0.5 or below -0.5 indicates a notable correlation and the other below values

suggests a less important correlation. A zero value means no linear correlation between the two variables. The value of the Pearson correlation coefficient is measured as in the following equation and is presented in a heatmap correlation of coefficients:

$$R_{xy} = \frac{\sum_{i=1}^n (x_i - \bar{x})(y_i - \bar{y})}{\sqrt{\sum_{i=1}^n (x_i - \bar{x})^2} \sqrt{\sum_{i=1}^n (y_i - \bar{y})^2}}$$

$$\Leftrightarrow R_{xy} = \frac{1}{N-1} \sum_{i=1}^n \left( \frac{x_i - \mu_x}{\sigma_x} \right) \left( \frac{y_i - \mu_y}{\sigma_y} \right) = \frac{cov(X,Y)}{\sigma^X \sigma^Y},$$

where  $\mu_x$  and  $\sigma_x$  are the mean and standard deviation of  $X$ , respectively, and  $\mu_y$  and  $\sigma_y$  are the mean and standard deviation of  $Y$ . The need for the two data samples to have Gaussian or Gaussian-like distribution.

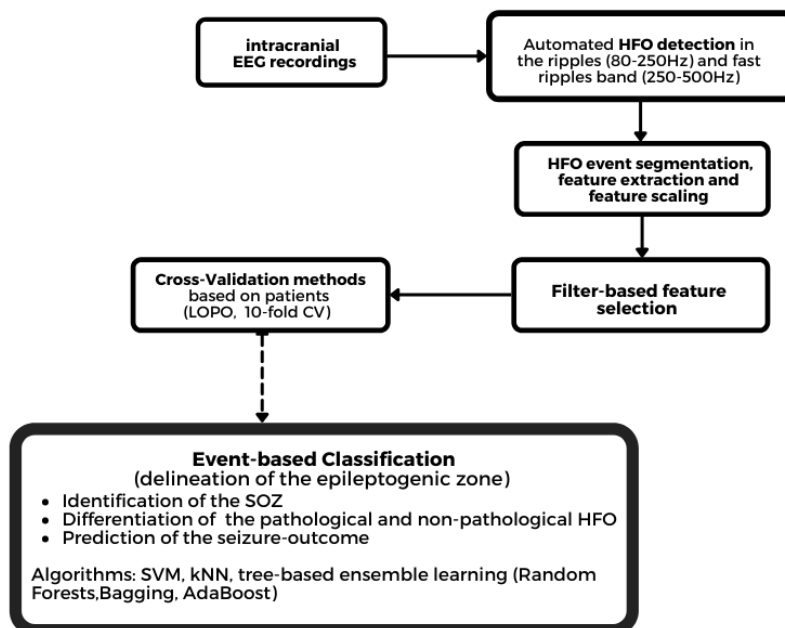
These filter feature selection methods, statistical and correlation, were applied before the classification of the events. Inside the cross-validation we used intrinsic or else embedded methods to measure the feature importance, as part of the learning process during training, on decision trees. The selected intrinsic method for Feature Importance was based on the Gini Impurity Index. Before moving on to the classifiers, feature normalization is required as the features have different ranges and is important to avoid bias. Normalization, also known as Min-Max scaling, is a scaling technique in which values are shifted and rescaled, so that they end up ranging between 0 and 1. Standardization is another feature scaling technique, where the values are centered around the mean with a unit standard deviation. Except SVM, K-nearest Neighborhood is also a distance-based machine learning algorithm, that is strongly affected by the range of the features and as a result feature scaling helps the classifier to perform better and faster. With standardization, the means of the attributes become zero and the resultant distribution has a unit standard deviation.

## Machine Learning Classification Approach

### Event-based Classification

In this classification problem, our goal is to categorize into two classes the normal and abnormal events related to the epileptogenesis. As defined previously, the HFO events that correspond to the red channels designate the pathological HFO area or else the epileptogenic area (resected + highest HFO rated channels) and the events that correspond to the salmon channels (remaining channels), designate the non-pathological HFO area or else the non-epileptogenic area. By solving this classification

problem, we differentiate the epileptic HFOs to the non-epileptic, identify the clinical SOZ and prove that by adding the highest HFO rated events into the epileptic area marked by the experts, we achieve very good results in predicting the seizure freedom not only intra-patient but also amongst all patients and subsets of them. Our reverse engineering approach on the classification problem, led us to apply and experiment amongst different supervised machine learning algorithms. All classifiers have been applied to normalized features. The first algorithms in the list were SVM and kNN, which had similar mediocre performance, then tree-based ensembles were tested and successfully increased the overall performance. The performance metrics of the proposed method were accuracy, specificity, sensitivity, recall and F1-score. Also, confusion matrixes are presented to explore the trade-off between different kinds of misclassification. Both the assessment of the classifier's report and the feature selection procedure were conducted following a double Cross Validation intra-subject. To ensure the robustness and generalization in the inter-subject case with the 20 patients, we implemented model optimization and the best cross validation strategy that followed according to its performance was the Leave One Out Cross Validation (Leave One Patient Out).



## Support Vector Machines

First on the algorithms' list was to test how an SVM classifier performs with different kernels. The quality of the features is highly important and largely determines the SVM classification performance results. **Support Vector Machines (SVM)** is one of the most popular machine learning algorithms with a rigorous theoretical foundation, commonly used for classification and regression analysis [106], [107]. In the literature, SVM has been widely used on EEG data for training predictive models. An SVM classifier, usually separates a given set of binary labelled training data and a hyperplane that is maximally distant from it, by finding the maximum margin. In its simplest form, an SVM is a linear classifier with a line as hyperplane, that is selected as the best separator between two classes, for example either class 1 epileptic HFO area or class 1 non-epileptic area salmon events. However, there are many cases (including ours), that the data are not linearly separable and the SVM needs to be solved non-linearly by using kernel tricks (mapping the feature set to a new space that the separation between classes becomes clearer), and then we can improve its performance by tuning optimization parameters[108]. A practical advantage of SVM is that even with high-dimensional data, different kernels can be plugged into the same learning machinery and studied independently of it. The best decision boundary and thus the optimal hyperplane is obtained by maximizing the margin between the different feature sets of the class. Margin is the distance between the hyperplane and the closest pattern (called support vectors) in each data class as shown in this figure 24:

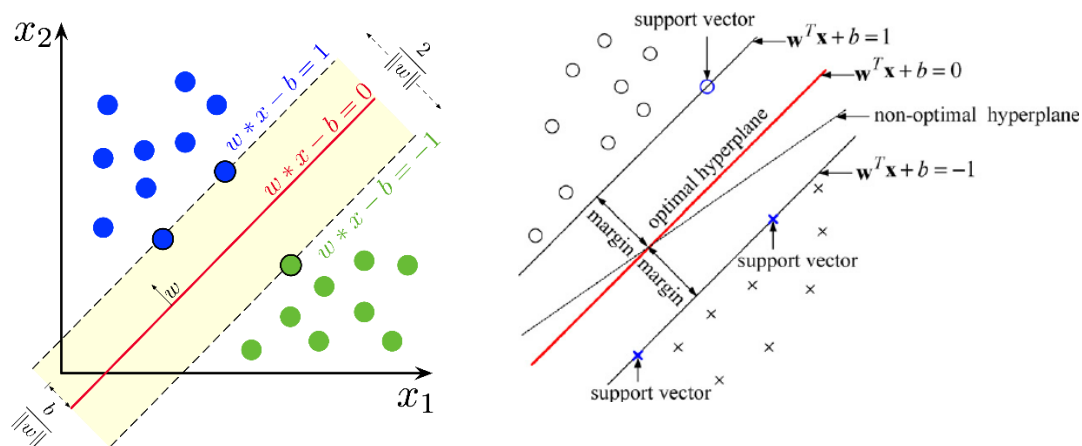


Figure 26 The core idea of SVM classifier (Source: Wikipedia)

The goal of the algorithm is to choose a separating hyperplane  $(w \cdot x_i + b) = 0$  which maximizes the interval between hyperplanes  $H_1 (w \cdot x_i + b) = -1$  and  $H_2 (w \cdot x_i + b) = 1$ . This goal is implemented by assuming that all the training data satisfy the following restrictions:

$$y_i(w \cdot x_i + b) \geq 1 \quad (5),$$

where  $y_i$  is the corresponding requested value. If  $y_i = 1$  then this means that  $x_i$  belongs to class 1 and if  $y_i = -1$  then it belongs to class 2. The distance of dotted hyperplane H1 from the beginning of the vector is  $|b| + 1/\|w\|$  and respectively the distance of H2 from the beginning of the vector is  $|b| - 1/\|w\|$ . So, the distance between H1 and H2 is  $2/\|w\|$  and the goal is to find the optimal pair that gives the maximum space by minimizing the quantity  $\|w\|$  considering the previous restrictions. This problem is followed by the Lagrange formulation. Given the Lagrange positive multipliers for any inequality constraint the Lagrange formulation and the primal problem consist of:

$$L_p = \frac{1}{2} \|w\|^2 - \sum_i \alpha_i [y_i(w x_i - b) - 1]$$

$$\min_{w,b} \left\{ \max_{\alpha_i} L_p \right\}$$

where  $\alpha_i$  are Lagrange multipliers  $\forall \alpha_i \geq 0$ .

After substituting the Karush-Kuhn-Tucker conditions (Gale 1951) into the primal Lagrangian, we derive the dual Lagrangian  $L_D$  and maximize it, subject to the following constraints :

$$L_D = \sum_i \alpha_i - \frac{1}{2} w(\alpha)w(\alpha)$$

$$w(\alpha) = \sum_i \alpha_i y_i x_i$$

$$\max_{\alpha_i} L_D \quad \text{subject to } \alpha_i \geq 0, \sum_i \alpha_i y_i = 0$$

Those points  $i$  for which the equation  $y_i(w \cdot x_i + b) \geq 1$  holds are called support vectors. After training the support vector machine and deriving Lagrange multipliers (they are equal to 0 for non-support vectors) one can classify by the vector of parameters  $\chi$  using the classification rule. Given a new data point  $x$  in the classifier, a label is assigned to it according to its relationship to the decision boundary and the corresponding function:

$$f(x) = \text{sign}(\langle w, \varphi(x) \rangle - b)$$

The SVMs can also be easily generalized to special linear cases by adding into the equation (5) slack variables  $\xi_i$  and tuning the restrictions with a new cost parameter  $C$ . The new parameter  $C$  characterizes the generalization of the classifier. Then we have:

$$y_i(w \cdot x_i + b) \geq 1 - \xi_i, \quad \xi_i \geq 0 \quad \forall i.$$

By working in a similar way to the first case, we solve the problem where the new restrictions are slightly different given  $C$ :

$$0 \leq \alpha_i \leq C$$

$$\sum_i \alpha_i y_i = 0$$

It is worth noting that all the training vectors appear in the dual  $L_D$  only as scalar

products. This means that we can apply various kernel functions  $\Phi$  to transform all the data into a high dimensional Hilbert feature space and use linear algorithms there:

$$\Phi: \mathbb{R}^N \rightarrow \mathbb{H}, \quad K(x, \hat{x}) = \Phi(x) \cdot \Phi(\hat{x}).$$

Some basic and commonly used kernel functions are linear, polynomial, RBF, sigmoid, and mathematically represented as follows:

- $K_{linear}(x_1, x_2) = x_1^T x_2$ ,
- $K_{polynomial}(x_1, x_2) = (x_1^T x_2 + 1)^d$ ,  $d$ : polynomial order
- $K_{sigmoid}(x_1, x_2) = \tanh(\gamma x_1^T x_2 + C)$
- $K_{RBF}(x_1, x_2) = e^{-\frac{\|x_1 - x_2\|^2}{2\sigma^2}} = e^{-\gamma \|x_1 - x_2\|^2}$ ,  $\gamma = \frac{1}{2\sigma^2}$

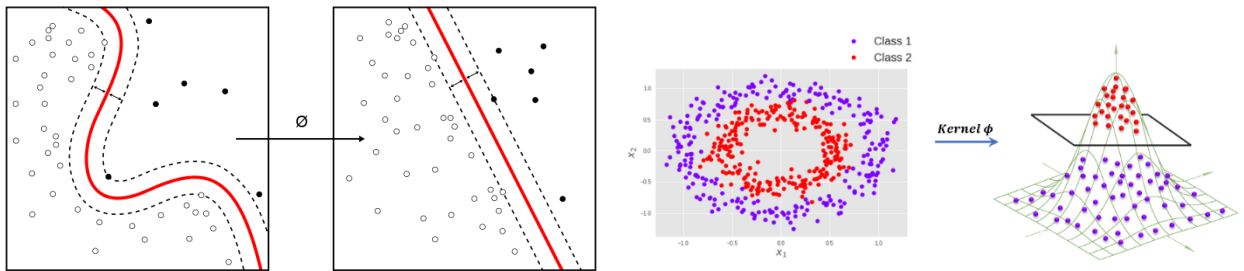


Figure 27 non-linearly separable data on the left, and after the kernel trick on the right the data is linearly separable in the feature space obtained by the kernel (source Wikipedia)

When the data is non-linearly separable, which happens in most of the real-world data problems, then we choose to allow some margin violation, because it is better to have a larger margin, even though some constraints are being violated. This approach is a soft-margin SVM. In this case, some datapoints will be in the incorrect side of the hyperplane misclassified. The loss of a misclassified point is called a slack variable and is added to the primal problem that we had for hard margin SVM. The slack variables add flexibility for misclassification in the classifier and is the main difference between hard and soft margin. A new regularization parameter  $C$  is measuring the tradeoff between minimizing the misclassification error and maximizing the margin. Practically, the important tuning parameters by the user are the gamma and  $C$ . The parameter gamma is related to how spread is the decision region, and the parameter  $C$  expresses the penalty for misclassifying a data point. Logarithmic scale values are usually used as a search area for gamma and by grid-searching  $C$  takes power of 10 values. A large value of  $C$  results in a low bias and high variance (soft margin) leading to underfitting, whereas a small value of  $C$  in a higher bias and lower variance (hard margin) leading to overfitting.

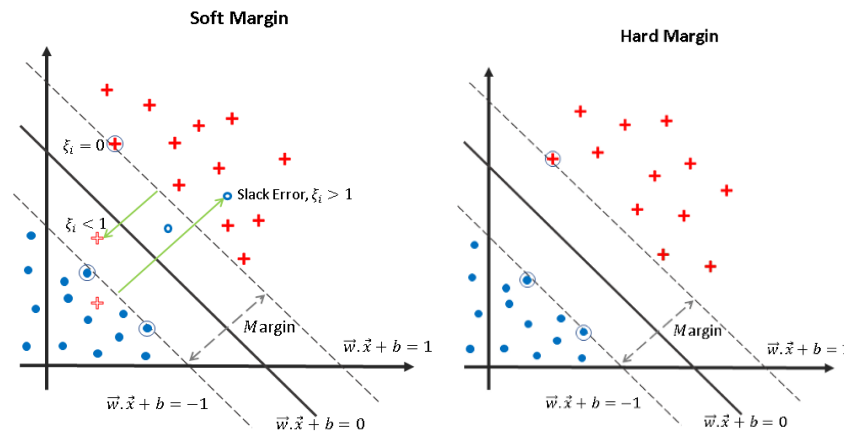


Figure 28 Hard Margin Vs Soft Margin source by Donthi Suraj

In this work, two main non-linear SVM classifiers were applied, one with a sigmoid kernel and one with a radial basis function (RBF). The input feature vector is already normalized but is recommended to be scaled with respect to a feature before being applied to the kernel function. When the absolute values of some features are very large or range widely, their inner product can be dominant in the kernel calculation. To prevent this from happening, we use a kernel scale in the RBF case that helps also to maintain the information. The RBF kernel function computes the similarity between data points. In the RBF kernel type, ' $\sigma$ ' is the variance and main width hyperparameter, and  $\|X_1 - X_2\|$  is the Euclidean distance (L2-norm) between two points  $X_1, X_2$ . Gamma parameter is inversely proportional to  $\sigma$  and can be seen as the inverse of the radius of influence of samples selected by the model as support vectors. It is evident from the kernel type, that the width of the region of similarity changes as  $\sigma$  changes. Finding the right  $\sigma$  for a given dataset is crucial and can be done by using hyperparameter tuning techniques like grid search cross validation. The gamma parameter defines how far the influence of a single training example reaches, with low gamma values meaning 'far' and high values 'close'. When gamma is very small, the model is too constrained and cannot capture the complexity or "shape" of the data.

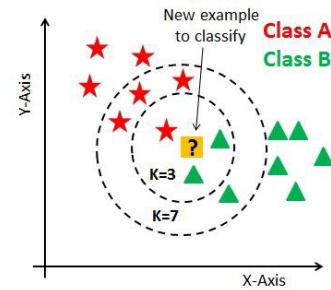
C is a trade-off between training error and the flatness of the solution. The larger C is the less the final training error will be, but usually increases the time needed for training, too. By increasing C too much, we risk losing the generalization properties of the classifier, because it will try to fit as best as possible all the training points. The goal is to find a C that keeps the training error small, but also generalizes well. In MATLAB, we can easily find the optimal hyperparameters of our model, that minimize the cross-validation loss, by using Bayesian optimization. The sigmoid kernel function was tested with different gamma values, but the results were not as good as with the radial basis function, especially intrasubject. For the implementation of SVM algorithms, we utilized those offered by the Statistics and Machine Learning Toolbox in MATLAB

software environment.

### k- Nearest Neighborhood

Another fundamental algorithm in supervised machine learning is the distance-based k-Nearest Neighborhood (k-NN), used both for regression and classification purposes. This non-parametric algorithm calculates the distances between the test data and all the training points in order to predict correctly its class. There are many distance metrics available for k-NN classification

except euclidean distance with different effects, such as correlation, Minkowsky, Chi square, Manhattan (also known as city block), Mahalanobis, Cosine, Hamming, and others. In k-NN classifier,  $k$  is the number of the nearest neighbors that are used to classify new points and is a tuning parameter that requires testing and validation. After setting the  $k$  number, the  $k$ -nearest neighbors of the test data are found and the test data is classified by a plurality vote of its neighbors. Generally, odd values of  $k$  are preferred to avoid confusion between two classes and a common way of finding an approximate default value of  $k$  is to square root the total number of data points in the dataset. K-NN requires feature scaling, because distance measures are sensitive to magnitudes and with the scaling all the features are weighted equally. This classifier works by classifying the new data points based on the similarity measure of the earlier stored data.



### Decision Trees

A decision tree is a non-parametric modelling approach that goes from observations about an item to conclusions about the item's target values, that are represented as decisions in its leaves. Decision trees learn from data to approximate a sine curve in a tree structure with condition states and if-then-else decision rules. The term classification and regression trees (CART) is an umbrella term used to refer to either of the above procedures, classification or regression and it was first introduced in 1984 [109]. For the classification trees, each leaf of a tree is labeled with a class or a probability distribution, signifying that the data has been classified into a certain subset of class. A decision tree is built by splitting the source set of data, constituting the root node of the tree into subsets—which constitute the successor children-nodes.

The deeper a tree goes, the more complex the decision rules are, and the model becomes fitter.

The splitting, which is a process of partitioning the data, is based on a set of splitting criteria based on classification features. The concept of constructing decision trees usually works top-down, by selecting a variable at each step that best splits the set of items. There are different algorithms that use different metrics for measuring the best splitting procedure. Generally, they measure the homogeneity of the target variable, and they provide a different metric for the quality of split. Two of the most common metrics are Gini impurity and Information Gain. In decision trees, “impurity” is a score used when deciding to split a node. The most common impurities are the Gini Impurity and Shannon Entropy. An improvement on the Gini impurity is known as “**Gini importance**” while an improvement on the Entropy is the **Information Gain**.

Some of the advantages of decision trees are that are interpretable and easy to understand, they can handle both numerical and categorical data, handle non-linear parameters efficiently and work fast. However, decision trees tend to overfit and lose their generalization capabilities, especially when they are particularly deep. Finally, they are not suitable for large data sizes, because one tree may grow complex and lead to overfitting. For that reason and to overcome the drawbacks of decision trees, Random Forest is often recommended, because RF is not relied on a single tree.

Another common feature selection technique that we used is feature importance ranking from tree-based models. The feature importances are essentially the way of the individual trees to improve in the splitting criterion and process. In other words, it is how much the score “impurity” was improved when splitting the tree using that specific variable. These methods can be used to rank features and then select a subset of them. However, the feature importances should be used properly, as they suffer from biases and sometimes present an unexpected behavior regarding highly correlated features. Regardless of how strong and fast they are, the random forest feature importances are biased when features that have different and a lot of categories exist in the vector. Besides, if two features are highly correlated, both of their scores largely decrease, regardless of the quality of the features.

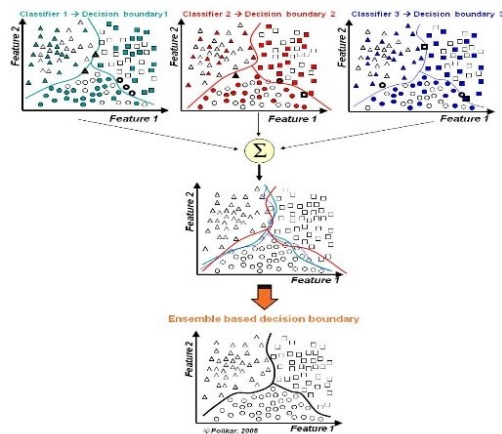


Figure 29 Combining classifiers with different decision boundaries reduce error (Source Scholarpedia).

## Ensemble learning

Ensemble systems or else ensembles are obtained by combining multiple diverse models, such as multiple classifier systems in our classification problem. One of the first questions that arise at complex classification concepts are related to the selection of the most appropriate classifier given our data. Ensemble systems can be often – just like in our case- surprisingly effective and useful when dealing with lack of adequate data (intra-patient) or with large volumes of data (inter-patient). The core idea of ensemble learning can be interpreted by looking into our daily lives. When we take advice and opinions from multiple experts before taking a final decision about a medical procedure, when we read different reviews from multiple sources before a purchase, when we evaluate job profiles from their references, then we follow the ensemble learning strategy. By combining all the individual decisions of several experts instead of one, at the end we are able to take an optimal decision without being biased or irrational. Therefore, ensemble methodology imitates our need to seek several opinions before making a crucial decision [110]. In applied machine learning, ensembles are strategically generated and combined to improve the model's performance, by minimizing the likelihood of an unfortunate poor model selection.

## Random Forests

Random Forest as an ensemble learning algorithm, is used for both regression and classification purposes. Trees used for regression and trees used for classification have some similarities, however they also have some differences, such as the splitting procedure (how to split). A random forest is simply a collection of decision trees whose results are aggregated into one final result. Every individual decision tree is constructed using a bootstrap version of the training data. The original training data is randomly sampled-with-replacement generating small subsets of data, known as bootstrap samples. Then these bootstrap samples are fed as training data to many

decision trees of large depths. Each of these decision trees is trained separately on these bootstrap samples. This aggregation of decision trees is called the Random Forest ensemble. Prediction of new samples is made through a majority voting system between trees, where the class that has collected the most votes from all the decision trees, becomes the final prediction outcome of the model. While the RF is inherently stochastic, it is considered to be robust to noise and remains resistant to overfitting. This concept is also known as Bagging or Bootstrap Aggregation. The fundamental difference of Bagging and general Random Forests is that in Random forests only a subset of features is selected at random out of the total. The best split feature from the subset is used to split each node in a tree, unlike in the method of bagging where all features are considered for splitting each node. Finally, out of bag score is a way of validating the RF model and is computed as the number of correctly predicted rows from the out of bag sample. The error rate in the “out of bag” samples of all trees in the forest is the estimate of the generalization error of the final model. An interesting aspect of Random Forest is that it can be also utilized for feature importance during training by using the Gini impurity index. The Gini index is a measure of node impurity. This impurity criterion is non-parametric. For a binary split, the Gini index of a  $t$  node can be calculated as follows:

$$G(t) = 1 - \sum_{j=1}^2 p(j)^2 ,$$

where  $p$  is the frequency of each  $j$  class passing through that node. A node with just one class (a pure node) has zero Gini index, otherwise the Gini index is positive. The specific feature is important in partitioning data into two separate classes, if the Gini index is low (here, target is pathological HFO, and control is non pathological HFO). More specifically, a tree with structure  $T$  that is trained on a learning sample of size  $N$ , has a goal to identify at each  $t$  node, a split  $s_t$  for which the sample  $N_t$  that pass through the node, is split into two child nodes  $t_R$  and  $t_L$  by maximizing the decrease that follows:

$$\Delta G(s, t) = G(t) - p_L G(t_L) - p_R G(t_R) ,$$

where  $p_L = N t_L / N_t$  ,  $p_R = N t_R / N_t$  . By adding all the weighted decreases of all  $t$  nodes using a specific feature and with  $X_m$  averaged over all trees, one can obtain the mean decrease in Gini (MDG) index as follows:

$$MDG(X_m) = \frac{1}{N_T} \sum_T \sum_{t \in T: u(s_t) = X_m} p(t) \Delta G(s, t)$$

where  $p(t) = N_t / N$  ,  $N_T$  is the number of trees in the forest, and  $u(s_t)$  is the feature used in the split of  $t$  node. MDG index reflects the average of a variable's total decrease in node impurity, weighted by the proportion of samples reaching that node across all trees of the ensemble model.

In this work, we estimated the MDG index for different subsets of features across many

independent runs of the RF model. It is performed feature selection during training, and we average the results to eliminate the stochastic nature of the algorithm, so as to ensure a stable feature ranking. In every run we keep up to 5 features, with the highest MDG indices, that are considered to be the most important features. When two or more models with feature ranking subsets are tied in terms of performance, we choose the model with the fewer features. In the current work,

For our computations, we used the MATLAB Toolbox Statistics and Machine Learning that offers two main objects that support bootstrap aggregation (bagging – bagged trees) `TreeBagger` and `ClassificationBaggedEnsemble`. The number of predictors-trees in the “forest” was set to 100 and the parameter concerning the number of features analyzed at each node to find the best split was set equal to the square root of the number of features. Similar approaches are followed by other studies [61, 62, 66].

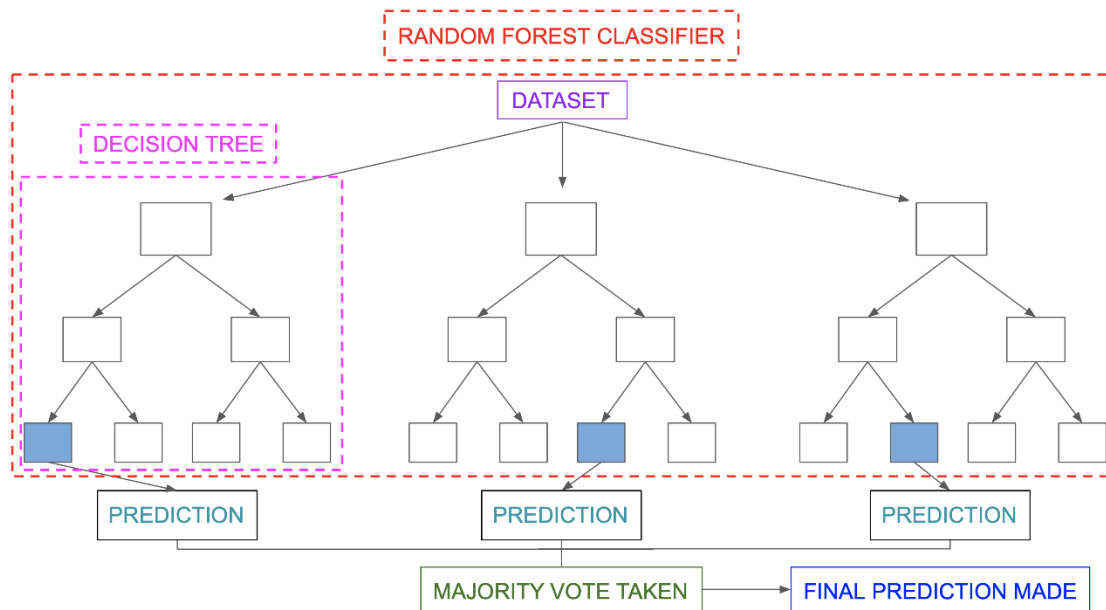


Figure 30 Simplified RF Classification (Source: Medium). A RF Classifier consists of numerous decision trees. Every decision tree has a root node, decision nodes and leaves. The leaf node is the final output-product of each tree. The final prediction of Random Forests follows a majority voting system.)

### Bagging and Boosting

Bootstrapping and Aggregation combined, form one ensemble model technique called Bagging. This technique was first proposed by Breiman (1996a,1996b). According to Wikipedia, Breiman's Random Forest algorithm is "Breiman's 'bagging' idea and random selection of features." This bagging idea is actually performed as a step within the Random Forest algorithm. In bagging, *all features* are considered for splitting a node, unlike in Random forests, where *only a subset of features* is selected at random out of the total and the best split feature from the subset is used to split each node in a decision tree. The main goal of this general technique that can be used in various

problem settings (both with classification and regression), is to reduce the variance and therefore improve tree-based predictions. The idea of bagged trees is relatively easy to understand. Given a sample dataset, many bootstrapped subsamples are pulled. A Decision Tree is formed on each of the bootstrapped subsamples. Then, a prediction is applied to each bootstrap sample and finally the results are aggregated (in case of classification simple voting system and in case of regression by averaging). In the final total prediction the variance will be reduced due to the Bagging's principle of averaging.

Boosting is another ensemble approach close to bagging, but with a basic difference. In bagging, the models run in parallel and are independent on each other whereas in boosting the models run in sequence and depend on the previous models. This is the model's key way of learning from previous mistakes. In contrast with bagging (simple averaging or voting system for the overall prediction), boosting weights each training example by how incorrectly was missclassified in an iterative procedure. An interesting aspect of boosting is the ability to track Therefore, boosting set of algorithms is generally less affected by overfitting. Boosting algorithms often use weak learners (i.e. low accurate classifiers) with the purpose to finally create a powerful "committee", a strong learner (i.e highly accurate classifier). A common weak learner often used in boosting is a two node tree (one level), called stump. One of the most popular boosting techniques, suitable for binary classification that was also used in this work, is Adaptive Boosting, referred as AdaBoost algorithm.

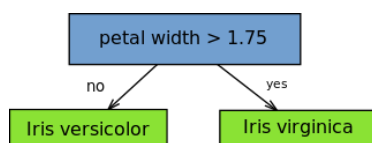


Figure 32 Example of A Weak Learner: Stump (Source: Wikipedia)



Figure 31 Framework for Ensemble Learning by MathWorks [113]

## AdaBoost

Adaptive Boosting (AdaBoost) algorithm was first developed and proposed by Freund and Schapire (1996). Boosting is considered one of the most competitive and powerful machine learning ideas conceived during 1990s. For that reason, AdaBoost gained very quickly a massive popularity. Adaptive means that the algorithm uses multiple

iterations to generate a single composite strong learner. There are two main versions of Adaboost and in this work we used *AdaBoost.M1* from Statistics and Machine Learning Toolbox in MATLAB. *AdaBoost.M1* is in general preferred in binary classification problems, whereas *AdaBoost.M2* in multiclass classification. Adaptive Boosting uses very shallow trees, often with one level referred as stumps. The order of stumps is very useful and important in AdaBoost.

Initially, the algorithm starts by selecting randomly a training subset. On iteration, AdaBoost model is being trained by selecting each time the train set based on the accurate prediction of the previous training. In that way, the model is actually practicing self-learning. Then, it assigns the heigher weight to wrong classified observations, in oder to give to these observations in the next iteration high probability for classification. This is done by assigning also the weight to the trained classifier in each iteration according to the accuracy of the classifier. The higher weight goes to the more accurate classifier. All these steps are iterating until the complete training set fits without any error or in most cases until reached the maximum number of estimators (hyperparameter). Finally, AdaBoost performs classification by “voting” across all of the learning-built models. The algorithmic steps of AdaBoost are further explained in [112] and performed comprehensively in the following frame:

1. Initialize the observation weights  $w_i = 1/N$ ,  $i = 1, 2, \dots, N$ .
2. For  $m = 1$  to  $M$ :
  - (a) Fit a classifier  $G_m(x)$  to the training data using weights  $w_i$ .
  - (b) Compute
 
$$\text{err}_m = \frac{\sum_{i=1}^N w_i I(y_i \neq G_m(x_i))}{\sum_{i=1}^N w_i}.$$
  - (c) Compute  $\alpha_m = \log((1 - \text{err}_m)/\text{err}_m)$ .
  - (d) Set  $w_i \leftarrow w_i \cdot \exp[\alpha_m \cdot I(y_i \neq G_m(x_i))]$ ,  $i = 1, 2, \dots, N$ .
3. Output  $G(x) = \text{sign} \left[ \sum_{m=1}^M \alpha_m G_m(x) \right]$ .

Figure 33 AdaBoost algorithmic steps

## Experimental Scenarios, Results and Evaluation

### Evaluation Metrics and Techniques

For the evaluation of our results, we need to choose important metrics to ensure that our models are robust and can be generalized. The following performance metrics and validation strategies were applied in this work:

### Classification Report

Some of the most important performance metrics are Accuracy, Sensitivity (sometimes called Recall), Specificity, Precision and F1 score. In our binary

classification problem, we define the statistical measures as follows:

- Sensitivity (Recall) =  $\frac{TP}{(TP+FN)}$
- Specificity =  $\frac{TN}{(TN+FP)}$
- Precision (PPV or Positive Predicted Value) =  $\frac{TP}{(TP+FP)}$
- Accuracy =  $\frac{(TP+TN)}{(TP+TN+FP+FN)}$
- F1 Score =  $\frac{2 \text{ Precision} \times \text{Recall}}{(\text{Precision} + \text{Recall})}$
- NPV (Negative Predictive Value) =  $\frac{TN}{(TN+FN)}$

Where in our binary problem we have two conditions P, which is the positive condition that means non-epileptic event and N, which is the negative condition that means epileptic event. As a result, we have the True Positives (TP), which is the number of cases correctly identified as non-epileptic, False Positives (FP), which is the number of cases incorrectly identified as epileptic, True Negatives (TN), which is the number of cases correctly identified as epileptic and False Negatives (FN), which is the number of cases incorrectly identified as non-epileptic. False Positives are often called type 1 Error (e.g. we predicted that an event is epileptic, while it's not actually) and False Negatives called type 2 Error (we predicted that an event is non-epileptic, while it is actually). Accuracy shows us overall how often our classifier predicts correctly. Precision shows us from all the cases that we have predicted as positive, how many were actually positive. F1-score is a useful metric, that represents the harmonic mean between precision and sensitivity, when a model has high precision and low sensitivity or vice versa, because it gives a more comparable balanced result in the classification report.

### **Confusion Matrix**

The confusion matrix gives us a representative visualization of the classifier's performance and it is widely used in many domains. In the table, each row represents the instances in an actual class, while each column represents the instances in a predicted class or vice versa. In our problem, sensitivity measures the proportion of true positives in the detection of events of interest, and specificity measures the proportion of true negatives. In the context of HFO event classification, sensitivity measures the proportion of actual non-epileptic HFOs correctly classified, and specificity measures the proportion of correctly classifying the epileptic HFOs. An

example of a confusion matrix layout with the evaluation metrics that we described before, it is shown in the following table.

		Predicted Class		
		Positive	Negative	
Actual Class	Positive	True Positive (TP)	False Negative (FN) Type II Error	<b>Sensitivity</b> $\frac{TP}{(TP + FN)}$
	Negative	False Positive (FP) Type I Error	True Negative (TN)	<b>Specificity</b> $\frac{TN}{(TN + FP)}$
		<b>Precision Value</b> $\frac{TP}{(TP + FP)}$	<b>Negative Predictive Value</b> $\frac{TN}{(TN + FN)}$	<b>Accuracy</b> $\frac{TP + TN}{(TP + TN + FP + FN)}$

## Validation Strategies

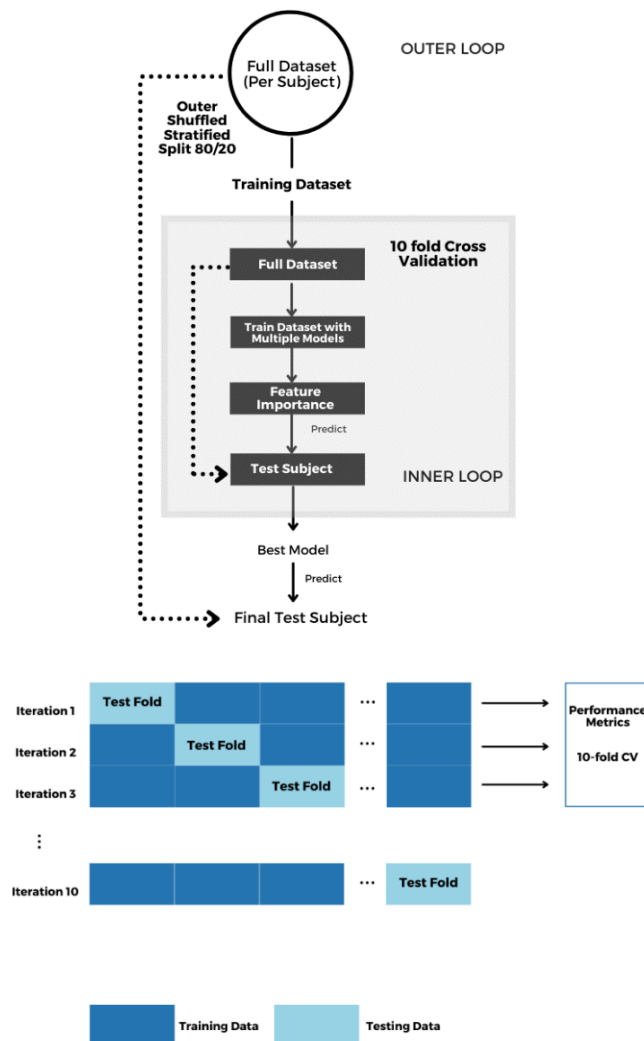
### Scenario 1 (Individual patient)

In the first scenario we demonstrate a ***nested cross-validation*** or else ***double cross validation*** that was necessary to overcome the problem of overfitting in our training dataset. In the training of an individual patient, the dataset available is imbalanced in many cases, including different seizure outcomes. More specifically, we avoided overfitting by splitting in the outer loop our dataset not randomly, but in a way that maintains the same distribution in each subset. This is a stratified split 80/20 and is called stratification method or stratified sampling, where the target variable is used to control the sampling process. The 80% will be the training dataset, which will be used in the inner loop as the new full dataset, and the 20% will remain unseen in the outer loop as test dataset that will be used in the final step. By using **stratified 10-fold cross-validation** in the inner loop, we ensure that the proportion of positive to negative examples found in the original distribution is respected in all the folds. In the inner loop at every fold of 10-fold CV we train multiple machine learning algorithms, such as SVM, k-NN, Random Forests. During the training of Random Forests, we get also the rankings from feature importance based on Mean Decrease Gini (MDG) index and it shows a great amount of redundancy inherent to the dataset. In the end of the 10-fold CV, we get the best model and make with it the prediction in the outer loop with the unseen test data. In the outer loop we evaluate the model's performance, while in the inner loop the classification procedure is being optimized (different supervised ML models). As a final result, the estimation of the final performance of our model with this technique remains unbiased and the selected features are more likely to be generalizable in case of unseen data.

The graphical representation of the double cross validation strategy with the inner 10-

fold CV applied in our experiments, are shown below:

Figure 34 Nested (Double) Cross Validation



## RESULTS SCENARIO 1

PATIENT 2 ILAE 1			
#EPILEPTIC=855 #NON-EPILEPTIC=252			
Metrics	Naïve Bayes	SVM	Bagging
Accuracy	76,55%	86,72% ± 0.3	95,75% ± 0.1
Sensitivity	-	97,19% ± 0.3	98,12% ± 0.2
Specificity	-	51,19% ± 0.6	87,69% ± 0.2
Precision	-	87,10% ± 0.3	96,43% ± 0.1
F1 Score	-	91,87% ± 0.4	97,27% ± 0.1

<b>PATIENT 10 ILAE 1</b>			
#EPILEPTIC=123 #NON-EPILEPTIC=46			
Metrics	<b>Naïve Bayes</b>	<b>SVM</b>	<b>Bagging</b>
Accuracy	70,58%	86,98% ± 0.3	92,89% ± 0.1
Sensitivity	-	97,56% ± 0.1	98,37% ± 0.1
Specificity	-	58,69% ± 0.2	78,26% ± 0.15
Precision	-	86,33% ± 0.2	92,36% ± 0.1
F1 Score	-	91,60% ± 0.15	95,27% ± 0.15

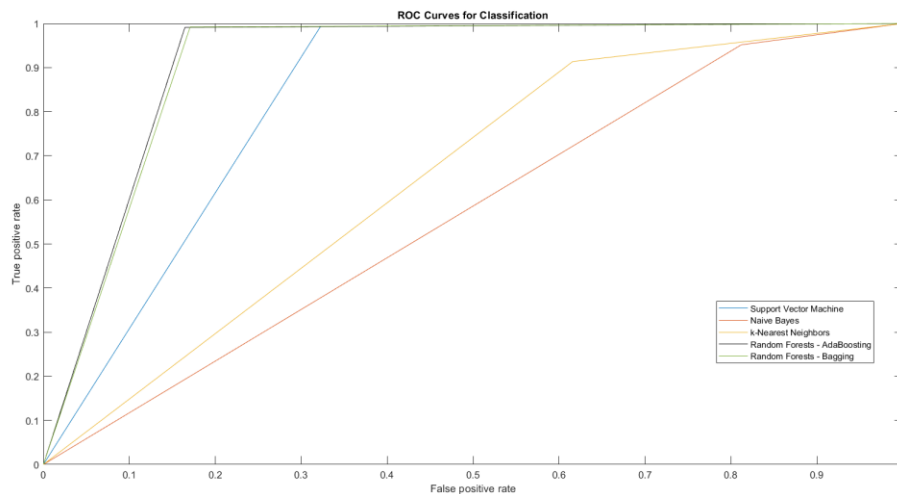
<b>PATIENT 8 ILAE 3</b>			
#EPILEPTIC=273 #NON- EPILEPTIC=192			
Metrics	<b>Naïve Bayes</b>	<b>SVM</b>	<b>Bagging</b>
Accuracy	59,57%	92,90% ± 0.2	97,41% ± 0.1
Sensitivity	-	96,33% ± 0.1	97,43% ± 0.1
Specificity	-	88,02% ± 0.3	97,39% ± 0.05
Precision	-	91,95% ± 0.2	98,15% ± 0.05
F1 Score	-	94,09% ± 0.1	97,79% ± 0.1

<b>PATIENT 9 ILAE 5</b>			
#EPILEPTIC =1110 #NON- EPILEPTIC=318			
Metrics	<b>Naïve Bayes</b>	<b>SVM</b>	<b>Bagging</b>
Accuracy	78,47%	87,39% ± 0.2	94,39% ± 0.1
Sensitivity	-	98,01% ± 0.3	98,82% ± 0.05
Specificity	-	50,31% ± 0.5	78,93% ± 0.15
Precision	-	87,31% ± 0.3	94,24% ± 0.1
F1 Score	-	92,35% ± 0.3	96,48% ± 0.1

<b>PATIENT 19 ILAE 6</b>			
#EPILEPTIC=747 #NON-EPILEPTIC=1326			
Metrics	<b>Naïve Bayes</b>	<b>SVM</b>	<b>Bagging</b>
Accuracy	65,11%	77,95% ± 0.3	91,31% ± 0.1
Sensitivity	-	52,20% ± 0.5	82,06% ± 0.2
Specificity	-	79,59% ± 0.3	96,53% ± 0.15
Precision	-	52,20% ± 0.5	93,01% ± 0.1
F1 Score	-	63,05% ± 0.3	87,19% ± 0.15

<b>PATIENT WITH ILAE 6</b>	
TOP FEATURES	<b>SCORES</b>
Kurtosis	0.0521
Duration	0.0220
Min	0.0122
Power	0.0054
Skewness	0.0037

Figure 35 ROC Curves in intra-subject prediction



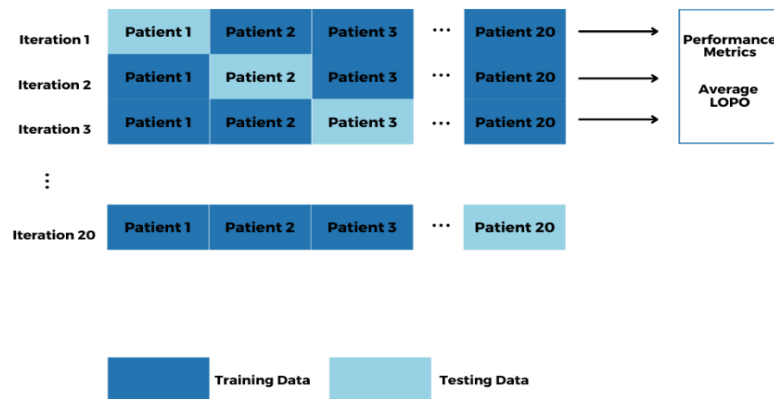
### **Scenario 2 (All patients - LOPO)**

In the current scenario, we use another validation strategy based on Leave One Out Cross Validation (LOOCV), which is the most robust way to test a model that contains data on a participant level. LOOCV is normally recommended to validate models built on smaller datasets where a standard test/train split may introduce significant bias into the model. After investigating intra-subject our dataset and all 20 patients separately, we move on to the overall classification of all patients with all the events. Leave-one-patient-out cross validation (LOPO CV) is a cross validation approach that utilizes each individual person as a “test” set. It is a specific type of k-fold cross validation, where the number of folds, k, is equal to the number of patients in the dataset. In each iteration for 20 patients, the model needs to train on 19 patients and is tested on the “left out” patient. As a result, the training size each time is consisted of the events from 19 patients and the test size of the events of one left-out patient, that becomes the test-subject. At the end, in order to assess the performance metrics of the entire model, we average all the performance reports for each leave one out subject.

We decided to apply a LOOCV in all patients, with a feature vector having averagely a size greater than 180.000 (num of observations) x 12 (num of features) in each iteration. The reason is that we wanted to make our model generalizable and because we had previously observed variations between some individual patients. However, LOPO is also the most computationally expensive amongst validation strategies with very low training speed in the overall process (In our case for 20 patients the training needs around 18 hours). Obviously, the training is slower, not just

because of the validation strategy, but also because of the classifiers dealing with a larger dataset. In the following results, we can see also the ranking of features (top 5 features for each subset) from the embedded feature importance-based selection. The final feature set is derived from internal feature rank after multiple iterations. For the Random Forest, the features selected repeatedly in the internal are used in the external validation.

Figure 36 Leave One Patient Out (LOPO CV)



## RESULTS SCENARIO 2

PATIENTS WITH ILAE 1	
TOP FEATURES	SCORES
Renyi Entropy	0.0523
Peak-to-peak	0.0324
Log-Energy Entropy	0.03032
Kurtosis	0.0234
Duration	0.0089

PATIENTS WITH ILAE 3	
TOP FEATURES	SCORES
Max	0.04724
Power	0.0316
Duration	0.0182
Renyi Entropy	0.0065
Log-Energy Entropy	0.0021

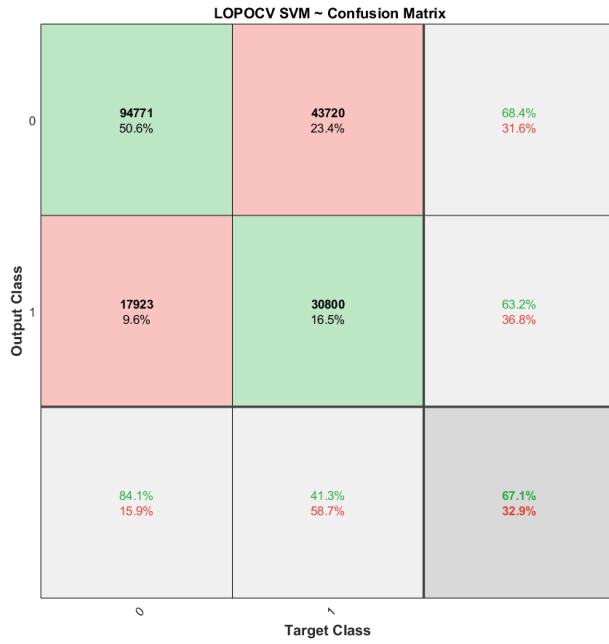
PATIENTS WITH ILAE 5	
TOP FEATURES	SCORES
Max	0.0852
Power	0.0728
Duration	0.0480
Renyi Entropy	0.0024

Log-Energy Entropy	0.0022
--------------------	--------

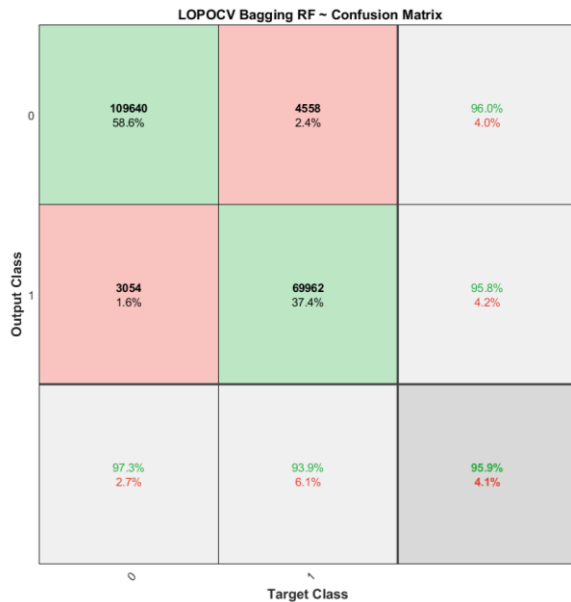
PATIENTS WITH ILAE 6	
TOP FEATURES	SCORES
Max	0.0521
Power	0.0220
Duration	0.0122
Renyi Entropy	0.0054
Log-Energy Entropy	0.0037

Average Leave One Patient Out CV				
#EPILEPTIC=90174 #NON-EPILEPTIC=97040				
Metrics	SVM	k-NN	Bagging	AdaBoost
Accuracy	67,12% ± 0.2	71,92% ± 0.1	95,92% ± 0.3	95,92% ± 0.3
Sensitivity	68,46% ± 0.3	75,01% ± 0.2	96,00% ± 0.3	96,01% ± 0.3
Specificity	63,24% ± 0.3	66,32% ± 0.3	95,79% ± 0.2	95,70% ± 0.2
Precision	84,10% ± 0.2	79,92% ± 0.1	97,32% ± 0.3	97,23% ± 0.3
F1 Score	75,47% ± 0.2	70,39% ± 0.2	95,89% ± 0.3	95,85% ± 0.3

		ACTUAL VALUES	
		0 (non-epileptic)	1 (epileptic)
PREDICTED VALUES	0	51.61% (TP) 94771	8.57% (FP) 17923
	1	22.35% (FN) 43720	17.45% (TN) 30800



		ACTUAL VALUES	
		0 (non-epileptic)	1 (epileptic)
PREDICTED VALUES	0	58.56% <b>(TP)</b> 109640	2.3% <b>(FP)</b> 4558
	1	1.62% <b>(FN)</b> 3054	37.37% <b>(TN)</b> 69962

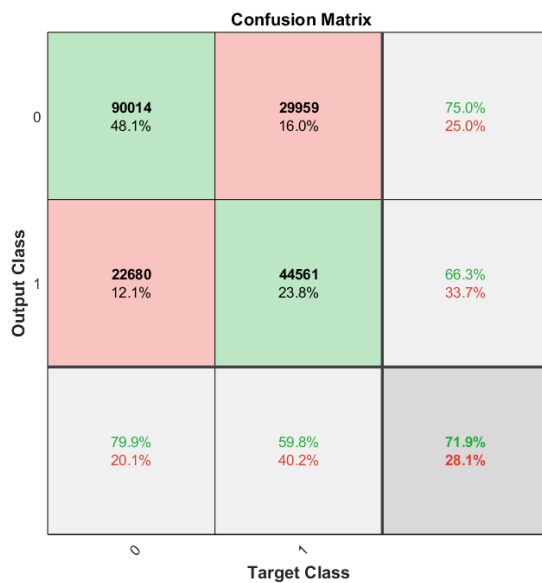


**ADAbost LOPOCV**



		ACTUAL VALUES		
		AdaBoost	0 (non-epileptic)	1 (epileptic)
PREDICTED VALUES	0	58.56% <b>(TP)</b> 109520	1.7% <b>(FP)</b> 3174	
	1	2.4% <b>(FN)</b> 4492	37.37% <b>(TN)</b> 70028	

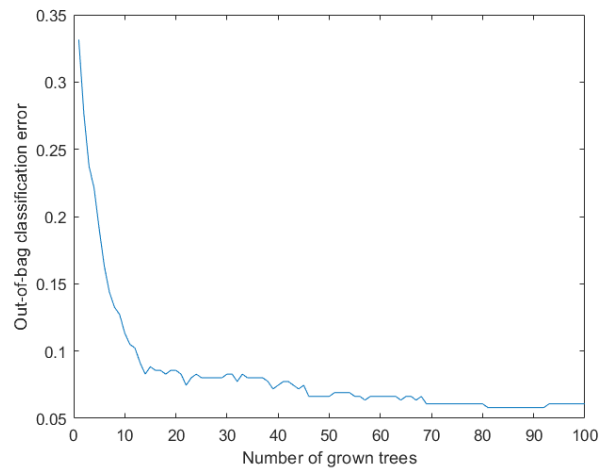
**k-NN LOPOCV**



		ACTUAL VALUES	
--	--	---------------	--

PREDICTED VALUES	k-NN	0 (non-epileptic)	1 (epileptic)
	0		48.04% (TP) 90014
1		15.00% (FN) 29959	24.80% (TN) 44561

Figure 37 Out Of Bag Error in Bagging RF, expresses the misclassification probability during training



### Hyperparameter Tuning

For each classifier, an iterative approach was followed in order to tune our model with the best set of optimal hyperparameters during training. By grid searching, we tried to find this optimal combination of hyperparameters. At first, we checked several default and proposed parameters in order to reject the less important, and then a 10-fold CV was performed, so as to select the best set of parameters that define the best model. In the literature, both SVM and tree-based algorithms are proposed with good results in dealing with intracranial data, but yet there is no way of knowing which is the best classifier in all cases, as it strongly depends on the datasets (and nature of the problem).

Algorithms	Hyperparameters (Tuning)	Training <sup>1</sup>	Comparison
<b>SVM (Non-linear)</b>	<ul style="list-style-type: none"> <li>▪ Kernel Function</li> <li>▪ Gamma</li> <li>▪ C</li> </ul>	Very Slow $O(n^2p+n^3)$	Generally good performance, but difficult to train inter-subject where the dataset is big
<b>k-NN</b>	<ul style="list-style-type: none"> <li>▪ Distance function</li> <li>▪ K</li> </ul>	Moderate	Mediocre performance, interpretable
<b>Decision Trees</b>	<ul style="list-style-type: none"> <li>▪ Max features</li> <li>▪ Split criterion</li> <li>▪ Min samples leaf</li> <li>▪ Min samples split</li> </ul>	Moderate $O(n^2p)$	Good performance, prone to overfitting
<b>Random Forests (Bagging)</b>	<ul style="list-style-type: none"> <li>▪ Max features</li> <li>▪ Split criterion</li> <li>▪ Min samples leaf</li> <li>▪ N estimators</li> </ul>	Slow $O(n^2p n_{trees})$	High performance intra-subject and inter-subject (medium and big datasets)
<b>Boosting</b>	<ul style="list-style-type: none"> <li>▪ Max features</li> <li>▪ Min samples leaf</li> <li>▪ N estimators</li> <li>▪ Learning rate</li> </ul>	Slow	High performance intra-subject and inter-subject (medium and big datasets)

Figure 38 COMPARISON TABLE OF ALGORITHMS

<sup>1</sup> In the training process,  $n$  is the number of training samples,  $p$  is the number of features and  $n_{trees}$  is the number of trees

## Chapter 5 Conclusions & Future Work

Drug-resistant patients constitute a significant percentage of clinical epilepsy, having the greatest burden of epilepsy-related disabilities. The best treatment choice for these complex cases is resective surgery. Multiple studies, have shown that HFO Zone is spatially associated with the Epileptogenic Zone and with HFO guidance in surgical treatment, we could increase the rate of seizure-free outcomes. Despite the encouraging findings over the last few years, there are still challenges and limitations for the establishment of HFOs as epileptogenic biomarkers to the clinical practice. Epileptic phenomena are dynamic and complex. There is also still a major barrier in detecting and localizing epileptic HFOs with non-invasive techniques, such as traditional scalp-EEG or MEG. Scalp-HFOs could be considered long-term indicators and might help in future identification of the Seizure Onset Zone in a larger group of epileptic patients. The main purpose of this thesis was to investigate HFO morphological characteristics, provide a distinct separation of pathological from non-pathological HFO and thus determine a clinically relevant HFO area. Up to now, the current techniques determine HFO area by its persistence in time and by testing against random effects. With this approach we might be able to avoid this by checking HFO's spectral and morphological features. Our results in the present work, indicate that the proposed machine learning approach with the HFO extracted features and their event-based classification, delineates successfully and precisely the epileptogenic zone in the individual patient. Moreover, we validated that the co-occurrence of Ripples and Fast Ripples designated the pathological HFO area with higher performance, than Ripples and Fast Ripples separately. HFO analysis showed that the HFO Zone is critical for the seizure outcome whether it is within the Seizure Onset Zone or outside. This prospective automated HFO definition proved to be reproducible in all patients, even in the most difficult ones according to their seizure outcome. With the current techniques, mostly drug-resistant patients that need to undergo epilepsy surgery may profit from the benefit of HFO as a biomarker in iEEG.

As for future steps, we suggest to make our classification models more generalizable by training and evaluating with a larger sufficient dataset and different epileptic cases. We could also apply different feature selection techniques and test deep learning approaches, for example transfer learning or Convolutional Neural Networks for improving HFO detection. A comparison between the efficiency of event-level and channel-wise HFO characterization would be also useful. Moreover, further experimentation and analysis of the electrophysiological content of the HFOs could

lead to better insights in relation with other cortical zones that are estimators of the Epileptogenic Zone. Finally, an important prerequisite for the establishment of HFOs in the clinical routine is more multicentre studies and research trials.

## References

- [1] “About Neuroscience,” *Department of Neuroscience*. <https://neuro.georgetown.edu/about-neuroscience/>
- [2] “Computational Neuroscience in Epilepsy - 1st Edition.” <https://www.elsevier.com/books/computational-neuroscience-in-epilepsy/soltesz/978-0-12-373649-9>
- [3] D. Sterratt, B. Graham, A. Gillies, and D. Willshaw, *Principles of Computational Modelling in Neuroscience*. Cambridge: Cambridge University Press, 2011. doi: 10.1017/CBO9780511975899.
- [4] V. Lai, H. K. Mak, A. W. Y. Yung, W. Y. Ho, and K. N. Hung, “Neuroimaging techniques in epilepsy,” *Hong Kong Med. J. Xianggang Yi Xue Za Zhi*, vol. 16, no. 4, pp. 292–298, Aug. 2010.
- [5] C. Juhász and F. John, “Utility of MRI, PET, and ictal SPECT in presurgical evaluation of non-lesional pediatric epilepsy,” *Seizure*, vol. 77, pp. 15–28, Apr. 2020, doi: 10.1016/j.seizure.2019.05.008.
- [6] B. E. Youngerman, A. V. Save, and G. M. McKhann, “Magnetic Resonance Imaging-Guided Laser Interstitial Thermal Therapy for Epilepsy: Systematic Review of Technique, Indications, and Outcomes,” *Neurosurgery*, vol. 86, no. 4, pp. E366–E382, Apr. 2020, doi: 10.1093/neuros/nyz556.
- [7] E. H. Reynolds, “Epilepsy and Neuroscience: Evolution and Interaction,” *Front. Neuroanat.*, vol. 14, p. 25, 2020, doi: 10.3389/fnana.2020.00025.
- [8] R. A. Stefanescu, R. G. Shivakeshavan, and S. S. Talathi, “Computational models of epilepsy,” *Seizure*, vol. 21, no. 10, pp. 748–759, Dec. 2012, doi: 10.1016/j.seizure.2012.08.012.
- [9] F. Wendling, “Computational models of epileptic activity: a bridge between observation and pathophysiological interpretation,” *Expert Rev. Neurother.*, vol. 8, no. 6, pp. 889–896, Jun. 2008, doi: 10.1586/14737175.8.6.889.
- [10] L. Dalic and M. J. Cook, “Managing drug-resistant epilepsy: challenges and solutions,” *Neuropsychiatr. Dis. Treat.*, vol. 12, pp. 2605–2616, Oct. 2016, doi: 10.2147/NDT.S84852.
- [11] M.-C. Picot *et al.*, “Cost-effectiveness analysis of epilepsy surgery in a controlled cohort of adult patients with intractable partial epilepsy: A 5-year follow-up study,” *Epilepsia*, vol. 57, no. 10, pp. 1669–1679, Oct. 2016, doi: 10.1111/epi.13492.
- [12] F. Rosenow and H. Lüders, “Presurgical evaluation of epilepsy,” *Brain J. Neurol.*, vol. 124, no. Pt 9, pp. 1683–1700, Sep. 2001, doi: 10.1093/brain/124.9.1683.
- [13] E. Tamilya, J. R. Madsen, P. E. Grant, P. L. Pearl, and C. Papadelis, “Current and Emerging Potential of Magnetoencephalography in the Detection and Localization of High-Frequency Oscillations in Epilepsy,” *Front. Neurol.*, vol. 8, p. 14, 2017, doi: 10.3389/fneur.2017.00014.
- [14] M. Dümpelmann, J. Jacobs, and A. Schulze-Bonhage, “Temporal and spatial characteristics of high frequency oscillations as a new biomarker in epilepsy,” *Epilepsia*, vol. 56, no. 2, pp. 197–206, 2015, doi: 10.1111/epi.12844.
- [15] T. Fedele *et al.*, “Resection of high frequency oscillations predicts seizure outcome in the individual patient,” *Sci. Rep.*, vol. 7, no. 1, p. 13836, Oct. 2017, doi: 10.1038/s41598-017-13064-1.
- [16] B. Elahian, M. Yeasin, B. Mudigoudar, J. W. Wheless, and A. Babajani-Feremi, “Identifying seizure onset zone from electrocorticographic recordings: A machine learning approach based on phase locking value,” *Seizure*, vol. 51, pp. 35–42, Oct. 2017, doi: 10.1016/j.seizure.2017.07.010.
- [17] Y. Varatharajah *et al.*, “Integrating artificial intelligence with real-time intracranial EEG monitoring to automate interictal identification of seizure onset zones in focal epilepsy,” *J. Neural Eng.*, vol. 15, no. 4, p. 046035, Aug. 2018, doi: 10.1088/1741-2552/aac960.
- [18] “About HFO Zurich,” *HFO Zurich*. <https://hfozuri.ch/research/> (accessed Oct. 08, 2021).
- [19] D. Lai *et al.*, “Channel-Wise Characterization of High Frequency Oscillations for Automated Identification of the Seizure Onset Zone,” *IEEE Access*, vol. 8, pp. 45531–45543, 2020, doi: 10.1109/ACCESS.2020.2978290.
- [20] S. Chaibi, Z. Sakka, T. Lajnef, M. Samet, and A. Kachouri, “Automated detection and classification of high frequency oscillations (HFOs) in human intracerebral EEG,” *Biomed. Signal Process. Control*, vol. 8, pp. 927–934, Oct. 2013, doi: 10.1016/j.bspc.2013.08.009.
- [21] N. Sciaraffa, M. A. Klados, G. Borghini, G. Di Flumeri, F. Babiloni, and P. Aricò, “Double-Step Machine Learning Based Procedure for HFOs Detection and Classification,” *Brain Sci.*, vol. 10, no. 4, Art. no. 4, Apr. 2020, doi: 10.3390/brainsci10040220.

- [22] S. A. Weiss *et al.*, “Localizing epileptogenic regions using high-frequency oscillations and machine learning,” *Biomark. Med.*, vol. 13, no. 5, pp. 409–418, doi: 10.2217/bmm-2018-0335.
- [23] “Multiband entropy-based feature-extraction method for automatic identification of epileptic focus based on high-frequency components in interictal iEEG | Scientific Reports.” <https://www.nature.com/articles/s41598-020-62967-z> (accessed Oct. 09, 2021).
- [24] H. Sugondo, A. Suci, and R. Achmad, “Quantitative EEG based on Renyi Entropy for Epileptic Classification,” p. 6.
- [25] Y. Zhang *et al.*, *Refining epileptogenic high-frequency oscillations using deep learning: a reverse engineering approach*. 2021. doi: 10.1101/2021.08.31.458385.
- [26] H. O. Lüders, I. Najm, D. Nair, P. Widdess-Walsh, and W. Bingman, “The epileptogenic zone: general principles,” *Epileptic. Disord.*, vol. 8, no. 2, pp. 1–9, Sep. 2006.
- [27] “About ILAE // International League Against Epilepsy.” <https://www.ilae.org/about-ilae>
- [28] J. Jacobs, P. LeVan, C.-É. Châtillon, A. Olivier, F. Dubeau, and J. Gotman, “High frequency oscillations in intracranial EEGs mark epileptogenicity rather than lesion type,” *Brain J. Neurol.*, vol. 132, no. Pt 4, pp. 1022–1037, Apr. 2009, doi: 10.1093/brain/awn351.
- [29] “A Neurosurgeon’s Overview the Brain’s Anatomy.” <https://www.aans.org/>.
- [30] “AANS Patient Resources - Neurosurgical Conditions and Treatments.” <https://www.aans.org/>
- [31] “ORGANIZATION OF THE NERVOUS SYSTEM - THE NERVOUS SYSTEM - Medical Physiology, 2e Updated Edition: with STUDENT CONSULT Online Access, 2e (MEDICAL PHYSIOLOGY (BORON)) 2nd Ed.” <https://doctorlib.info/physiology/medical-physiology-molecular/11.html>
- [32] “Neuroanatomy: The Basics,” *Dana Foundation*. <https://www.dana.org/article/neuroanatomy-the-basics/>
- [34] “Nerve Tissue | SEER Training.” <https://training.seer.cancer.gov/anatomy/nervous/tissue.html>
- [35] “Peripheral nervous system - Queensland Brain Institute - University of Queensland.” <https://qbi.uq.edu.au/brain/brain-anatomy/peripheral-nervous-system>
- [36] “Introduction to the Nervous System | SEER Training.” <https://training.seer.cancer.gov/anatomy/nervous/>
- [37] “Action potentials and synapses,” Nov. 22, 2016. <https://qbi.uq.edu.au/brain-basics/brain/brain-physiology/action-potentials-and-synapses>
- [38] “What Are Glial Cells and What Do They Do?” *Verywell Health*. <https://www.verywellhealth.com/what-are-glial-cells-and-what-do-they-do-4159734>
- [39] “Types of glia,” Nov. 22, 2016. <https://qbi.uq.edu.au/brain-basics/brain/brain-physiology/types-glia>
- [40] E. G. Jones and A. Peters, Eds., *Cerebral Cortex: Comparative Structure and Evolution of Cerebral Cortex, Part II*. Springer US, 1990. doi: 10.1007/978-1-4615-3824-0.
- [41] “Lobes of the Brain | Introduction to Psychology.” <https://courses.lumenlearning.com/waymaker-psychology/chapter/reading-parts-of-the-brain/>
- [42] “Lobes of the brain,” Dec. 02, 2016. <https://qbi.uq.edu.au/brain/brain-anatomy/lobes-brain>
- [43] I. M. Colrain, C. L. Nicholas, and F. C. Baker, “Alcohol and the Sleeping Brain,” *Handb. Clin. Neurol.*, vol. 125, pp. 415–431, 2014, doi: 10.1016/B978-0-444-62619-6.00024-0.
- [44] “The Functional Significance of Theta and Upper Alpha Oscillations. - PsycNET.” <https://psycnet.apa.org/doiLanding?doi=10.1027%2F1618-3169.52.2.99>
- [45] B. R. Cornwell, L. L. Johnson, T. Holroyd, F. W. Carver, and C. Grillon, “Human Hippocampal and Parahippocampal Theta during Goal-Directed Spatial Navigation Predicts Performance on a Virtual Morris Water Maze,” *J. Neurosci.*, vol. 28, no. 23, pp. 5983–5990, Jun. 2008, doi: 10.1523/JNEUROSCI.5001-07.2008.
- [46] G. Pfurtscheller and A. Aranibar, “Event-related cortical desynchronization detected by power measurements of scalp EEG,” *Electroencephalogr. Clin. Neurophysiol.*, vol. 42, no. 6, pp. 817–826, Jun. 1977, doi: 10.1016/0013-4694(77)90235-8.
- [47] K. D. Rana and L. M. Vaina, “Functional Roles of 10 Hz Alpha-Band Power Modulating Engagement and Disengagement of Cortical Networks in a Complex Visual Motion Task,” *PLoS ONE*, vol. 9, no. 10, p. e107715, Oct. 2014, doi: 10.1371/journal.pone.0107715.
- [48] O. M. Klimecki, S. Leiberg, M. Ricard, and T. Singer, “Differential pattern of functional brain

- plasticity after compassion and empathy training," *Soc. Cogn. Affect. Neurosci.*, vol. 9, no. 6, pp. 873–879, Jun. 2014, doi: 10.1093/scan/nst060.
- [49] C. Lainscsek, M. E. Hernandez, J. Weyhenmeyer, T. J. Sejnowski, and H. Poizner, "Non-Linear Dynamical Analysis of EEG Time Series Distinguishes Patients with Parkinson's Disease from Healthy Individuals," *Front. Neurol.*, vol. 4, p. 200, Dec. 2013, doi: 10.3389/fneur.2013.00200.
- [50] O. Dimigen, M. Valsecchi, W. Sommer, and R. Kliegl, "Human Microsaccade-Related Visual Brain Responses," *J. Neurosci. Off. J. Soc. Neurosci.*, vol. 29, pp. 12321–31, Sep. 2009, doi: 10.1523/JNEUROSCI.0911-09.2009.
- [51] "Who Gets Epilepsy?" *Epilepsy Foundation*. <https://www.epilepsy.com/learn/about-epilepsy-basics/who-gets-epilepsy>
- [52] "Types of Seizures | Johns Hopkins Medicine." <https://www.hopkinsmedicine.org/health/conditions-and-diseases/epilepsy/types-of-seizures>
- [53] "Epilepsy: A Comprehensive Textbook." <https://www.ilae.org/education/books-on-epilepsy/epilepsy-a-comprehensive-textbook>
- [54] "Treating Seizures and Epilepsy," *Epilepsy Foundation*. <https://www.epilepsy.com/learn/treating-seizures-and-epilepsy>
- [55] S. T. Sarmast, A. M. Abdullahi, and N. Jahan, "Current Classification of Seizures and Epilepsies: Scope, Limitations and Recommendations for Future Action," *Cureus*, vol. 12, no. 9, p. e10549, doi: 10.7759/cureus.10549.
- [56] F. M. C. Besag and M. J. Vasey, "Prodrome in epilepsy," *Epilepsy Behav. EB*, vol. 83, pp. 219–233, Jun. 2018, doi: 10.1016/j.yebeh.2018.03.019.
- [57] "Seizures," *Epilepsy Canada Epilepsi*. <https://www.epilepsy.ca/seizures>
- [58] J. J. Falco-Walter, I. E. Scheffer, and R. S. Fisher, "The new definition and classification of seizures and epilepsy," *Epilepsy Res.*, vol. 139, pp. 73–79, Jan. 2018, doi: 10.1016/j.eplepsyres.2017.11.015.
- [59] G. H. Glover, "Overview of Functional Magnetic Resonance Imaging," *Neurosurg. Clin. N. Am.*, vol. 22, no. 2, pp. 133–139, Apr. 2011, doi: 10.1016/j.nec.2010.11.001.
- [60] F. Pittau, F. Dubeau, and J. Gotman, "Contribution of EEG/fMRI to the definition of the epileptic focus," *Neurology*, vol. 78, pp. 1479–87, Apr. 2012, doi: 10.1212/WNL.0b013e3182553bf7.
- [61] D. Caligari Conti, "Magnetic Resonance Imaging," Mar. 2016.
- [62] G. D. Rubin, "Computed tomography: revolutionizing the practice of medicine for 40 years," *Radiology*, vol. 273, no. 2 Suppl, pp. S45–74, Nov. 2014, doi: 10.1148/radiol.14141356.
- [63] "Computed Tomography - an overview | ScienceDirect Topics." <https://www.sciencedirect.com/topics/neuroscience/computed-tomography>
- [64] H. Health, "Patient Basics: Positron Emission Tomography (PET Scan) | 2 Minute Medicine," Nov. 09, 2014. <https://www.2minutemedicine.com/patient-basics-positron-emission-tomography-pet-scan/>
- [65] J. J. Vaquero and P. Kinahan, "Positron Emission Tomography: Current Challenges and Opportunities for Technological Advances in Clinical and Preclinical Imaging Systems," *Annu. Rev. Biomed. Eng.*, vol. 17, pp. 385–414, 2015, doi: 10.1146/annurev-bioeng-071114-040723.
- [66] K. Lameka, M. D. Farwell, and M. Ichise, "Chapter 11 - Positron Emission Tomography," in *Handbook of Clinical Neurology*, vol. 135, J. C. Masdeu and R. G. González, Eds. Elsevier, 2016, pp. 209–227. doi: 10.1016/B978-0-444-53485-9.00011-8.
- [67] "EEG (Electroencephalography): The Complete Pocket Guide," *Imotions Publish*, Aug. 27, 2019. <https://imotions.com/blog/eeg/>
- [68] "Frontiers | Epileptic neuronal networks: methods of identification and clinical relevance. | Neurology." <https://www.frontiersin.org/articles/10.3389/fneur.2013.00008/full>
- [69] G. Buzsáki, C. A. Anastassiou, and C. Koch, "The origin of extracellular fields and currents — EEG, ECoG, LFP and spikes," *Nat. Rev. Neurosci.*, vol. 13, no. 6, pp. 407–420, Jun. 2012, doi: 10.1038/nrn3241.
- [70] M. Cohen, "It's about Time," *Front. Hum. Neurosci.*, vol. 5, p. 2, 2011, doi: 10.3389/fnhum.2011.00002.
- [71] A. K. Shah and S. Mittal, "Invasive electroencephalography monitoring: Indications and presurgical planning," *Ann. Indian Acad. Neurol.*, vol. 17, no. Suppl 1, pp. S89–S94, Mar. 2014, doi: 10.4103/0972-2327.128668.

- [72] J. Parvizi and S. Kastner, "Human Intracranial EEG: Promises and Limitations," *Nat. Neurosci.*, vol. 21, no. 4, pp. 474–483, Apr. 2018, doi: 10.1038/s41593-018-0108-2.
- [73] Y. Wang *et al.*, "Expert consensus on clinical applications of high-frequency oscillations in epilepsy," *Acta Epileptol.*, vol. 2, no. 1, p. 8, Jun. 2020, doi: 10.1186/s42494-020-00018-w.
- [74] A. Bragin, C. L. Wilson, J. Almajano, I. Mody, and J. Engel, "High-frequency oscillations after status epilepticus: epileptogenesis and seizure genesis," *Epilepsia*, vol. 45, no. 9, pp. 1017–1023, Sep. 2004, doi: 10.1111/j.0013-9580.2004.17004.x.
- [75] "Hippocampal and entorhinal cortex high-frequency oscillations (100--500 Hz) in human epileptic brain and in kainic acid--treated rats with chronic seizures - PubMed." <https://pubmed.ncbi.nlm.nih.gov/9952257/> (accessed Oct. 08, 2021).
- [76] A. Bragin, S. K. Benassi, F. Kheiri, and J. Engel, "Further evidence that pathologic high-frequency oscillations are bursts of population spikes derived from recordings of identified cells in dentate gyrus," *Epilepsia*, vol. 52, no. 1, pp. 45–52, Jan. 2011, doi: 10.1111/j.1528-1167.2010.02896.x.
- [77] L. P. Andrade-Valenca, F. Dubeau, F. Mari, R. Zelmann, and J. Gotman, "Interictal scalp fast oscillations as a marker of the seizure onset zone," *Neurology*, vol. 77, no. 6, pp. 524–531, Aug. 2011, doi: 10.1212/WNL.0b013e318228bee2.
- [78] "High-frequency oscillations, extent of surgical resection, and surgical outcome in drug-resistant focal epilepsy." <https://www.ncbi.nlm.nih.gov/pmc/articles/PMC3712982/>
- [79] S. A. Weiss *et al.*, "Ictal high frequency oscillations distinguish two types of seizure territories in humans," *Brain J. Neurol.*, vol. 136, no. Pt 12, pp. 3796–3808, Dec. 2013, doi: 10.1093/brain/awt276.
- [80] T. Akiyama *et al.*, "Focal resection of fast ripples on extraoperative intracranial EEG improves seizure outcome in pediatric epilepsy," *Epilepsia*, vol. 52, no. 10, pp. 1802–1811, Oct. 2011, doi: 10.1111/j.1528-1167.2011.03199.x.
- [81] K. Kerber *et al.*, "Differentiation of specific ripple patterns help to identify epileptogenic areas for surgical procedures," *Clin. Neurophysiol. Off. J. Int. Fed. Clin. Neurophysiol.*, vol. 125, Dec. 2013, doi: 10.1016/j.clinph.2013.11.030.
- [82] J. Jacobs *et al.*, "Removing high-frequency oscillations: A prospective multicenter study on seizure outcome," *Neurology*, vol. 91, no. 11, pp. e1040–e1052, Sep. 2018, doi: 10.1212/WNL.0000000000006158.
- [83] J. Xiang *et al.*, "Quantification of Interictal Neuromagnetic Activity in Absence Epilepsy with Accumulated Source Imaging," *Brain Topogr.*, vol. 28, no. 6, pp. 904–914, Nov. 2015, doi: 10.1007/s10548-014-0411-5.
- [84] C. Hatlestad-Hall *et al.*, "Source-level EEG and graph theory reveal widespread functional network alterations in focal epilepsy." 2020. doi: 10.1101/2020.12.17.20248426.
- [85] I. E. Scheffer *et al.*, "ILAE classification of the epilepsies: Position paper of the ILAE Commission for Classification and Terminology," *Epilepsia*, vol. 58, no. 4, pp. 512–521, 2017, doi: 10.1111/epi.13709.
- [86] "Types of Epilepsy Surgery," *Epilepsy Foundation*. <https://www.epilepsy.com/learn/treating-seizures-and-epilepsy/surgery/types-epilepsy-surgery>
- [87] "Temporal Lobe Epilepsy (TLE)," *Epilepsy Foundation*. <https://www.epilepsy.com/learn/types-epilepsy-syndromes/temporal-lobe-epilepsy-aka-tle>
- [88] D. Cheng, X. Yan, K. Xu, X. Zhou, and Q. Chen, "The effect of interictal epileptiform discharges on cognitive and academic performance in children with idiopathic epilepsy," *BMC Neurol.*, vol. 20, no. 1, p. 233, Jun. 2020, doi: 10.1186/s12883-020-01807-z.
- [89] Y. Lv, Z. Wang, L. Cui, D. Ma, and H. Meng, "Cognitive correlates of interictal epileptiform discharges in adult patients with epilepsy in China," *Epilepsy Behav. EB*, vol. 29, no. 1, pp. 205–210, Oct. 2013, doi: 10.1016/j.yebeh.2013.07.014.
- [90] A. Hufnagel, M. Dümpelmann, J. Zentner, O. Schijns, and C. E. Elger, "Clinical relevance of quantified intracranial interictal spike activity in presurgical evaluation of epilepsy," *Epilepsia*, vol. 41, no. 4, pp. 467–478, Apr. 2000, doi: 10.1111/j.1528-1157.2000.tb00191.x.
- [91] A. B. Martin *et al.*, "Temporal dynamics and response modulation across the human visual system in a spatial attention task: an ECoG study," *J. Neurosci.*, Nov. 2018, doi: 10.1523/JNEUROSCI.1889-18.2018.
- [92] J.-P. Lachaux, N. Axmacher, F. Mormann, E. Halgren, and N. E. Crone, "High-frequency neural activity and human cognition: past, present and possible future of intracranial EEG

- research," *Prog. Neurobiol.*, vol. 98, no. 3, pp. 279–301, Sep. 2012, doi: 10.1016/j.pneurobio.2012.06.008.
- [93] M. Zijlmans, P. Jiruska, R. Zelman, F. S. S. Leijten, J. G. R. Jefferys, and J. Gotman, "High-Frequency Oscillations as a New Biomarker in Epilepsy," *Ann. Neurol.*, vol. 71, no. 2, pp. 169–178, Feb. 2012, doi: 10.1002/ana.22548.
- [94] A. Bragin, I. Mody, C. L. Wilson, and J. Engel, "Local generation of fast ripples in epileptic brain," *J. Neurosci. Off. J. Soc. Neurosci.*, vol. 22, no. 5, pp. 2012–2021, Mar. 2002.
- [95] G. Buzsáki, "Large-scale recording of neuronal ensembles," *Nat. Neurosci.*, vol. 7, no. 5, pp. 446–451, May 2004, doi: 10.1038/nn1233.
- [96] D. Whitmer, G. Worrell, M. Stead, I. K. Lee, and S. Makeig, "Utility of independent component analysis for interpretation of intracranial EEG," *Front. Hum. Neurosci.*, vol. 4, p. 184, 2010, doi: 10.3389/fnhum.2010.00184.
- [97] G. A. Worrell *et al.*, "High-frequency oscillations in human temporal lobe: simultaneous microwire and clinical macroelectrode recordings," *Brain J. Neurol.*, vol. 131, no. Pt 4, pp. 928–937, Apr. 2008, doi: 10.1093/brain/awn006.
- [98] J. Jacobs *et al.*, "Value of electrical stimulation and high frequency oscillations (80-500 Hz) in identifying epileptogenic areas during intracranial EEG recordings," *Epilepsia*, vol. 51, no. 4, pp. 573–582, Apr. 2010, doi: 10.1111/j.1528-1167.2009.02389.x.
- [99] L. Menendez de la Prida, R. J. Staba, and J. A. Dian, "Conundrums of high-frequency oscillations (80-800 Hz) in the epileptic brain," *J. Clin. Neurophysiol. Off. Publ. Am. Electroencephalogr. Soc.*, vol. 32, no. 3, pp. 207–219, Jun. 2015, doi: 10.1097/WNP.000000000000150.
- [100] J. Jacobs *et al.*, "High-frequency electroencephalographic oscillations correlate with outcome of epilepsy surgery," *Ann. Neurol.*, vol. 67, no. 2, pp. 209–220, Feb. 2010, doi: 10.1002/ana.21847.
- [101] J. Y. Wu, R. Sankar, J. T. Lerner, J. H. Matsumoto, H. V. Vinters, and G. W. Mathern, "Removing interictal fast ripples on electrocorticography linked with seizure freedom in children," *Neurology*, vol. 75, no. 19, pp. 1686–1694, Nov. 2010, doi: 10.1212/WNL.0b013e3181fc27d0.
- [102] M. A. van 't Klooster *et al.*, "Tailoring epilepsy surgery with fast ripples in the intraoperative electrocorticogram," *Ann. Neurol.*, vol. 81, no. 5, pp. 664–676, May 2017, doi: 10.1002/ana.24928.
- [103] D. Purves *et al.*, "Stages of Sleep," *Neurosci. 2nd Ed.*, 2001 Available: <https://www.ncbi.nlm.nih.gov/books/NBK10996/>
- [104] J. Jacobs *et al.*, "High-frequency oscillations (HFOs) in clinical epilepsy," *Prog. Neurobiol.*, vol. 98, no. 3, pp. 302–315, Sep. 2012, doi: 10.1016/j.pneurobio.2012.03.001.
- [105] "(PDF) Fractal dimension analysis of spatio-temporal patterns using image processing and nonlinear time-series analysis | Debasmita Banerjee και Amit Kumar Jha - Academia.edu." [https://www.academia.edu/49026671/Fractal\\_dimension\\_analysis\\_of\\_spatio\\_temporal\\_patterns\\_using\\_image\\_processing\\_and\\_nonlinear\\_time\\_series\\_analysis](https://www.academia.edu/49026671/Fractal_dimension_analysis_of_spatio_temporal_patterns_using_image_processing_and_nonlinear_time_series_analysis)
- [106] B. E. Boser, I. M. Guyon, and V. N. Vapnik, "A training algorithm for optimal margin classifiers," in *Proceedings of the fifth annual workshop on Computational learning theory*, 1992, pp. 144–152.
- [107] "Theoretical foundations of the potential function method in pattern recognition learning. | BibSonomy." <https://www.bibsonomy.org/bibtex/22d5200f2631a82c1ccb33db90ee38d10/naufraghi>
- [108] B. Schölkopf and A. J. Smola, *Learning with Kernels: Support Vector Machines, Regularization, Optimization, and Beyond*. Cambridge, MA, USA: MIT Press, 2001.
- [109] D. H. Moore II, "Classification and regression trees, by Leo Breiman, Jerome H. Friedman, Richard A. Olshen, and Charles J. Stone. Brooks/Cole Publishing, Monterey, 1984, 358 pages," *Cytometry*, vol. 8, no. 5, pp. 534–535, 1987, doi: 10.1002/cyto.990080516.
- [110] "Pattern Classification Using Ensemble Methods | Series in Machine Perception and Artificial Intelligence." <https://www.worldscientific.com/worldscibooks/10.1142/7238>
- [112] T. Hastie, R. Tibshirani, and J. Friedman, *The Elements of Statistical Learning: Data Mining, Inference, and Prediction, Second Edition (Springer Series in Statistics)*. 2009